UNIVERSIDADE ESTADUAL PAULISTA
"JÚLIO DE MESQUITA FILHO"
Câmpus de São José do Rio Preto

Leonardo Pereira Serantola

A Study of Limit Cycles and Global Centers for some Systems

São José do Rio Preto
2024

Leonardo Pereira Serantola

A Study of Limit Cycles and Global Centers for some Systems

Tese apresentada como parte dos requisitos para obtenção do título de Doutor em Matemática, junto ao Programa de Pós-Graduação em Matemática, do Instituto de Biociências, Letras e Ciências Exatas da Universidade Estadual Paulista "Júlio de Mesquita Filho", Câmpus de São José do Rio Preto.

Orientador: Prof. Dr. Márcio Ricardo Alves Gouveia
Coorientador: Prof. Dr. Jaume Llibre

Financiadora: CAPES

São José do Rio Preto
2024

S481s

Serantola, Leonardo Pereira
A study of limit cycles and global centers for some systems / Leonardo Pereira Serantola. -- São José do Rio Preto, 2024
101 p. : il.

Tese (doutorado) - Universidade Estadual Paulista (UNESP), Instituto de Biociências Letras e Ciências Exatas, São José do Rio Preto
Orientador: Márcio Ricardo Alves Gouveia
Coorientador: Jaume Llibre

1. matemática. 2. sistemas dinâmicos. 3. ciclo limite. 4. centro global. 5. ciclo canard. I. Título.

Sistema de geração automática de fichas catalográficas da Unesp. Biblioteca da Universidade Estadual Paulista (UNESP), Instituto de Biociências Letras e Ciências Exatas, São José do Rio Preto. Dados fornecidos pelo autor(a).

Essa ficha não pode ser modificada.

Leonardo Pereira Serantola

A Study of Limit Cycles and Global Centers for some Systems

Tese apresentada como parte dos requisitos para obtenção do título de Doutor em Matemática, junto ao Programa de Pós-Graduação em Matemática, do Instituto de Biociências, Letras e Ciências Exatas da Universidade Estadual Paulista "Júlio de Mesquita Filho", Câmpus de São José do Rio Preto.

Financiadora: CAPES

Comissão Examinadora

Prof. Dr. Márcio Ricardo Alves Gouveia
Orientador

Prof. Dr. Cláudio A. Buzzi
UNESP - Campus de São José do Rio Preto

Profa. Dra. Cláudio Pessoa
UNESP - Campus de São José do Rio Preto

Prof. Dr. Rodrigo D. Euzebio
UFG - Universidade Federal de Goiás

Prof. Dr. Tiago Carvalho
USP - Campus de Riberirão Preto

São José do Rio Preto
19 de agosto de 2024

À Minha esposa, Yuki,
Às minhas filhas, Catarina, Bárbara e Milena,
À minha mãe, Sebastiana Inez,
dedico.

AGRADECIMENTOS

O meu muito obrigado à minha esposa e minhas filhas que sempre me apoiaram ao longo desta empreitada, à minha mãe, ao meu orientador Márcio Ricardo Alves Gouveia e ao meu co-orientador Jaume Llibre que me recebeu em Barcelona com muita atenção e cordialidade. Não posso me esquecer também do meu muito obrigado aos meus amigos Paulo Santana que me ajudou muito ao longo do doutorado, Lucas Arakaki e Mateus Pereira que me ajudaram muito em dúvidas de listas de exercícios. Agradeço também à CAPES por todo suporte financeiro fornecido.

O presente trabalho foi realizado com apoio da Coordenação de Aperfeiçoamento de Pessoal de Nível Superior - Brasil (CAPES) - Código de Financiamento 001, à qual agradeço.

"Não é o conhecimento, mas o ato de aprender,
não a posse, mas o ato de chegar lá,
que concede a maior satisfação."
Carl Friedrich Gauss

RESUMO

Esta tese é baseada em três assuntos estudados concomitantemente. No primeiro assunto, estudamos ciclos limite para uma classe de sistemas diferenciais contínuos por partes, onde lidamos com ciclos limite (existência e número máximo) em sistemas diferenciais contínuos por partes com uma separação de uma linha não regular, onde temos um centro linear e um centro isócrono (quatro tipos diferentes) em cada uma das duas regiões que o plano é dividido por uma linha não regular. No segundo assunto, estudamos novas famílias de centros cúbicos globais, onde lidamos com a pesquisa de centros globais em um determinado sistema baseado em um teorema que esclarece a existência de centros locais sobre certas condições dos parâmetros envolvidos. No terceiro assunto, estudamos ciclos limite para um sistema diferencial quadrático linear contínuo por partes, onde lidamos com um sistema diferencial contínuo por partes composto por um campo quadrático e um campo linear separados pela linha $x = 0$, que não apresenta ciclos limite quando consideramos eles isoladamente, mas quando aplicamos a regularização de Sotomayor-Teixeira, este sistema contínuo por partes apresenta um ciclo limite na origem e, mais ainda, o sistema se transforma em um sistema slow fast.

Palavras-chave: Sistemas dinâmicos, Ciclos limite, Sistemas diferenciais contínuos por partes, Ciclos canard, Centro global.

ABSTRACT

This thesis is based on three subjects studied. In the first subject, we study limit cycles for a class of discontinuous piecewise differential systems, where we deal with limit cycles (existence and maximum number) in discontinuous piecewise differential system separated by a non regular line where we have a linear center and a isochronous center (4 different types) in each one of the two regions that the plane is divided by the non regular line. In the second subject, we study new families of global cubic centers, where we deal with the search of global centers in a determined system, based on a theorem that elucidades under some parameters conditions the existence of local centers. In the third subject, we study limit cycles for a quadratic-linear discontinuous piecewise differential system, where we deal with a discontinuous piecewise differential system composed by a quadratic and a linear system separated by the line $x = 0$*, that do not present limit cycles when we consider them isolatedly, but when we apply the Sotomayor-Teixeira regularization, this piecewise discontinuous system presents a limit cycle at the origin and, moreover, the system transforms in a slow fast system.*

Keywords: Dynamical systems, Limit cycles, Piecewise discontinuous differential systems, Canard cycles, Global center.

LIST OF FIGURES

1.1 Discontinuity region. Figure made by the author. 17
1.2 Types of limit cycles studied. Figure made by the author. 18
1.3 Type of trajectories. Figure made by the author. 23
1.4 Two hyperbolic sectors. Figure made by the author. 29
1.5 Phase portraits of non-degenerate singular points. Figure made by the author. . 30
1.6 Phase portraits of semi-hyperbolic singular points. Figure made by the author. . 31
1.7 Phase portraits of nilpotent singular points. Figure made by the author. 33

2.1 Examples of limit cycles. Figure made by the author. 45
2.2 Examples of limit cycles. Figure made by the author. 47
2.3 Examples of limit cyles. Figure made by the author. 48
2.4 Examples of limit cyles. Figure made by the author. 49

3.1 Desingularization of blow up's. Figure made by the author. 56
3.2 Desingularization of blow up's. Figure made by the author. 58

4.1 Critical manifold. Figure made by the author. 62
4.2 Sliding region between the interval $(0, 1)$ on the y axis. Figure made by the author. 63
4.3 Sliding region between the interval $(0, 1)$ on the y axis. Figure made by the author. 64
4.4 Phase portrait for the vector field X_{pert} in $\epsilon = 0$. Figure made by the author. . . 66
4.5 Graph of the quadratic surface. Figure made by the author. 66
4.6 Atractor node. Figure made by the author. 67
4.7 Repulsor node. Figure made by the author. 67
4.8 Attractor node. Figure made by the author. 68
4.9 Improper attractor node. Figure made by the author. 68
4.10 Improper repulsor node. Figure made by the author. 69
4.11 Improper attractor node. Figure made by the author. 69
4.12 Bifurcation diagram for X_{pert}. Figure made by the author. 70
4.13 Limit periodic sets. Figure made by the author. 70
4.14 lps of type I and III. Figure made by the author. 71
4.15 The curve c_0. Figure made by the author. 72
4.16 The canard cycle Γ_h. Figure made by the author. 72
4.17 Phase portrait for the chart $\{\overline{\epsilon} = 1\}$. Figure made by the author. 78
4.18 Phase portrait for the charts $\{\overline{a} = \pm 1\}$. Figure made by the author. 79
4.19 Phase portrait for the charts $\{\overline{x} = \pm 1\}$. Figure made by the author. 81
4.20 Phase portrait for the charts $\{\overline{y} = \pm 1\}$. Figure made by the author. 83
4.21 General phase portrait obtained from the charts. Figure made by the author. . . 84
4.22 Representation of the lines N and S. Figure made by the author. 85

4.23 Tridimensional representation of the center manifold M. Figure made by the author. 87
4.24 Center manifold $C_\gamma(A)$. Figure made by the author. 87

CONTENTS

1 Introduction **17**
1.1 Limit Cycles for a Class of Discontinuous Piecewise Differential Systems . . 18
1.1.1 A Brief Introduction on Non-Smooth Systems 18
1.1.2 Limit Cycles in Non-Smooth Systems 20
1.1.3 The Interaction Between Trajectories of $X, Y \in \mathcal{X}$ and Σ 21
1.1.4 Displacement Function 24
1.1.5 Topological Equivalence in Ω^r 24
1.1.6 Results about Isochronous Centers 25
1.2 New Families of Global Cubic Centers 28
1.2.1 Equilibrium Points 34
1.2.2 Vertical Blow Up 34
1.2.3 The Poincaré Compactification 35
1.2.4 Characterization of the Global Centers 36

2 Limit Cycles for a Class of Discontinuous Piecewise Differential Systems 37
2.1 Proof of Theorem 2 37
2.2 Proof of Theorem 3 39
2.3 Proof of Theorem 4 41
2.4 Proof of Theorem 5 43
2.5 Exhibition of Limit Cycles 45
2.5.1 Exhibition of Limit Cycles under the Assumptions of Statement (a) of Theorem 2 45
2.5.2 Exhibition of Limit Cycles under the Assumptions of Statement (a) of Theorem 3 46
2.5.3 Exhibition of Three Limit Cycles under the Assumptions of Statement (a) of Theorem 4 47
2.5.4 Exhibition of Limit Cycles Under the Assumptions of Statement (a) of Theorem 5 48

3 Results on New Families of Global Cubic Centers **50**
3.0.1 Skecth of the Proof of Theorem 13 51
3.0.2 The Proofs According to the Previous Sketch 54

4 Canard Limit Cycles in Piecewise Linear Differential Systems Through Regularization and Blow Up **60**
4.1 Regularization 62
4.2 Hopf Bifurcation 64

4.3 Analysis for the Perturbed Regularized Fields in the Charts 76
4.4 Center Manifolds and Melnikov Integral 86
4.5 Melnikov Integral 88

5 Conclusion **93**

References **94**

1 Introduction

This thesis is composed by three different subjects related mainly to limit cycles and centers. In this chapter we introduce the concepts and definitions needed for an whole understanding of Chapter 2 and 3. In the first section we deal with limit cycles for a specific class of discontinuous piecewise systems, in the second section we study local and global centers for a determined class of systems and, in Chapter 4, we study the canard phenomenon in a non-smooth system of Lièenard type where we use regularization and blow-up techniques.

In a general view, the first subject is based on the study of the existence of limit cycles at the origin of $\mathbb{R}^2$, with a discontinuity region Σ and two regions Σ^+ and Σ^-, where are acting the normal form of the linear center at the origin and one of the four normal forms of cubic isochronous centers extracted from the Theorem 1, represented as X_1 and X_2 in the Figure 1.1.

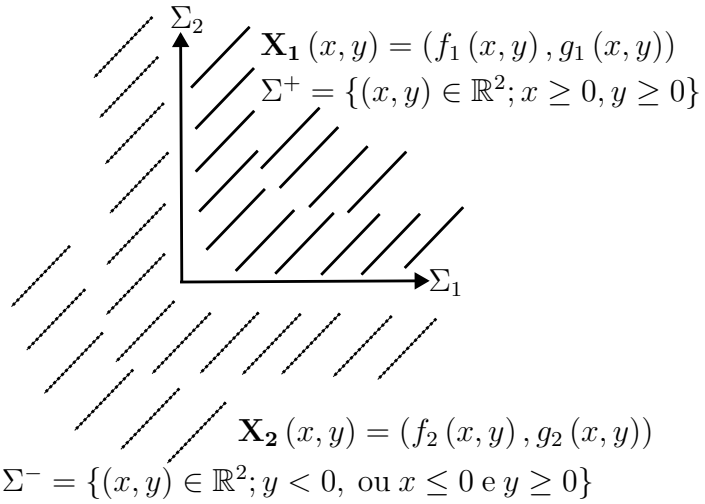

Figura 1.1: Discontinuity region. Figure made by the author.

We consider different configurations of limit cycles, with only one intersection with each one of the semi-axes and with two intersections with each one of the semi-axes, as showed in Figure 1.2. The cases that present only intersections with one semi-axis (two intersections) as showed in 1.2 were already studied in [1]. We found limit cycles with the combinations $X_c - X_i$, $i \in \{1, 2, 3, 4\}$, regardless the order (i.e., $X_c = X_1$ or $X_i = X_1$), in the case with only one intersection with each one of the semi-axes. In the cases with two intersections with each one of the semi-axes, limit cycles do not exist.

The second subject studied consists in a search of the existence of global center for a determined planar system (1.3) already studied in a past article [64], related to the search of local centers (Theorem 12). Based on system (1.3) and the parameters conditions

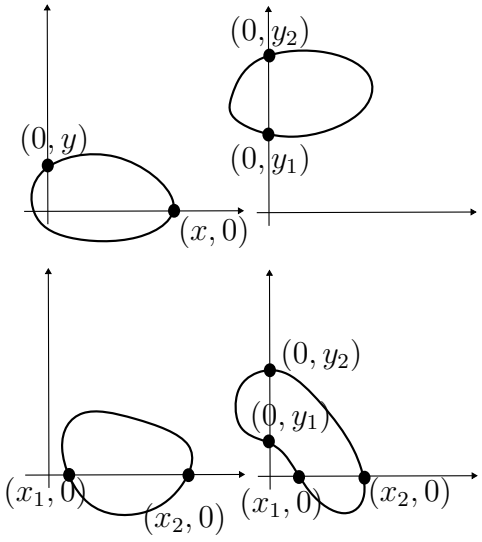

Figura 1.2: Types of limit cycles studied. Figure made by the author.

estabilished on the statements of the Theorem 12 related to the existence of local centers, we analyse parameters conditions that determine the existence of a global center at the origin of the coordinate system in $\mathbb{R}^2$. The system (1.3) has applications in astrophysics.

We begin this study through the application of the Poincaré compactification to the system (1.3) for analysing the infinite equilibria that possibly emerge in the chart U_1 and in the origin of the chart U_2, which is enough to cover every infinite equilibrium point that can exist in system (1.3). Then, we need to become as a necessary condition the Jacobian matrices related to the infinite equilibria null, with the purpose of verifying if these infinite equilibria can be formed by a meeting of hyperbolic sectors. After this, we apply the vertical blow up in all infinite equilibria of the charts U_1 and U_2 to examinate if they are saddles, nodes or saddle-nodes. The meeting of hyperbolic sectors can emerge only in the case that the infinite equilibrium point is a saddle (all the infinite equilibria must be formed by a meeting of hyperbolic sectors, otherwise the system (1.3) can not present a global center). Through these actions, conditions about the parameters are estabilished and then we can verify if the origin is the unique finite equilibrium point of the system (1.3). Then the system (1.3) present a global center under one of the ten statements of Theorem 12 and additional conditions obtained from this analysis.

A detailed analysis of the third subject studied can be found in Chapter 4.

1.1 Limit Cycles for a Class of Discontinuous Piecewise Differential Systems

1.1.1 A Brief Introduction on Non-Smooth Systems

In the last years a considerable interest in studying non-smooth systems grew. A central motivation is due to the many applications in real problems and the rich dynamics that these systems have. For example, applications of non-smooth systems is found in physics, control systems, eletrical engineering, dynamics of neurons, climate changes and problems involving impact, friction, and others, see for instance [13, 19, 23, 30, 34, 46, 48, 67, 75, 76, 79] and applications therein. A good reason for which non-smooth systems are

suitable models for several practical problems is the fact that they can take fast transitions between two states so fast that we can figure them as being discontinuous, as those which occur in on/off electrical systems, see [30]. Therefore, instead of assuming smooth changes in the position or the velocity of some state, a non-smooth model may use discontinuous functions (step or sign functions, for example) to get a more realistic phase portrait of the problem.

The study of the discontinuous piecewise differential systems has attracted attention of mathematicians during these past decades due to their applications. These piecewise differential systems in the plane are formed by different differential systems defined in distinct regions, separated by a curve. Filipov, in 1988, provided the theoretical bases for these kinds of differential systems. Nowadays, a vast literature of these differential systems is available. For instance, see the books of [30], [52], [53] and [73]. As for the smooth differential systems, the study of the existence and location of limit cycles on the piecewise differential systems is also of great importance.

In a piecewise system we have a sudden break in the law that governs the vector field. This break could be subtle like in a non smooth continuous system, i.e., a kind of system that keeps the continuity despite the loss of diferenciability, but this break could be stronger, like in the situation that we have a loss of continuity in the vector field too. In other words, when a piecewise non-smooth system is of class C^0 but not of class C^1, we have a continuous system and when we have a system that is neither of class C^0, we have a discontinuous system.

It is important to notice that non-smooth systems present more complex dynamics than analogous smooth systems, even in the simplest situations. In fact, nonlinearities and nondeterminism appear, for example, in systems without equilibria. It happens basically due to the existence of a positive co-dimension manifold where the system is discontinuous, i.e., these systems have branches of smooth systems with interaction at the discontinuity region. The dynamics is therefore as complex than the complexity of those branches and the geometry of the manifold, with the simplest case being a non-smooth linear system having a straight line as a discontinuity set. Another important element in the study of non-smooth systems is the notion of trajectories. The indeterminacy relies on the way that the trajectories of each branch interact on the discontinuity set, because outside this set the dynamics is governed according to the existence and uniqueness theorem from the classical theory of ordinary differential equations. There are some distinct conventions in the literature as, for instance, the Filippov convention [37] used in this thesis, the paper of Broucke, Pugh and Simic [13] and the Barbashin's, Caratheodory's and Utkin's conventions, see [30]. Related to the nondeterminism, probabilistic approaches can also take place, see for instance [74].

We briefly introduce a non-smooth system for the particular discontinuity set that we consider throughout this chapter. We denote Σ the discontinuity set or switching manifold that is the separating boundary of the region $\Sigma^+ = Q_1 = \{(x, y) \in \mathbb{R}^2; x > 0 \text{ and } y > 0\}$, being Q_1 the first quadrant and $\Sigma^- = \mathbb{R}^2 \backslash Q_1 \cup \Sigma$. Indeed, we estabilish $\Sigma = \Sigma_1 \cup \Sigma_2$ where $\Sigma_1 = \left\{f_1^{-1}(0); x \geq 0\right\}$ and $\Sigma_2 = \left\{f_2^{-1}(0), y \geq 0\right\}$, with $f_1(x, y) = y$ and $f_2(x, y) = x$.

We designate by $\mathcal{X}$ the space of C^r vector fields on $\mathbb{R}^2$ (vector fields that present all the partial derivatives continuous until order r), equipped with the C^r-topology, i.e., two vector fields $X = (P_1, Q_1)$ and $Y = (P_2, Q_2)$ are close in the C^r-topology if $P_1 - P_2$, $Q_1 - Q_2$ and all their partial derivatives until the order r are small enough too, with

$r \geq 1$, and by Ω^r the space of vector fields $Z : \mathbb{R}^2 \to \mathbb{R}^2$ given by

$$Z(x,y) = \begin{cases} X(x,y) & \text{if} \quad (x,y) \in \Sigma^+, \\ Y(x,y) & \text{if} \quad (x,y) \in \Sigma^-, \end{cases} \tag{1.1}$$

where $X = (X_1, X_2)$, $Y = (Y_1, Y_2) \in \mathcal{X}$ and the trajectories of Z are solutions of the non-smooth system $\dot{q} = Z(q)$. Moreover the space Ω^r is equipped with the product topology, and we note that Z is multivalued at the points of Σ.

1.1.2 Limit Cycles in Non-Smooth Systems

A limit cycle is a periodic orbit of a differential system which is isolated in the set of all periodic orbits of the system. In order to determine the dynamics of a given planar differential system, we need to know if it has or not limit cycles and if it has, how many and what are their distribution on the plane.

Limit cycles appear in many areas of research. For example, for explaining physical phenomena like in van der Pol equation [77], or in the Belousov-Zhavotinsky model [8]. In addition the limit cycles are useful in control theory, electrical circuits, economics, etc.

The limit cycles, which are the central problem of the Hilbert 16th problem have their dynamics related to study the existence, the number and the distribution of limit cycles and, moreover, the appearance and robustness of such objects. In the non-smooth context the Hilbert question becomes even harder, because beyond limit cycles there exist other types of different periodic trajectories like the sliding ones, related to the so-called sliding motion.

The simplest non-smooth system consists of a continuous non-smooth linear system separated by a straight line and it is known that such systems have at most one limit cycle, see [35, 56, 65, 66]. On the other hand, if the non-smooth linear system is discontinuous and separated by a straight line, there exists some results providing an upper bound for the number of limit cycles, see [12, 16, 36, 41, 44, 57, 72]. Although several papers indicated that such an upper bound may be three, in the paper [20], the upper bound is limited by eight limit cycles.

A particular kind of non-smooth linear system is considered by Llibre and Teixeira in [61], where the authors proved that, when both of linear systems are of the center type, the continuous or discontinuous non-smooth linear system has no limit cycles. Moreover, it was proved that a continuous non-smooth linear system separated by two paralell straight lines, formed by three linear centers does not present limit cycles. But when are considered two paralell straight lines with discontinuous systems, formed by three linear centers presents at most one limit cycle and, moreover, were found particular cases of such systems having a limit cycle. Thus the results obtained from [61] suggest that the switching manifold plays an important role in the existence of limit cycles.

In this thesis we consider a non-regular switching manifold at the origin. This approach was considered by others authors as for instance, Llibre and Zhang [63], where they proved that non-smooth linear systems formed by three linear centers and separated by the set $\Sigma = \{(x,y)\,;\ y = 0 \text{ or } x = 0 \text{ and } y \geq 0\}$ can have at most three limit cycles. With this set Σ and considering saddles and centers, the same bound was obtained in [81] but when is considered a focus-focus type system, five limit cycles was gotten. There is also the work from Braga and Mello [12] which studies the number of crossing limit cycles bifurcating from two or three period annuli in discontinuous planar linear Hamiltonian differential systems with three zones.

When the separation line is formed by two semi-straight lines that coincide in the origin, forming an angle θ with the x-axis, with $\theta \in (0, \pi)$, Cardin and Torregrosa [18] proved that the system with a perturbation of the linear center presents five limit cycles. With the same separation line, but fixing $\theta = \pi/2$, Huan and Yang [43] provided an example of a focus-focus type system with five limit cycles as well. The authors also proved that is enough to study the case when the angle is $\theta = \pi/2$, because they showed that there is an invertible linear transformation that takes the system with $\theta \in (0, \pi)$ in the system with $\theta = \pi/2$.

The case that we have two centers separated by two semi-straight lines with an inicial point in common, as far as we know, two papers worked with these kind of problems, see [33, 80], where the authors provide upper bounds for the number of crossing limit cycles in some types of center-center systems having two or four intersection with the switching manifold.

1.1.3 The Interaction Between Trajectories of $X, Y \in \mathcal{X}$ and Σ

Consider the Lie derivatives $Xf(p) = \langle \nabla f(p), X(p) \rangle$, with $\langle ., . \rangle$ being the usual inner product in $\mathbb{R}^2$. For our purpose we assume that $X(p) \neq 0$, because we work only with cases where the vector field is not null at the point p in the discontinuity region Σ. We classify the points on Σ according to one of the three following types described below and considering $\Sigma_1 = \left\{ f_1^{-1}(0) ; x \geq 0 \right\}$ and $\Sigma_2 = \left\{ f_2^{-1}(0), y \geq 0 \right\}$, with $f_1(x, y) = y$ and $f_2(x, y) = x$.

Generic points on Σ. If $\langle \nabla f(p), X(p) \rangle \neq 0$ and $\langle \nabla f(p), Y(p) \rangle \neq 0$, we distinguish the following regions on the set $\Sigma \setminus \{(0, 0)\}$.

- $\Sigma_i^c \subseteq \Sigma_i$ is the crossing region when $(Xf_i)(Yf_i) > 0$ in Σ_i^c, $i = 1, 2$.
- $\Sigma_i^e \subseteq \Sigma_i$ is the escaping region when $(Xf_i) > 0$ and $(Yf_i) < 0$ in Σ_i^e, $i = 1, 2$.
- $\Sigma_i^s \subseteq \Sigma_i$ is the sliding region when $(Xf_i) < 0$ and $(Yf_i) > 0$ in Σ_i^s, $i = 1, 2$.

Dynamics on $\Sigma_i^e \cup \Sigma_i^s$ **and** Σ_i**-regular points**. When $q \in \Sigma_i^e \cup \Sigma_i^s$, $i = 1, 2$, following the Filippov convention described in [37], we can define the **sliding vector field** associated to $Z \in \Omega^r$. Hence the **sliding vector field** associated to $Z \in \Omega^r$ is the vector field Z^s tangent to $\Sigma_i^e \cup \Sigma_i^s$ at q and given by

$$Z^s(q) = \frac{Y(q) f_i(q) X(q) - X(q) f_i(q) Y(q)}{Y(q) f_i(q) - X(q) f_i(q)}.$$

We say that $q \in \Sigma_i$ is Σ_i-regular if $(Xf_i(q))(Yf_i(q)) > 0$ or $(Xf_i(q))(Yf_i(q)) < 0$ and $Z^s(q) \neq 0$, i.e., $q \in \Sigma_i^e \cup \Sigma_i^s$ and it is a regular point of Z^s.

Σ_i**-singular points and tangential points**. The points of Σ_i that are not Σ_i-regular are denominated Σ_i-singular. We have two subsets in the set of Σ_i-singular, namely Σ_i^t and Σ_i^p. Any point $q \in \Sigma_i^p$ is called a **pseudo equilibrium** of Z and it is characterized by $Z^s(q) = 0$. Any point $q \in \Sigma_i^t$ is called a **tangential singularity** or a **tangency point** of Z and it is characterized by $(Xf_i(q))(Yf_i(q)) = 0$, where q is a tangential contact point between the trajectories of X and/or Y with Σ_i at the point $q \in \Sigma_i$.

Contact order and visibility of tangent trajectories to Σ. For a given vector field $W \in \mathcal{X}$, we say that r is the contact order of the trajectory Γ_W with Σ at p when we have $W^k f_i(p) = 0, \forall k = 1, \ldots, r-1$ and $W^r f_i(p) \neq 0$, where $W^r f_i(p) = W(W^{r-1} f_i(p))$,

with $k \geq 2$. If $W = X$ or Y, we say that $p \in \Sigma$ is an **invisible tangential point** when the contact order with Γ_X (or Γ_Y) passing through p is even and $X^r f_i(p) < 0$ (respectively $Y^r f_i(p) > 0$). On the other hand, we say that $p \in \Sigma$ is a **visible tangent point** when the contact order with Γ_X (or Γ_Y) passing through p is odd or,if it is even, the condition $X^r f_i(p) > 0$ is satisfied (respectively $Y^r f_i(p) < 0$). A tangential singularity $p \in \Sigma_i^t$ is **singular** if p is an invisible tangent point for both X and Y. On the other hand, $p \in \Sigma_i^t$ is **regular** when it is not singular.

Critical elements and Σ-non-regular points. We say that p is a **critical element** of the system X if p is an equilibrium point or a pseudo equilibrium or a tangency point. Let p be an equilibrium point of X. We say that p is **real** if $p \in \Sigma^+$, otherwise we say that p is *virtual*. The same definition follows analogously for the system Y. Moreover, we say that p is a Σ-**non-regular point** if Σ is non-regular at p. Therefore, it is not possible to use Lie derivatives to classify such points. Nevertheless, we say that they are of **crossing type** if the trajectories cross it from one side of Σ to another. We say that they are of **sliding or escaping type** if they are at the boundary of sliding or escaping regions of Σ_i^s or Σ_i^e respectively. We say that they are of **regular tangential type** if either X or Y has a tangential contact to them. Finally, we say that they are of **singular tangential type** when neither X or Y has trajectories out of the region Σ that can reach it.

Regular and closed trajectories of non-smooth systems. Let $W \in \mathcal{X}$ and denote its flow by $\phi_W(t,p)$, i.e.,

$$\frac{d}{dt}\phi_W(t,p) = W(\phi_W(t,p)),\ \phi_W(0,p) = p,$$

where $t \in I = I(p,W) \subset \mathbb{R}$, and I being an interval that depends on $p \in V$ and W. The next two definitions state the concepts of the local and global trajectory of the non-smooth systems and there are slight modifications of those presented in [37]. The following definition can be found in [40], except by item (vi) that we added due to the non-regular shape of Σ.

Definition 1. *The local trajectory $\phi_Z(t,p)$ of a non-smooth vector field Z given by* (1.1) *is defined as follows:*

- *(i) For $p \in \Sigma^+ \setminus \Sigma^-$ and $q \in \Sigma^- \setminus \Sigma^+$ the trajectory is given by $\phi_Z(t,p) = \phi_X(t,p)$ and $\phi_Z(t,q) = \phi_Y(t,q)$ respectively, where $t \in I$.*

- *(ii) For $p \in \Sigma_i^c$ such that $Xf(p) > 0$ and $Yf(p) > 0$ and the time origin at p, the trajectory is defined as $\phi_Z(t,p) = \phi_X(t,p)$ for $t \in I \cap \{t \geq 0\}$ and $\phi_Z(t,p) = \phi_Y(t,p)$ for $t \in I \cap \{t \leq 0\}$. For the case $Xf(p) < 0$ and $Yf(p) < 0$ the definition is analogous, but with reversing time.*

- *(iii) Taking the origin of the time at p, for $p \in \Sigma_i^e$ the trajectory is defined as $\phi_Z(t,p) = \phi_{Z^s}(t,p)$ for $t \in I \cap \{t \leq 0\}$ and it is either $\phi_Z(t,p) = \phi_X(t,p)$ or $\phi_Y(t,p)$ or $\phi_Z(t,p) = \phi_{Z^s}(t,p)$ for $t \in I \cap \{t \geq 0\}$. For the case $p \in \Sigma_i^s$ the definition is analogous, but with reversing time.*

- *(iv) For p a regular tangent point and taking the origin of the time at p, the trajectory is defined as $\phi_Z(t,p) = \phi_1(t,p)$ for $t \in I \cap \{t \leq 0\}$ and $\phi_Z(t,p) = \phi_2(t,p)$ for $t \in I \cap \{t \geq 0\}$, where each ϕ_1 and ϕ_2 is either ϕ_X or ϕ_Y or ϕ_{Z^s}.*

- *(v) For p a singular tangent point, we have that $\phi_Z(t,p) = p, \forall t \in I$.*

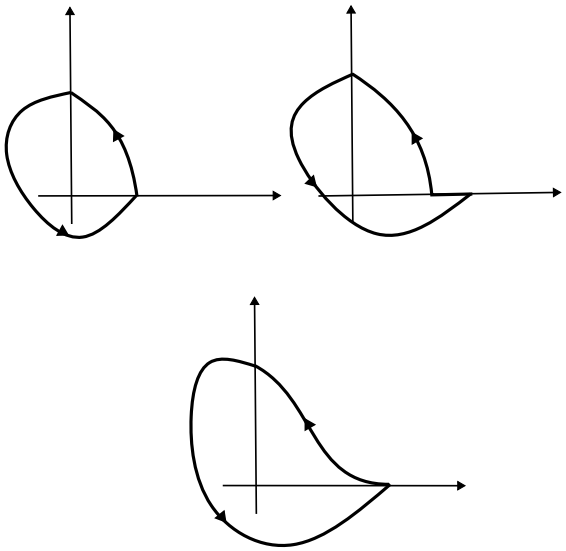

Figura 1.3: Type of trajectories. Figure made by the author.

- *(vi) For $p = (0,0)$, the non-regular point of Σ, the trajectory is defined as in (ii), (iii), (iv) or (v) if p is a Σ-non-regular point of crossing, escaping/sliding, regular tangential or singular tangential type, respectively.*

The following definition is presented in [14].

Definition 2. *A global trajectory $\Gamma_Z(t, p_0)$ of $Z \in \Omega^r$, passing through p_0 is an union:*

$$\Gamma_Z(t, p_0) = \bigcup_{i \in \mathbb{Z}} \{\sigma_i(t, p_i); t_i \leq t \leq t_{i+1}\},$$

of preserving orientation local trajectories $\sigma_i(t, p_i)$, satisfying

$$\sigma_i(t_{i+1}, p_i) = \sigma_{i+1}(t_{i+1}, p_{i+1}) = p_{i+1}$$

and $t_i \to \pm\infty$ as $i \to \pm\infty$. A global trajectory is a positive (respectively negative) global trajectory if $i \in \mathbb{N}$ (respectively $-i \in \mathbb{N}$) and $t_0 = 0$.

Definition 3. *Let $\Gamma_Z(t, q)$ be a global trajectory of system (1.1). We say that Γ_Z is periodic when Γ_Z is periodic in the variable t, i.e., if there exists $T > 0$ such that $\Gamma_Z(t + T, q) = \Gamma_Z(t, q)$.*

Next definition introduces the different types of periodic trajectories.

Definition 4. *Consider the non-smooth vector fields (1.1). A closed global trajectory Δ is a*

- *(i) crossing periodic trajectory if it is isolated and does not contain points or segments in $\Sigma_i^s \cup \Sigma_i^e$,*
- *(ii) sliding periodic trajectory if it is isolated and contain points or segments in $\Sigma_i^s \cup \Sigma_i^e$,*
- *(iii) tangential periodic trajectory if it is isolated and contains points in Σ_t,*

In Figure 1.3, we have periodic trajectories, the upper left is a crossing cycle, the upper right is a sliding cycle, the lower left is a tangential cycle and the lower right is an example of internally center type.

In this thesis we work only with crossing periodic trajectories. Due to the similarity between a limit cycle from the smooth dynamical systems theory and a crossing periodic trajectory, from now on we also call it a limit cycle. We emphasize, nonetheless, that it refers to an object from the non-smooth context and it is not a classical limit cycle.

Concerning item (iv), we also remark that in the literature an internally center type periodic trajectory does not need to be tangent to a specific region. We also notice that, due to the discontinuities, two types of internal center types periodic trajectories take place. On one hand, we have those whose outer small neighborhoods attract or repel trajectories asymptotically without reach the periodic trajectory. On the other hand, it can be reached in finite time through sliding trajectories on Σ, which is a general case.

1.1.4 Displacement Function

An important tool to study hyperbolicity and stability of periodic trajectories is the displacement function. Consider X and Y vector fields with centers at the origin, $P_0 = (x_0, y_0)$ an initial condition and assume that both centers of X and Y rotate counterclockwise. Denote the solutions associated to the linear vector fields $X \in \Omega^r$ and $Y \in \Omega^r$ by the maps $(t_0, P_0) \mapsto (x_1(t_0, P_0), x_2(t_0, P_0))$ and $(t_0, P_0) \mapsto (y_1(t_0, P_0), y_2(t_0, P_0))$, where x_1, x_2 are the vector components of the system X and y_1, y_2 are the vector components of the system Y. Let $P = (r, 0) \in \Sigma_1$ be a point such that $P \notin \Sigma_1^{e,s} \cup \Sigma^t$, let $t^+ > 0$ be the smallest time such that $X(t^+, P) \cap \Sigma_2 \neq \emptyset$ and let $t^- > 0$ be the smallest time such that $Y(-t^-, P) \cap \Sigma_2 \neq \emptyset$. The first half return map associated with the vector field X is given implicitly by the transition function $\rho_1(P) = (0, x_2(t^+, P))$. Similarly, the first half return map associated with the vector field Y is given by $\rho_2(P) = (0, y_2(-t^-, P))$. Therefore, the first return map associated with the system formed by X and Y is

$$\rho : \Gamma \subset \Sigma_1 \to \Sigma_1,\ \rho(P) = \left(\rho_2^{-1} \circ \rho_1\right)(P),$$

where Γ is a suitable set formed by crossing points of Σ_1. If P^* is such that $\rho(P^*) = P^*$, then the trajectory passing through P^* is periodic and, moreover, is isolated, which means that it is a limit cycle, provided that $|\rho'(P^*)| \neq 1$.

Equivalently, one can also define the displacement function by $P \mapsto d(P) = \rho(P) - P$, i.e., periodic trajectories that correspond to zeroes of this map. Moreover, if $d(P^*) = 0$ satisfies $d'(P^*) \neq 0$, then the limit cycle passing through P^* is hyperbolic. In this case, if $d'(P^*) > 0$ (respectively $d'(P^*) < 0$) the limit cycle is unstable (respectively stable). We notice that a limit cycle τ could be neither stable or unstable, which means that this kind of limit cycle is denominated by semi-stable and happens when τ is the α-limit set for all trajectories contained in the intern region of τ (extern region) and close to it, and the ω-limit set for all trajectories that are closed to τ in the extern region (intern region).

1.1.5 Topological Equivalence in Ω^r

We say that two non-smooth systems $Z = (X^+, X^-, f)$ and $\overline{Z} = \left(\overline{X}^+, \overline{X}^-, \overline{f}\right)$ are Σ-topologically equivalent if there exist a homeomorphism h satisfying the following conditions:

- h sends the set $f^{-1}(0)$ to $\overline{f}^{-1}(0)$;

- h sends the trajectories of X^+ (respectivelly X^-) restricted to Σ^+ (respectivelly Σ^-) to the trajectories of $\overline{X}^+$ (respectivelly $\overline{X}^-$) restricted to Σ^+ (respectivelly Σ^-), preserving the orientation of the time;
- h sends critical elements (equilibrium point, tangency point, ...) of Z to critical elements of $\overline{Z}$;
- h sends sliding (respectively escaping) regions of Z to sliding (respectivelly escaping) regions of $\overline{Z}$.

1.1.6 Results about Isochronous Centers

These last decades a big interest has appeared for studying the discontinuous piecewise differential systems. This is mainly due to the fact that these differential systems allow to modelize many natural phenomena. In order to describe the dynamics of a differential system, we need to control its periodic orbits and, in special, its limit cycles, i.e., we need to solve something related to the extended 16th Hilbert problem. Here, for the class of discontinuous piecewise differential systems formed by a linear center and an isochronous center with cubic homogeneous nonlinearities separated by a non-regular line, we solve a problem that is related to the extended 16th Hilbert problem, i.e., we provide an upper bound for the maximum number of limit cycles that these differential systems can exhibit and additionally we prove that this upper bound is reached.

The study of the piecewise differential systems began with Andronov, Vitt and Khaikin and until nowadays these systems have received attention of many researchers, mainly due to their applications for modeling many natural phenomena that appear in electronics, mechanics, economy, etc., see for instance the books of di Bernardo *et al.* [2008] and Simpson [2010], the survey of Makarenkov and Lamb [2012], as well as the lots of references cited in these last three works. See also the references [10, 9, 28, 55].

The simplest class of discontinuous piecewise differential systems is the planar one, formed by two pieces separated by a straight line, having a linear differential system in each piece. In this specific class, several authors have tried to determine the maximum number of limit cycles in this type of discontinuous piecewise differential system, but it remains open to know if this maximum is three, see for instance [54] and the references inside.

As usual the dot in differential systems denotes derivative with respect to the time t and this will be the notation followed in the whole thesis.

For the discontinuous piecewise differential systems here studied, we can study their limit cycles using the first integrals of the linear center and of the isochronous centers with cubic homogeneous nonlinearities (4 different families) acting in the regions Σ^+ and Σ^-, which form the discontinuous piecewise differential system separated by the non-regular curve Σ.

A center is isochronous if the period of all integral curves in a neighborhood of the origin is constant. the equations are most easily written when the arc length l is the variable

$$\ddot{l} + k^2 l = 0,$$

where k is a real constant. In [70] Pleshkan classifies the isochronous centers with cubic homogeneous nonlinearities as follows.

Theorem 1. *A cubic polynomial differential system of the form*

$$X = \left\{ \dot{x} = -y + P(x,y), \ \ \dot{y} = x + Q(x,y), \right.$$

where P and Q are homogeneous polynomials of degree three has an isochronous center at the origin of coordinates if and only if after a linear change of variables and a rescaling of the time, it can be written as one of the four following differential systems:

$$X_1 = \begin{cases} \dot{x} = -y + x^3 - xy^2, \\ \dot{y} = x + x^2 y - y^3, \end{cases} \qquad H_1 = \frac{x^2+y^2}{1+2xy}.$$

$$X_2 = \begin{cases} \dot{x} = -y + x^3 - 3xy^2, \\ \dot{y} = x + 3x^2 y - y^3, \end{cases} \qquad H_2 = \frac{(x^2+y^2)^2}{1+4xy}.$$

$$X_3 = \begin{cases} \dot{x} = -y + 3x^2 y, \\ \dot{y} = x - 2x^3 + 9xy^2, \end{cases} \qquad H_3 = \frac{4-9x^2+27y^2}{(1-3x^2)^3}.$$

$$X_4 = \begin{cases} \dot{x} = -y - 3x^2 y, \\ \dot{y} = x + 2x^3 - 9xy^2, \end{cases} \qquad H_4 = \frac{4+9x^2-27y^2}{(1+3x^2)^3}.$$

The H_i is a first integral of the system X_i for $i \in \{1,2,3,4\}$.

One of the aims here is to study the maximum number of limit cycles of the discontinuous piecewise differential systems (1.1) formed by an arbitrary linear differential center at the origin $(0,0)$, namely

$$X_c = \left\{ \dot{x} = -ax - \frac{(a^2+w^2)\,y}{d}, \ \ \dot{y} = dx + ay, \right.$$

in Σ^+ (resp. Σ^-), where $\omega > 0$, $d > 0$, $a \in \mathbb{R}$, $a \neq 0$ (for more details on these linear differential systems see Lemma 1 of [61]), and by one of the four cubic global isochronous centers X_i in Σ^- (resp. Σ^+) after an arbitrary linear change of variables.

The differential system X_c has the first integral:

$$H(x,y) = (dx+ay)^2 + y^2\omega^2.$$

Now we denote the discontinuity curve as follows

$$\Sigma = \Sigma_1 \cup \Sigma_2 = \{(x,0)\,; x > 0\} \cup \{(0,y)\,; y > 0\}.$$

We have four cases to aote that in statementalize, i.e., the linear center X_c with each one of the four cubic isochronous centers X_i of Theorem 1. The result of this analysis provides the next four theorems.

Each theorem has three cases enumerated as follows:

- **Case 1**. We study the limit cycles that intersect Σ_1 and Σ_2 exactly in one point (see Figure 2.1), considering the linear center and one of the isochronous centers in the regions Σ^+ and Σ^- (the regions where are located the vector fields in this case are irrelevant).

- **Case 2**. We have the linear differential center in the region R_1 and one of the isochronous centers in the region R_2 and we study the limit cycles that intersect Σ_1 and Σ_2 exactly in two points in each one of them.

- **Case 3**. Finally, in the third case we have one of the isochronous centers in the region R_1 and the linear differential center in the region R_2 and again we study the limit cycles that intersect Σ_1 and Σ_2 exactly in two points in each one of them.

Our main results are the following ones.

Theorem 2. *Consider a piecewise differential system* (1.1) *formed by a general linear center with singularity at the origin and the first isochronous center X_1 after an arbitrary linear change of variables, with the discontinuity curve Σ and the regions Σ^+ and Σ^- defined as above. Then the following statements hold.*

(a) In case (1) the maximum number of limit cycles is one and there are piecewise differential systems under the assumptions of this theorem with one limit cycle, see Figure 2.1, assuring that $(1+2a_1x^2\alpha_1)\left(1+\dfrac{2b_1d^2x^2\beta_1}{a^2+\omega^2}\right)\neq 0$.

(b) In cases (2) and (3) there are no limit cycles.

Theorem 3. *Consider a piecewise differential system* (1.1) *formed by a general linear center with singularity at the origin and the second isochronous center X_2 after an arbitrary linear change of variables, with the discontinuity curve Σ and the regions Σ^+ and Σ^- defined as above. Then the following statements hold.*

(a) In case (1) the maximum number of limit cycles is one and there are piecewise differential systems under the assumptions of this theorem with one limit cycle, see Figure 2.2. We must assure that $(1+4a_1x^2\alpha_1)(1+4b_1y^2\beta_1)\neq 0$.

(b) In cases (2) and (3) there are no limit cycles.

Theorem 4. *Consider a piecewise differential system* (1.1) *formed by a general linear center with singularity at the origin and the third isochronous center X_3 after an arbitrary linear change of variables, with the discontinuity curve R and the regions Σ^+ and Σ^- defined as above. Then the following statements hold.*

(a) In case (1) the maximum number of limit cycles is three and there are piecewise differential systems under the assumptions of this theorem with three limit cycles, see Figure 2.3. We must assume that $(-1+3a_1^2x^2)^3(-1+3b_1^2y^2)^3\neq 0$.

(b) In case (2) and (3) there are no limit cycles.

Theorem 5. *Consider a piecewise differential system* (1.1) *formed by a general linear center with singularity at the origin and the fourth isochronous center X_4 after an arbitrary linear change of variables, with the discontinuity curve Σ and the regions Σ^+ and Σ^- defined as above. Then the following statements hold.*

(a) In case (1) the maximum number of limit cycles is one and there are piecewise differential systems under the assumptions of this theorem with one limit cycle, see Figure 2.4.

(b) In case (2) and (3) there are no limit cycles.

Theorems 2, 3, 4 and 5 are proved in Chapter 2 with details.

Note that in statement (a) of Theorems 4 we proved that an upper bound for the maximum number of limit cycles is three and we found an example of discontinuous piecewise differential systems under the assumptions of that statement having three limit cycles. The cases involving only global isochronous centers X_i and X_j with $i \neq j$ remains open.

1.2 New Families of Global Cubic Centers

An equilibrium point p of a differential system in the plane $\mathfrak{t}^2$ is a center if there exists a neighbourhood U of p such that $U \setminus \{p\}$ is filled with periodic orbits. A difficult classical problem in the qualitative theory of differential systems in the plane $\mathfrak{t}^2$ is the problem of distinguish between a focus and a center.

A global center is a center p such that $\mathfrak{t}^2 \setminus \{p\}$ is filled with periodic orbits. Another difficult problem in the qualitative theory of differential systems in $\mathfrak{t}^2$ is to distinguish inside a family of centers the ones which are global.

In [64] Lloyd, Pearson and Romanovsky characterized when the origin of coordinates is a local center for the family of cubic polynomial differential systems (1.3). This system

Here we characterize when the origin of this family of differential system (1.3) is a global center.

The notion of center first appears in the work of Huygens in 1656 on the pendulum clock (look at [45, 69]), but only with the works of Poincaré (see [71]) in 1881 and Dulac (see [31]) in 1908 the notion of center was rigorously defined.

A polynomial differential system in the plane $\mathbb{R}^2$ of degree n is a differential system of the form

$$\dot{x} = P(x, y), \qquad \dot{y} = Q(x, y), \tag{1.2}$$

where P and Q are polynomials in the variables x and y, and the n is the maximum of the degrees of the polynomials P and Q.

The classification of centers for polynomial differential systems of degree two has been done just by the authors Kapteyn [47] and Bautin [7]. For higher degrees only exist partial results.

There are several works studying the global centers of different families of polynomial differential systems, as for instance in [38] and [59] where the authors proved that polynomial differential systems of even degree cannot have global centers because such systems always have orbits coming from and going to infinity. However to classify all polynomial differential systems of odd degree having a global center is a very difficult problem. This last problem was proposed by Conti in 1998, see his Problem 14.1 in [25], and up to now only few partial results exist for certain families of polynomial differential systems of odd degree, for more details see for instance [24, 39, 42, 59].

Our objective here is to classify the global centers of the following cubic polynomial differential systems

$$\begin{aligned} \dot{x} &= y - Cx^2 + (B + 2D)\,xy + Cy^2 + Px^3 + Gx^2y - (H + 3P)\,xy^2 + Ky^3, \\ \dot{y} &= -x + Dx^2 + (E + 2C)\,xy - Dy^2 - Kx^3 - (H + 3P)\,x^2y - Gxy^2 + Py^3. \end{aligned} \tag{1.3}$$

when they have a center at the origin of coordinates.

It was given in [64] the classification of the cubic systems (1.3) having a local center at the origin of coordinates. This classification is presented in Chapter 3 together with the proof of the main theorem.

In order to determine the global centers of the family of cubic polynomial differential systems (1.3), the dynamics of these systems near infinity play a main role. So we need the Poincaré compactification for studying these dynamics.

Roughly speaking the Poincaré compactification consists in identifying the plane $\mathfrak{t}^2$ with the interior of the unit closed disc $\mathbb{D}^2$ centered at the origin of coordinates, and the boundary of this disc, the circle $\mathbb{S}^1$, with the infinity of $\mathfrak{t}^2$. After the polynomial differential system defined in $\mathfrak{t}^2$ is extended analytically to the whole closed disc $\mathbb{D}^2$. In this way we

can study the dynamics of the polynomial differential systems in a neighbourhood of the infinity. All the details on the Poincaré compactification can be found in [6, Chapter 5].

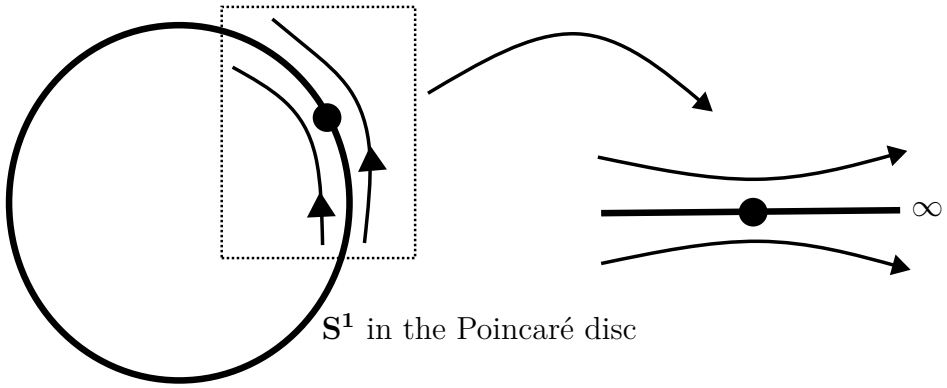

Figura 1.4: Two hyperbolic sectors. Figure made by the author.

In Figure 1.4, we have an equilibrium point on the infinity line whose local phase portrait is formed by two hyperbolic sectors, whose two separatrices are contained in the infinity line.

We note that in order to the origin of a polynomial differential system be a global center, this system either does not have equilibrium points at infinity in the Poincaré compactification, or the local phase portraits of all its infinite equilibrium points are formed by two hyperbolic sectors having their two separatrices at infinity, see Figure 1.4 (the notion of infinite equilibrium points will be clear in the subsection that explains the Poincaré compactification). This implies that the Jacobian matrix at any infinite equilibrium point of the system must be identically zero, otherwise the infinite equilibrium point would be either hyperbolic, or semi-hyperbolic, or nilpotent, and it is known that the local phase portraits of such kind of equilibrium points are not formed by two hyperbolic sectors having their two separatrices contained at infinity and this argumentation can be justified through the three theorems enunciated below. For details of the proofs, see Chapters (2) and (3) of [6].

Theorem 6. *Let* $(0,0)$ *be an isolated singular point of a vector field* X*, given by*

$$\begin{aligned} \dot{x} &= ax + by + W(x,y), \\ \dot{y} &= cx + dy + Z(x,y), \end{aligned} \tag{1.4}$$

where W *and* Z *are analytic in a neighborhood of the origin with* $W(0,0) = Z(0,0) = DW(0,0) = DZ(0,0) = 0$*. Let* λ_1 *and* λ_2 *be the eigenvalues of the linear part of* $DX(0)$ *of the system at the origin. Then the following statements hold.*

(i) If λ_1 *and* λ_2 *are real and* $\lambda_1\lambda_2 < 0$*, then* $(0,0)$ *is a saddle (see Figure 1.5(a)). If we denote by* E_1 *and* E_2 *the eigenspaces of respectively* λ_1 *and* λ_2*, then one can find two invariant analytic curves, tangent respectively to* E_1 *and* E_2 *at* 0*, on one of which points are attracted towards the origin, and on one of which points are repelled away from the origin. On these invariant curves* X *is* C^ω*-linearizable, i.e., linearizable through an analytical change of variables. There exists a* C^∞ *coordinate change transforming* (1.4) *into one of the following normal forms:*

$$\begin{aligned} \dot{x} &= \lambda_1 x, \\ \dot{y} &= \lambda_2 y, \end{aligned}$$

in the case $\dfrac{\lambda_2}{\lambda_1} \in \mathbb{R} \setminus \mathbb{Q}$, *and*

$$\begin{aligned} \dot{x} &= x\left(\lambda_1 + f\left(x^k y^l\right)\right), \\ \dot{y} &= y\left(\lambda_2 + g\left(x^k y^l\right)\right), \end{aligned}$$

in the case $\dfrac{\lambda_2}{\lambda_1} = -\dfrac{k}{l} \in \mathbb{Q}$, *with* $k, l \in \mathbb{N}$ *and where* f *and* g *are* C^∞ *functions. All systems* (1.4) *are* C^0*-conjugate to*

$$\begin{aligned} \dot{x} &= x, \\ \dot{y} &= -y. \end{aligned}$$

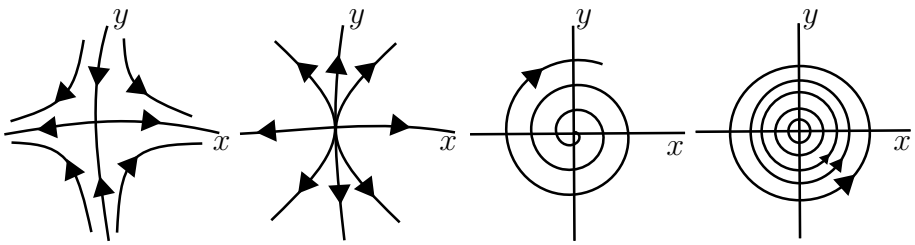

(a) (b) (c) (d)

Figura 1.5: Phase portraits of non-degenerate singular points. Figure made by the author.

(ii) If λ_1 *and* λ_2 *are real with* $|\lambda_2| \geq |\lambda_1|$ *and* $\lambda_1\lambda_2 > 0$, *then* $(0,0)$ *is a node (see Figure 1.5(b)). If* $\lambda_1 > 0$ *(respectively <0) then it is repelling or unstable (respectively attracting or stable). There exists a* C^∞ *coordinate change transforming* (1.4) *into*

$$\begin{aligned} \dot{x} &= \lambda_1 x, \\ \dot{y} &= \lambda_2 y, \end{aligned}$$

in case $\dfrac{\lambda_2}{\lambda_1} \neq \mathbb{N}$, *and into*

$$\begin{aligned} \dot{x} &= \lambda_1 x, \\ \dot{y} &= \lambda_2 y + \delta x^m, \end{aligned}$$

for some $\delta = 0$ *or* 1, *in case* $\lambda_2 = m\lambda_1$ *with* $m \in \mathbb{N}$ *and* $m \geq 1$. *All systems* (1.4) *are* C^0*-conjugate to*

$$\begin{aligned} \dot{x} &= \delta x, \\ \dot{y} &= \delta y, \end{aligned}$$

with $\delta \pm 1$ *and* $\lambda_1\delta > 0$.

(iii) If $\lambda_1 = \alpha + i\beta$ *and* $\lambda_2 = \alpha - i\beta$ *with* $\alpha,\ \beta \neq 0$, *then* $(0,0)$ *is a strong focus (see Figure 1.5(c)) into*

$$\begin{aligned} \dot{x} &= \alpha x + \beta y, \\ \dot{y} &= -\beta x + \alpha y. \end{aligned}$$

All systems (1.4) *are* C^0 *conjugate to*

$$\begin{aligned} \dot{x} &= \delta x, \\ \dot{y} &= \delta y, \end{aligned}$$

with $\delta = \pm 1$ *and* $\alpha\delta > 0$.

(iv) If $\lambda_1 = i\beta$ and $\lambda_2 = -i\beta$ with $\beta \neq 0$, then $(0,0)$ is a linear center, topologically, a weak focus or a center (see Figure 1.5(c) and (d)).

Theorem 7. *Let $(0,0)$ be an isolated singular point of the vector field X given by*

$$\begin{aligned} \dot{x} &= W(x,y), \\ \dot{y} &= \lambda y + Z(x,y), \end{aligned} \tag{1.5}$$

where W and Z are analytic in a neighborhood of the origin with $W(0,0) = Z(0,0) = DW(0,0) = DZ(0,0) = 0$ and $\lambda > 0$. Let $y = f(x)$ be the solution of the equation $\lambda y + Z(x,y) = 0$ in a neighborhood of the point $(0,0)$, and suppose that the function $g(x) = W(x, f(x))$ has the expression $g(x) = a_m x^m + o(x^m)$, where $m \geq 2$ and $a_m \neq 0$. Then there always exists an invariant analytic curve, called the strong unstable manifold, tangent at 0 to the y-axis, on which X is analytically conjugate to

$$\dot{y} = \lambda y;$$

it represents repelling behavior since $\lambda > 0$. Moreover the following statements hold.

(i) If m is odd and $a_m < 0$, then $(0,0)$ is a topological saddle (see Figure 1.6(a)). Tangent to the x-axis there is a unique invariant C^∞ curve, called the center manifold, on which X is C^∞ conjugate to

$$\dot{x} = -x^m \left(1 + a x^{m-1}\right), \tag{1.6}$$

for some $a \in \mathbb{R}$. If this invariant curve is analytic, then on it X is C^ω-conjugate to (1.6), i.e, conjugate through an analytic change of coordinates.

System X is C^∞-conjugate to

$$\begin{aligned} \dot{x} &= -x^m (1 + a x^{m-1}), \\ \dot{y} &= \lambda y, \end{aligned}$$

and is C^0-conjugate to

$$\begin{aligned} \dot{x} &= -x, \\ \dot{y} &= y. \end{aligned}$$

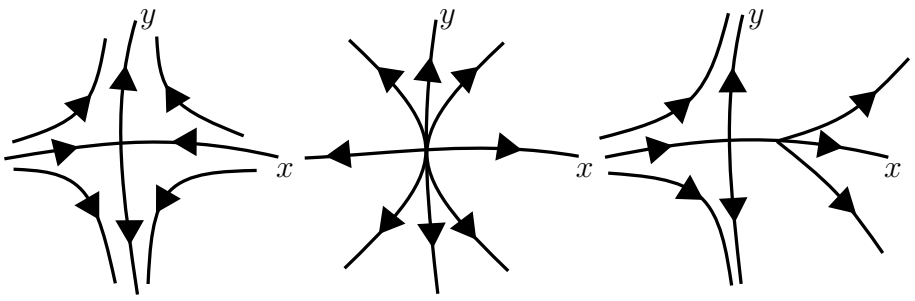

(a) (b) (c)

Figura 1.6: Phase portraits of semi-hyperbolic singular points. Figure made by the author.

(ii) If m is odd and $a_m > 0$, then $(0,0)$ is an unstable topological node (see Figure 1.6(b)). Every point not belonging to the strong unstable manifold lies on an invariant C^∞ curve, called a center manifold, tangent to the x-axis at the origin, and on which X is C^∞-conjugate to

$$\dot{x} = x^m \left(1 + ax^{m-1}\right), \tag{1.7}$$

for some $a \in \mathbb{R}$. All these center manifolds are mutually infinitely tangent to each other, and hence at most one of them can be analytic, in which system X is C^∞-conjugate to

$$\begin{aligned} \dot{x} &= x^m \left(1 + ax^{m-1}\right), \\ \dot{y} &= \lambda y, \end{aligned}$$

and is C^0-conjugate to

$$\begin{aligned} \dot{x} &= x, \\ \dot{y} &= y. \end{aligned}$$

(iii) If m is even, then $(0,0)$ is a saddle-node, that is, a singular point whose neighborhood is the union of one parabolic and two hyperbolic sectors (see Figure 1.6(c)). Modulo changing x into $-x$, we suppose that $a_m > 0$. Every point to the right of the strong unstable manifold (side $x > 0$) lies on a invariant C^∞-curve, called a center manifold, tangent to the x-axis at the origin, and on which X is C^∞-conjugate to

$$\dot{x} = x^m \left(1 + ax^{m-1}\right), \tag{1.8}$$

for some $a \in \mathbb{R}$. All these center manifolds coincide on the side $x \leq 0$ and are hence infinitely tangent at the origin. At most one of these center manifolds can be analytic, in which case X is C^ω-conjugate on it to (1.8). System X is C^∞-conjugate to

$$\begin{aligned} \dot{x} &= x^m \left(1 + ax^{m-1}\right), \\ \dot{y} &= \lambda y, \end{aligned}$$

and is C^0-conjugate to

$$\begin{aligned} \dot{x} &= x^2, \\ \dot{y} &= y. \end{aligned}$$

Definition 5. *A jet is a kind of operation that transforms a differential function f into a truncated Taylor polynomial in each point of the function domain. The jet of order k is a truncated Taylor polynomial around a determined point of order k.*

Theorem 8. *Let $(0,0)$ be an isolated singular point of the vector field X given by*

$$\begin{aligned} \dot{x} &= y + W(x,y), \\ \dot{y} &= Z(x,y), \end{aligned}$$

where W and Z are analytic in a neighborhood of the point $(0,0)$ and also $j_1 W(0,0) = j_1 Z(0,0) = 0$, where j_1 represents the jet of order one. Let $y = f(x)$ be the solution of the equation $y + W(x,y) = 0$ in a neighborhood of the point $(0,0)$, and consider $F(x) = Z(x, f(x))$ and $G(x) = \left(\dfrac{\partial W}{\partial x} + \dfrac{\partial Z}{\partial y}\right)(x, f(x))$. Then the following holds:

(1) If $F(x) \equiv G(x) \equiv 0$, then the phase portrait of X is given by (1.7)(a).

(2) If $F(x) \equiv 0$ and $G(x) = bx^n + o(x^n)$ for $n \in \mathbb{N}$ with $n \geq 1$ and $b \neq 0$, then the phase portrait of X is given by Figure 1.7(b) or (c).

(3) If $G(x) \equiv 0$ *and* $F(x) = ax^m + o(x^m)$ *for* $m \in \mathbb{N}$ *with* $m \geq 1$ *and* $a \neq 0$*, then*

(i) If m *is odd and* $a > 0$*, then the origin of* X *is a saddle (see Figure 1.7(d)) and if* $a < 0$*, then it is a center or a focus (see Figure 1.7(e)-(g));*

(ii) If m *is even then the origin of* X *is a cusp as in Figure 1.7(h).*

(4) If $F(x) = x^m + o(x^m)$ *and* $G(x) = bx^n + o(x^n)$ *with* $m \in \mathbb{N}$*,* $m \geq 2$*,* $n \in \mathbb{N}$*,* $n \geq 1$*,* $a \neq 0$ *and* $b \neq 0$*, then we have*

(i) If m *is even, and*

(i1) $m < 2n + 1$*, then the origin of* X *is a cusp as in Figure 1.7(h);*

(i2) $m > 2n + 1$*, then the origin of* X *is a saddle-node as in Figure 1.7(i) or (j);*

(ii) If m *is odd and* $a > 0$ *then the origin of* X *is a saddle as in Figure 1.7(d);*

(iii) If m *is odd,* $a < 0$ *and*

(iii.1) Either $m < 2n+1$*, or* $m = 2n+1$ *and* $b^2 + 4a(n+1) < 0$*, then the origin of* X *is a center or a focus (see Figure 1.7(e)-(g));*

(iii.2) n *is odd and either* $m > 2n + 1$*, or* $m = 2n + 1$ *and* $b^2 + 4a(n+1) \geq 0$ *then the phase portrait of the origin of* X *consists of one hyperbolic and one elliptic sector as in Figure 1.7(k);*

(iii.3) n *is even and either* $m > 2n+1$*, or* $m = 2n+1$ *and* $b^2+4a(n+1) \geq 0$*, then the origin of* X *is a node as in Figure 1.7(l), (m). The node is attracting if* $b < 0$ *and repelling if* $b > 0$*.*

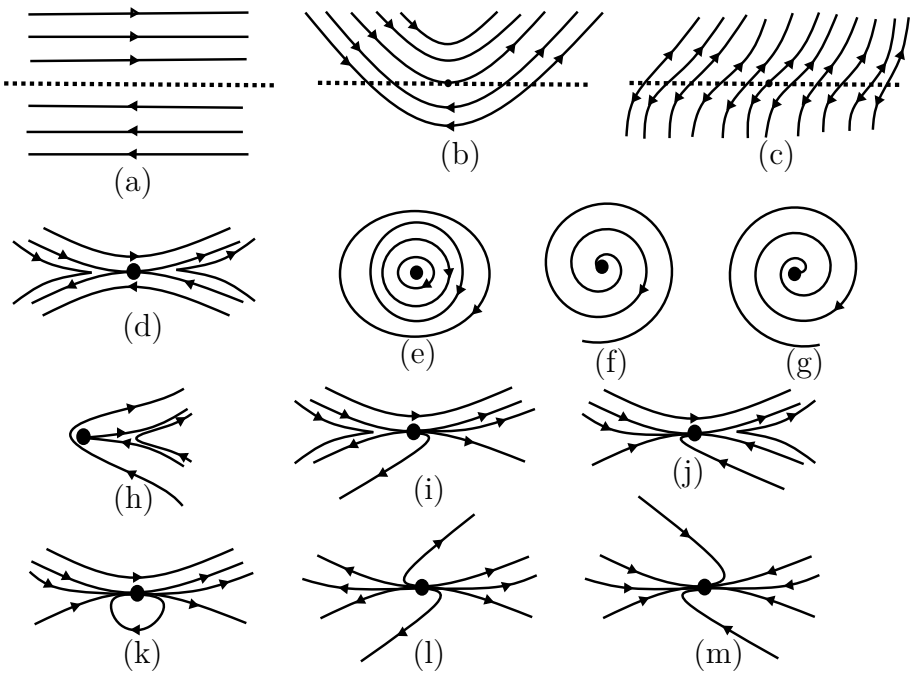

Figura 1.7: Phase portraits of nilpotent singular points. Figure made by the author.

Our main theorem is enunciated and proved in Chapter 3. It tells about the parameters values conditions to obtain global centers in the equilibrium point at the origin from the result obtained in [64], which is also enunciated in Chapter 3.

Now we present some useful notions and results that we need for proving Theorem 13 in Chapter 3.

1.2.1 Equilibrium Points

A point (x_0, y_0) is an equilibrium of the differential system (1.2) if $P(x_0, y_0) = Q(x_0, y_0) = 0$. The equilibrium (x_0, y_0) is *hyperbolic* if all eigenvalues of the Jacobian matrix of the differential system evaluated at (x_0, y_0) have real part different from zero, and it is *semi-hyperbolic* if the Jacobian matrix presents only one eigenvalue equal to zero.

The classification of the local phase portraits of the hyperbolic and semi-hyperbolic equilibria can be found in Theorems 2.15 and 2.19 of [6], respectively, enunciated here in Theorems 6 and 7. In this work when appears concepts related to local phase portraits of hyperbolic or semi-hyperbolic equilibrium points, we will be using implicitly these two theorems. But when the Jacobian matrix evaluated at an equilibrium point is identically zero, the local phase portrait at this equilibrium point must be analysed through special changes of variables called blow up's (for more details on the blow up method, see for instance [2] and [6]).

1.2.2 Vertical Blow Up

Consider a real planar polynomial differential system given by

$$\dot{x} = P(x, y) = P_n(x, y) + \ldots, \quad \dot{y} = Q(x, y) = Q_n(x, y) + \ldots, \tag{1.9}$$

with P and Q being coprime polynomials, P_n and Q_n being homogeneous polynomials of degree $n \in \mathbb{N}$ and the dots representing higher order terms in x and y. We are assuming that the origin is a singular point, since $n > 0$. Taking polar coordinates $(x, y) \mapsto (r, \theta)$, system (1.9) becomes

$$\dot{r} = \mathcal{R}(\theta) r + \ldots, \qquad \dot{\theta} = \mathcal{F}(\theta) + \ldots, \tag{1.10}$$

where $\mathcal{R}$ and $\mathcal{F}$ are polynomials in $\cos(\theta)$ and $\sin(\theta)$ and the dots means higher order terms in r. If $\mathcal{F} \not\equiv 0$ we say that the origin is a non-discritical singular point. In this case, all the solution curves tending to the origin in forward or backward time are tangent to the solutions $\theta^* \in (0, 2\pi)$ of the equation $\mathcal{F}(\theta) = 0$. We call $\mathcal{F}$ the characteristic polynomial of (1.9) at the origin and θ^* a *characteristic direction*. In cartesian coordinates $\mathcal{F}$ writes as

$$\mathcal{F}(x, y) = xQ_n(x, y) - yP_n(x, y). \tag{1.11}$$

If $\mathcal{F} \equiv 0$ the origin is a discritical singular point. In this case we deduce from (1.11) that $P_n = xW_{n-1}$ and $Q_n = yW_{n-1}$, where $W_{n-1} \not\equiv 0$ is a homogeneous polynomial of degree $n - 1$. If $y - vx$ is a factor of W_{n-1} and $v = \tan(\theta^*)$, $\theta^* \in [0, 2\pi)$, then θ^* is a singular direction.

The homogeneous polar blow up is the mapping $(r, \theta) \mapsto (r\cos(\theta), r\sin(\theta)) = (x, y)$, with $r \in \mathbb{R}$ and $\theta \in (0, 2\pi)$. This map transforms the origin of system (1.9) into the circle $r = 0$, which is called the exceptional divisor. After the polar blow up and after cancelling

an appearing common factor r^{m-1}, system (1.9) becomes system (1.10). If $\mathcal{F} \equiv 0$ then this common factor is r^m.

It is known that the orbits starting or ending at the origin start or end tangent to the straight lines given by the characteristic directions. For more details on the characteristic directions, see for instance [4].

Suppose that we have an equilibrium point at the origin of coordinates, as in the differential system (1.9) and that this equilibrium is linearly zero. Then for studying its local phase portrait we do vertical blow up's.

We define the vertical blow up in the y direction as the change of variables $(u, v) = (x, y/x)$. This change transforms the origin of system (1.9) in the straight line $u = 0$ and analyzing the dynamics of the differential system in a neighbourhood of this straight line we are analyzing the local phase portrait of the equilibrium point at the origin of system (1.9). But before doing a vertical blow up, in order that we do not lose information, we must avoid that the direction $x = 0$ be a characteristic direction of the origin of system (1.9). If $x = 0$ is a characteristic direction we do a convenient twist $(x, y) = (u, u + \alpha v)$ with $\alpha \neq 0$ in order that the new vertical straigh line $u = 0$ are not a characteristic direction.

1.2.3 The Poincaré Compactification

Let $X = (P, Q)$ be a planar polynomial vector field of degree n. The Poincaré compactified system $p(X)$ is an analytic vector field on the 2-dimensional sphere $\mathbb{S}^2$.

Initially we identify the plane $\mathbb{R}^2$ with the plane $y_3 = 1$ of $\mathbb{R}^3$, and define the Poincaré sphere $\mathbb{S}^2 = \{(y_1, y_2, y_3) \in \mathbb{R}^3; y_1^2 + y_2^2 + y_3^2 = 1\}$. We consider the northern hemisphere $H_+ = (y \in \mathbb{S}^2 : y_3 > 0\}$, the southern hemisphere $H_- = \{y \in \mathbb{S}^2 : y_3 < 0\}$ and the equator $\mathbb{S}^1 = \{y \in \mathbb{S}^2; y_3 = 0\}$ of the sphere $\mathbb{S}^2$.

The projections of the plane $y_3 = 1$ on the sphere $\mathbb{S}^2$ are defined as $f_\pm : \mathbb{R}^2 \longrightarrow H_\pm$, $f_\pm(y_1, y_2, 1) = (y_1^2 + y_2^2 + 1)^{-1/2}(y_1, y_2, 1)$. These two diffeomorphisms establish two copies of the vector field X, one X_+ in H_+ and another X_- in H_-. Then we have the vector field $X' = X_+ \cup X_-$ defined in $\mathbb{S}^2 \backslash \mathbb{S}^1$ and the infinity of the plane $y_3 = 1$, i.e., $\mathbb{R}^2$ is identified with the equator $\mathbb{S}^1$.

The *Poincaré compactified vector field* $p(X)$ is the analytic extension of X' from $H_+ \cup H_-$ to $\mathbb{S}^2$ doing $p(X) = y_3^{n-1} X'$, and the *Poincaré disc* $\mathbb{D}$ is obtained by the projection of the closed northern hemisphere on $y_3 = 0$ under the projection $(y_1, y_2, y_3) \mapsto (y_1, y_2)$. The dynamics presented by the vector field $p(X)$ near $\mathbb{S}^1$ is the dynamics near the infinity of the vector field X.

We can define local charts $\phi_i : U_i \longrightarrow \mathbb{R}^2$ and $\psi_i : V_i \longrightarrow \mathbb{R}^2$ by $\phi_i(y_1, y_2, y_3) = \psi_i(y_1, y_2, y_3) = (y_a/y_i, y_b/y_i) = (u, v)$, with $a \neq i$, $b \neq i$ and $a < b$. The expression of the vector field $p(X)$ in the chart U_1 is

$$\dot{u} = v^n \left(Q\left(\frac{1}{v}, \frac{u}{v}\right) - uP\left(\frac{1}{v}, \frac{u}{v}\right)\right), \quad \dot{v} = -v^{n+1} P\left(\frac{1}{v}, \frac{u}{v}\right),$$

and in the chart U_2 is

$$\dot{u} = v^n \left(P\left(\frac{u}{v}, \frac{1}{v}\right) - uQ\left(\frac{u}{v}, \frac{1}{v}\right)\right), \quad \dot{v} = -v^{n+1} Q\left(\frac{u}{v}, \frac{1}{v}\right).$$

The expressions of $p(X)$ on the charts V_1 and V_2 are the same than in the charts U_1 and U_2 but multiplied by $(-1)^{n-1}$, respectively. In the charts U_i and V_i for $i = 1, 2$ the

points of the infinity are of the form $(u, 0)$. The infinity $\mathbb{S}^1$ is invariant under the flow of $p(X)$. For more details in Poincaré compactification see [6, Chapter 5].

The equilibrium points of the vector field X are called *finite* equilibrium points of X or of $p(X)$, while the equilibrium points of the vector field $p(X)$ in $\mathbb{S}^1$ are called *infinite* equilibrium points of X or of $p(X)$.

1.2.4 Characterization of the Global Centers

Due to all that was explained in section 1.2, we arrive at the following two propositions.

Proposition 9. *Assume that a planar polynomial differential system has a global center and has infinite equilibrium points. Then the local phase portraits of these equilibria must be formed by two hyperbolic sectors, and consequently, having their two separatrices contained in the circle of the infinity. Moreover, the Jacobian matrix at these infinite equilibria must be identically zero.*

The next result characterizes when a polynomial differential system in $\mathbb{R}^2$ has a global center. For a proof, see Theorem 1.2 of [42].

Proposition 10. *A polynomial differential system* (1.2) *with finitely many infinite equilibria has a global center if and only if it has a unique finite singular point which is a center and all the infinite equilibria have their local phase portraits formed by two hyperbolic sectors.*

2 Limit Cycles for a Class of Discontinuous Piecewise Differential Systems

In this chapter we prove the Theorems 2, 3, 4 and 5 by the use of the first integrals of the isochronous centers and the first integral of the linear center. Furthermore, we provide some numeric examples related to these theorems exhibiting limit cycles.

2.1 Proof of Theorem 2

Now we prove the Theorem 2 through a initial linear change of variables and the application of the closing equation, that uses the first integrals from the isochronous centers from Theorem 1.

After doing the following arbitrary linear change of coordinates $x = a_1x + b_1y$, $y = \alpha_1x + \beta_1y$ with $a_1\beta_1 - b_1\alpha_1 \neq 0$, the isochronous center X_1 becomes

$$\begin{aligned}
\dot{x} = & -x^3\left(-a_1+\alpha_1\right)\left(a_1+\alpha_1\right)+2x^2y\left(a_1b_1-\alpha_1\beta_1\right)+\frac{y\left(b_1^2+\beta_1^2\right)}{b_1\alpha_1-a_1\beta_1} \\
& +x\left(y^2\left(b_1-\beta_1\right)\left(b_1+\beta_1\right)+\frac{a_1b_1+\alpha_1\beta_1}{b_1\alpha_1-a_1\beta_1}\right), \\
\dot{y} = & -x^2y\left(-a_1+\alpha_1\right)\left(a_1+\alpha_1\right)+y^3\left(b_1-\beta_1\right)\left(b_1+\beta_1\right)-\frac{y\left(a_1b_1+\alpha_1\beta_1\right)}{b_1\alpha_1-a_1\beta_1} \\
& +x\left(\frac{a_1^2+\alpha_1^2}{-b_1\alpha_1+a_1\beta_1}+2y^2\left(a_1b_1-\alpha_1\beta_1\right)\right).
\end{aligned}$$

The corresponding first integral of this differential system is

$$H_1\left(x,y\right)=\frac{\left(a_1x+b_1y\right)^2+\left(x\alpha_1+y\beta_1\right)^2}{1+2\left(a_1x+b_1y\right)\left(x\alpha_1+y\beta_1\right)}.$$

Proof of statement (a) *of Theorem* 2. We analize the presence or not of limit cycles that intersect the discontinuity curve R in the two points $(x,0)$ and $(0,y)$, with x and y positives. These two points must satisfy the following two equations

$$\begin{aligned}
E_1 &= H\left(x,0\right)-H\left(0,y\right)=0, \\
E_2 &= H_1\left(x,0\right)-H_1\left(0,y\right)=0,
\end{aligned}$$

or equivalently

$$E_1 = d^2x^2 - a^2y^2 - w^2y^2 = 0,$$
$$E_2 = \frac{A}{(1+2a_1x^2\alpha_1)\left(1+\dfrac{2b_1d^2x^2\beta_1}{a^2+\omega^2}\right)} = 0,$$

that we must solve. We must assure that the denominator in E_2 never will be zero, i.e., $(1+2a_1x^2\alpha_1)\left(1+\dfrac{2b_1d^2x^2\beta_1}{a^2+\omega^2}\right) \neq 0$ and A represents

$$\begin{aligned} A = \; & x^4\left(-\frac{2a_1b_1^2d^2\alpha_1}{a^2+\omega^2} + \frac{2a_1^2b_1d^2\beta_1}{a^2+\omega^2} + \frac{2b_1d^2\alpha_1^2\beta_1}{a^2+\omega^2} - \frac{2a_1d^2\alpha_1\beta_1^2}{a^2+\omega^2}\right) \\ & + x^2\left(a_1^2+\alpha_1^2 - \frac{b_1^2d^2}{a^2+\omega^2} - \frac{d^2\beta_1^2}{a^2+\omega^2}\right). \end{aligned}$$

From all the solutions x and y of system $E_1 = E_2 = 0$, only one satisfies $x > 0$ and $y > 0$, namely

$$(x,0) = \left(\sqrt{\frac{-a^2a_1^2 + b_1^2d^2 - a_1^2w^2 - a^2\alpha_1^2 - w^2\alpha_1^2 + d^2\beta_1^2}{2\left(-a_1b_1^2d^2\alpha_1 + a_1^2b_1d^2\beta_1 + b_1d^2\alpha_1^2\beta_1 - a_1d^2\alpha_1\beta_1^2\right)}}, 0\right)$$

and

$$(0,y) = \left(0, d\sqrt{\frac{-a^2a_1^2 + b_1^2d^2 - a_1^2w^2 - a^2\alpha_1^2 - w^2\alpha_1^2 + d^2\beta_1^2}{2\left(a^2+\omega^2\right)\left(-a_1b_1^2d^2\alpha_1 + a_1^2b_1d^2\beta_1 + b_1d^2\alpha_1^2\beta_1 - a_1d^2\alpha_1\beta_1^2\right)}}\right),$$

when x and y are real.

In section 2.5, we provide a discontinuous piecewise differential system under the assumptions of statement (a) of Theorem 2 having one limit cycle. So this upper bound is reached. ■

Now we supply the proofs related to the item (b), beginning by the case 2 and finishing by the case 3.

Proof of statement (b) of Theorem 2. **Case 2:** We analize the presence of limit cycles that intersect the discontinuity curve R at the points $(x_1,0)$, $(x_2,0)$, $(0,y_1)$ and $(0,y_2)$ with $0 < x_1 < x_2$ and $0 < y_1 < y_2$, i.e., limit cycles that have two intersection crossing points with R_x and R_y.

Since we are in Case 2, the linear differential center is located in region R_1 and the first isochronous center is located in the region R_2. The study of the existence or not of limit cycles is based on a system with four equations and the four unknowns x_1, x_2, y_1 and y_2, obtained using the first integrals H and H_1, i.e.,

$$\begin{aligned} F_1 &= H(x_1,0) - H(0,y_1) = 0, \\ F_2 &= H_1(0,y_1) - H_1(0,y_2) = 0, \\ F_3 &= H(0,y_2) - H(x_2,0) = 0, \\ F_4 &= H_1(x_2,0) - H_1(x_1,0) = 0. \end{aligned}$$

Since

$$F_2 = \frac{(y_1-y_2)(y_1+y_2)(b_1^2+\beta_1^2)}{(1+2b_1y_1^2\beta_1)(1+2b_1y_2^2\beta_1)},$$

it is zero if and only if $y_1 = y_2$ or $y_1 = -y_2$, because $b_1^2 + \beta_1^2 \neq 0$ due to the fact that $a_1\beta_1 - b_1\alpha_1 \neq 0$, and these solutions cannot satisfy $0 < y_1 < y_2$. So we do not have any limit cycles in Case 2.

Case 3: In this case the discontinuous piecewise differential system is the same than in the previous case, with the exception that the positions of the linear center and the cubic isochronous center involved are inverted, i.e., the differential linear center is located in the region R_2 and the first isochronous center is located in the region R_1. Therefore, we consider the system of four equations and four unknowns

$$\begin{aligned} G_1 &= H_1(x_1, 0) - H_1(0, y_1) = 0, \\ G_2 &= H(0, y_1) - H(0, y_2) = 0, \\ G_3 &= H_1(0, y_2) - H_1(x_2, 0) = 0, \\ G_4 &= H(x_2, 0) - H(x_1, 0) = 0. \end{aligned}$$

Since

$$G_2 = \left(a^2 + w^2\right)(y_1 - y_2)(y_1 + y_2) = 0,$$

we have $y_1 = y_2$ or $y_1 = -y_2$, which prevents the existence of limit cycles in this case. ■

In summary, the proof of Theorem 2 is done.

2.2 Proof of Theorem 3

Now we prove (3) through a initial linear change of variables and the application of the closing equation, that uses the first integrals from the isochronous centers from Theorem (1).

After the following linear change of coordinates $x = a_1x + b_1y$, $y = \alpha_1x + \beta_1y$ with $a_1\beta_1 - b_1\alpha_1 \neq 0$, the transformed isochronous center X_2 is

$$\begin{aligned} \dot{x} = \; & \frac{-1}{b_1\alpha_1 - a_1\beta_1}\left(x^3\left(b_1\alpha_1^3 - 3a_1^2b_1\alpha_1 + a_1^3\beta_1 - 3a_1\alpha_1^2\beta_1\right) - y\left(b_1^2 + \beta_1^2\right) + 6a_1x^2y\alpha_1\right. \\ & \left.\left(b_1^2 + \beta_1^2\right) + 2b_1y^3\beta_1\left(b_1^2 + \beta_1^2\right) - x\left(a_1b_1 + \alpha_1\beta_1 + 3y^2\left(b_1\alpha_1 + a_1\beta_1\right)\left(b_1^2 + \beta_1^2\right)\right)\right), \\ \dot{y} = \; & \frac{-1}{b_1\alpha_1 - a_1\beta_1}\left(2a_1x^3\alpha_1\left(a_1^2 + \alpha_1^2\right) + 3x^2y\left(a_1^2 + \beta_1^2\right)\left(b_1\alpha_1 + a_1\beta_1\right) + y\left(a_1b_1 + \alpha_1\beta_1\right)\right. \\ & \left.+y^3\left(b_1^3\alpha_1 - 3a_1b_1^2\beta_1 - 3b_1\alpha_1\beta_1^2 + a_1\beta_1^3\right) - x\left(a_1^2 + \alpha_1^2 + 6b_1y^2\left(a_1^2 + \alpha_1^2\right)\beta_1\right)\right). \end{aligned}$$

The corresponding first integral for this vector field is:

$$H_2(x, y) = \frac{\left(\left(a_1x + b_1y\right)^2 + \left(x\alpha_1 + y\beta_1\right)^2\right)^2}{1 + 4\left(a_1x + b_1y\right)\left(x\alpha_1 + y\beta_1\right)}.$$

Proof of statement (a) *of Theorem* 3. We analize the presence or not of limit cycles that intersect the discontinuity curve R in two points: $(x, 0)$ and $(0, y)$ with x and y positives. Then we have the system

$$\begin{aligned} I_1 &= H(x, 0) - H(0, y) = 0, \\ I_2 &= H_2(x, 0) - H_2(0, y) = 0, \end{aligned}$$

of two equations and two unknowns x and y to solve:

$$I_1 = d^2x^2 - a^2y^2 - \omega^2y^2 = 0,$$
$$I_2 = \frac{B}{(1+4a_1x^2\alpha_1)(1+4b_1y^2\beta_1)} = 0,$$

where

$$\begin{aligned} B = \; & a_1^4x^4 - b_1^4y^4 - 4a_1b_1^4x^2y^4\alpha_1 + 2a_1^2x^4\alpha_1^2 + x^4\alpha_1^4 + 4a_1^4b_1x^4y^2\beta_1 - 2b_1^2y^4\beta_1^2 + \\ & 8a_1^2b_1x^4y^2\alpha_1^2\beta_1 + 4b_1x^4y^2\alpha_1^4\beta_1 - 8a_1b_1^2x^2y^4\alpha_1\beta_1^2 - y^4\beta_1^4 - 4a_1x^2y^4\alpha_1\beta_1^4. \end{aligned}$$

We must assure that $(1+4a_1x^2\alpha_1)(1+4b_1y^2\beta_1) \neq 0$. From all the solutions found for this system, only one satisfies $x > 0$ and $y > 0$ and therefore we have at most one limit cycle in this case passing through the points

$$(x,0) = \left(\frac{1}{2}\sqrt{\frac{r}{s}}, 0\right) \text{ and } (0,y) = \left(0, \frac{d}{2}\sqrt{\frac{r}{(a^2+\omega^2)\,s}}\right),$$

if they are real, where $r = -a^4a_1^4 + b_1^4d^4 - 2a^2a_1^4\omega^2 - a_1^4\omega^4 - 2a^4a_1^2\alpha_1^2 - 4a^2a_1^2\omega^2\alpha_1^2 - 2a_1^2\omega^4\alpha_1^2 - a^4\alpha_1^4 - 2a^2\omega^2\alpha_1^4 - \omega^4\alpha_1^4 + 2b_1^2d^4\beta_1^2 + d^4\beta_1^4$ and $s = -a_1b_1^4d^4\alpha_1 + a^2a_1^4b_1d^2\beta_1 + a_1^4b_1d^2\omega^2\beta_1 + 2a^2a_1^2b_1d^2\alpha_1^2\beta_1 + 2a_1^2b_1d^2\omega^2\alpha_1^2\beta_1 + a^2b_1d^2\alpha_1^4\beta_1 + b_1d^2\omega^2\alpha_1^4\beta_1 - 2a_1b_1^2d^4\alpha_1\beta_1^2 - a_1d^4\alpha_1\beta_1^4$.

In section 2.5 we provide a discontinuous piecewise differential system under the assumptions of statement (a) of Theorem 3, having one limit cycle. So, this upper bound is reached. ■

Now we supply the proofs for the cases 2 and 3 related to the item (b) of Theorem (3).

Proof of statement (*b*) *of Theorem* 3. **Case 2:** We analize the presence of limit cycles that intersect the discontinuity curve R at the points $(x_1,0)$, $(x_2,0)$, $(0,y_1)$ and $(0,y_2)$ satisfying $0 < x_1 < x_2$ and $0 < y_1 < y_2$. First we consider that the linear differential center is located in the region R_1 and the second isochronous center is located in the region R_2. Again the study of the existence or not of limit cycles is based on the following system of four equations and four unknowns x_1, x_2, y_1 and y_2 obtained using the first integrals H and H_2

$$\begin{aligned} J_1 &= H(x_1,0) - H(0,y_1) = 0, \\ J_2 &= H_2(0,y_1) - H_2(0,y_2) = 0, \\ J_3 &= H(0,y_2) - H(x_2,0) = 0, \\ J_4 &= H_2(x_2,0) - H_2(x_1,0) = 0, \end{aligned}$$

i.e.,

$$\begin{aligned} J_1 &= d^2x_1^2 - a^2y_1^2 - \omega^2y_1^2 = 0, \\ J_2 &= \frac{(y_1-y_2)(y_1+y_2)(y_1^2+y_2^2+4b_1y_1^2y_2^2\beta_1)(b_1^2+\beta_1^2)^2}{(1+4b_1y_1^2\beta_1)(1+4b_1y_2^2\beta_1)} = 0, \\ J_3 &= -d^2x_2^2 + a^2y_2^2 + \omega^2y_2^2 = 0, \\ J_4 &= -\frac{(x_1-x_2)(x_1+x_2)(x_1^2+x_2^2+4a_1x_1^2x_2^2\alpha_1)(a_1^2+\alpha_1^2)^2}{(1+4a_1x_1^2\alpha_1)(1+4a_1x_2^2\alpha_1)} = 0. \end{aligned} \tag{2.1}$$

Now we adopt the tool of the Gröebner basis for studying the solutions of system (2.1), i.e., we obtain a list of polynomials that have the same solutions than that of the original

system. This adoption is necessary for searching possible solutions, due to the complexity of the original system (2.1). Through the application of the Gröebner basis to the system (2.1), we have chance to get a simpler system equivalently to the system (2.1) in the sense that these two systems supply the same solutions (on the development done ahead, for example, we find an equation of the transformed system through Gröebner basis in only one variable y_2). For more details about Gröebner basis, see for instance the reference [26], chapter 2. The new equivalent polynomial system has ten equations. One of these ten equations is

$$-\left(a^2+\omega^2\right) y_2^4 \left(a^2 a_1\alpha_1 + a_1\omega^2\alpha_1 - b_1 d^2\beta_1\right) = 0.$$

Therefore, if $a^2a_1\alpha_1 + a_1\omega^2\alpha_1 - b_1d^2\beta_1 \neq 0$, then $y_2 = 0$ and the condition $0 < y_1 < y_2$ is not satisfied.

If $a^2a_1\alpha_1 + a_1\omega^2\alpha_1 - b_1d^2\beta_1 = 0$ and $\alpha_1 \neq 0$, isolating the parameter a_1, we get $a_1 = b_1d^2\beta_1/\left(a^2+\omega^2\right)^2\alpha_1$. Calculating again the Gröebner basis, we obtain the three equations

$$y_1^2 + y_2^2 + 4b_1y_1^2y_2^2\beta_1 = 0, \quad d^2x_2^2 - a^2y_2^2 - \omega^2y_2^2 = 0, \quad x_1^2 + x_2^2 + 4b_1x_2^2y_1^2\beta_1 = 0.$$

From this system we obtain only solutions that are not real and the real solution zero. Hence in this case the discontinuous piecewise differential systems have no limit cycles.

Finally, if $a^2a_1\alpha_1 + a_1\omega^2\alpha_1 - b_1d^2\beta_1 = 0$ and $\alpha_1 = 0$, the equation $J_4 = 0$ becomes

$$(x_1 - x_2)(x_1 + x_2)(x_1^2 + x_2^2)a_1^4 = 0.$$

Since $a_1 \neq 0$, otherwise $a_1\beta_1 - b_1\alpha_1 = 0$, it follows that either $x_1 = x_2$ or $x_1 = -x_2$ or $x_1 = x_2 = 0$. Hence there are no solutions satisfying that $0 < x_1 < x_2$.

In summary, in this case the discontinuous piecewise differential systems never have limit cycles.

Case 3: In this case the discontinuous piecewise differential systems are the same that of Case 2 with the exception that the positions of the linear center and the isochronous center involved are inverted. Therefore, we consider the following system

$$\begin{aligned} L_1 &= H_2(x_1, 0) - H_2(0, y_1) = 0,\\ L_2 &= H(0, y_1) - H(0, y_2) = 0,\\ L_3 &= H_2(0, y_2) - H_2(x_2, 0) = 0,\\ L_4 &= H(x_2, 0) - H(x_1, 0) = 0. \end{aligned}$$

Since $L_2 = \left(a^2+\omega^2\right)(y_1 - y_2)(y_1 + y_2) = 0$ if and only if $y_1 = y_2$ or $y_1 = -y_2$, in this case the discontinuous piecewise differential system can not have limit cycles too.

This completes the proof of Theorem 3. ■

2.3 Proof of Theorem 4

Now we prove (4) through a initial linear change of variables and the application of the closing equation, that uses the first integrals from the isochronous centers from Theorem (1).

After the following linear change of coordinates $x = a_1x + b_1y$, $y = \alpha_1x + \beta_1y$ with $a_1\beta_1 - b_1\alpha_1 \neq 0$, the isochronous center X_3 becomes

$$\begin{aligned}
\dot{x} = \; & \frac{1}{b_1\alpha_1 - a_1\beta_1}\left(a_1x^3\left(-2a_1^2b_1 + 9b_1\alpha_1^2 - 3a_1\alpha_1\beta_1\right) - 2b_1^2y^3\left(b_1^2 - 3\beta_1^2\right) + y\left(b_1^2 + \beta_1^2\right)\right. \\
& +3x^2y\left(-2a_1^2b_1^2 + 3b_1^2\alpha_1^2 + 4a_1b_1\alpha_1\beta_1 - a_1^2\beta_1^2\right) \\
& \left. +\left(a_1b_1 + \alpha_1\beta_1 - 3b_1y^2\left(2a_1b_1^2 - 5b_1\alpha_1\beta_1 - a_1\beta_1^2\right)\right)\right), \\
\dot{y} = \; & \frac{1}{b_1\alpha_1 - a_1\beta_1}\left(2a_1^2x^3\left(a_1^2 - 3\alpha_1^2\right) - 3a_1x^2y\left(-2a_1^2b_1 + b_1\alpha_1^2 + 5a_1\alpha_1\beta_1\right)\right. \\
& +x\left(-a_1^2 - \alpha_1^2 - b_1\alpha_1 + a_1\beta_1 + 3y^2\left(2a_1^2b_1^2 + b_1^2\alpha_1^2 - 4a_1b_1\alpha_1\beta_1 - 3a_1^2\beta_1^2\right)\right), \\
& \left. -y\left(a_1b_1 + \alpha_1\beta_1\right) + b_1y^3\left(2a_1b_1^2 + 3b_1\alpha_1\beta_1 - 9a_1\beta_1^2\right)\right).
\end{aligned}$$

The corresponding first integral is

$$H_3 = \frac{4 - 9\left(a_1x + b_1y\right)^2 + 27\left(x\alpha_1 + y\beta_1\right)^2}{\left(1 - 3\left(a_1x + b_1y\right)^2\right)^3}.$$

Proof of statement (a) *of Theorem* 4. We analize the presence or not of limit cycles that intersect the discontinuity curve R in two points: $(x, 0)$ and $(0, y)$. So doing

$$\begin{aligned}
M_1 &= H\left(x, 0\right) - H\left(0, y\right) = 0, \\
M_2 &= H_3\left(x, 0\right) - H_3\left(0, y\right) = 0,
\end{aligned}$$

we obtain the system

$$\begin{aligned}
M_1 = \; & d^2x^2 - \left(a^2 + \omega^2\right)y^2 = 0, \\
M_2 = \; & -\frac{27}{\left(-1 + 3a_1^2x^2\right)^3\left(-1 + 3b_1^2y^2\right)^3}\left(4a_1^4x^4 - a_1x^2 - 4a_1^6x^6 - x^2\alpha_1^2 + \right. \\
& y^2\left(b_1^2 - 9a_1^4b_1^2x^4 + 9a_1^6b_1^2x^6 + 9b_1^2x^2\alpha_1^2 + \beta_1^2 - 9a_1^2x^2\beta_1^2 + 27a_1^4x^4\beta_1^2 - 27a_1^6x^6\beta_1^2\right) \\
& \left. +y^4\left(-4b_1^4 + 9a_1^2b_1^4x^2 - 27b_1^4x^2\alpha_1^2\right) + y^6\left(4b_1^6 - 9a_1^2b_1^6x^2 + 27b_1^6x^2\alpha_1^2\right)\right) = 0.
\end{aligned}$$

We must assure that $\left(-1 + 3a_1^2x^2\right)^3\left(-1 + 3b_1^2y^2\right)^3 \neq 0$. Using the Gröebner basis, we obtain an equation that is a polynomial in the y^2 of degree three and in this polynomial does not appear the variable x. So this polynomial has at most three positive zeros for the variable y, which using the equation $M_1 = 0$ can provide at most three limit cycles having $x > 0$.

In section 2.5 we provide a discontinuous piecewise differential system under the assumptions of statement (a) of Theorem 4 having three limit cycles. So this upper bound is reached. ■

Proof of statement (b) *of Theorem* 4. We analize the presence of limit cycles that intersect the discontinuity curve R at the points $(x_1, 0)$, $(x_2, 0)$, $(0, y_1)$, $(0, y_2)$, with $0 < x_1 < x_2$ and $0 < y_1 < y_2$. The coordinates of these four points must satisfy the equations

$$\begin{aligned}
N_1 &= H\left(x_1, 0\right) - H\left(0, y_1\right) = 0, \\
N_2 &= H_3\left(0, y_1\right) - H_3\left(0, y_2\right) = 0, \\
N_3 &= H\left(0, y_2\right) - H\left(x_2, 0\right) = 0, \\
N_4 &= H_3\left(x_2, 0\right) - H_3\left(x_1, 0\right) = 0.
\end{aligned} \tag{2.2}$$

For the two pieces N_1 and N_3 contained in the positive quadrant R_1 forming a limit cycle belonged to the linear center X_c, located at the origin of coordinates, we have that these pieces must travell in the same sense, either counterclockwise or clockwise. So such a possible limit cycle does not exist. ■

Proof of statement (c) *of Theorem* 4. Now the discontinuous piecewise differential systems are the same of the ones of statement (b), with the difference that the position of the two vector fields involved is inverted. Here the system that we must solve is

$$\begin{aligned} P_1 &= H_3(x_1,0) - H_3(0,y_1) = 0,\\ P_2 &= H(0,y_1) - H(0,y_2) = 0,\\ P_3 &= H_3(0,y_2) - H_3(x_2,0) = 0,\\ P_4 &= H(x_2,0) - H(x_1,0) = 0. \end{aligned}$$

Since

$$P_2 = \left(a^2+\omega^2\right)(y_1-y_2)(y_1+y_2) = 0,$$

we get that $y_1 = y_2$ or $y_1 = -y_2$, so the condition $0 < y_1 < y_2$ is not satisfied. This completes the proof of the theorem. ■

2.4 Proof of Theorem 5

Now we prove (5) through a initial linear change of variables and the application of the closing equation, that uses the first integrals from the isochronous centers from Theorem (1).

After the following linear change of coordinates $x = a_1x + b_1y$, $y = \alpha_1x + \beta_1y$ with $a_1\beta_1 - b_1\alpha_1 \neq 0$, the transformed isochronous center X_4 is

$$\begin{aligned} \dot{x} = \; & \frac{1}{b_1\alpha_1 - a_1\beta_1}\Big(y\left(b_1^2+\beta_1^2\right) - a_1x^3\left(-2a_1^2b_1 + 9b_1\alpha_1^2 - 3a_1\alpha_1\beta_1\right) + 2b_1^2y^3\left(b_1^2 - 3\beta_1^2\right)\\ & -3x^2y\left(-2a_1^2b_1^2 + 3b_1^2\alpha_1^2 + 4a_1b_1\alpha_1\beta_1 - a_1^2\beta_1^2\right)\\ & +x\left(a_1b_1 + \alpha_1\beta_1 + 3b_1y^2\left(2a_1b_1^2 - 5b_1\alpha_1\beta_1 - a_1\beta_1^2\right)\right)\Big),\\ \dot{y} = \; & \frac{1}{b_1\alpha_1 - a_1\beta_1}\Big(-2a_1^2x^3\left(a_1^2 - 3\alpha_1^2\right) + 3a_1x^2y\left(-2a_1^2b_1 + b_1\alpha_1^2 + 5a_1\alpha_1\beta_1\right)\\ & -b_1y^3\left(2a_1b_1^2 + 3b_1\alpha_1\beta_1 - 9a_1\beta_1^2\right) - y\left(a_1b_1 + \alpha_1\beta_1\right) - x\left(a_1^2 + \alpha_1^2\right.\\ & \left.+3y^2\left(2a_1^2b_1^2 + b_1^2\alpha_1^2 - 4a_1b_1\alpha_1\beta_1 - 3a_1^2\beta_1^2\right)\right)\Big). \end{aligned}$$

The corresponding first integral for this vector field is

$$H_4(x,y) = \frac{4 + 9\left(a_1x + b_1y\right)^2 - 27\left(x\alpha_1 + y\beta_1\right)^2}{\left(1 + 3\left(a_1x + b_1y\right)^2\right)^3}.$$

We shall need the following theorem.

Theorem 11 (Descartes Theorem)**.** *Consider the real polynomial* $p(x) = a_{i_1}x^{i_1} + a_{i_2}x^{i_2} + \ldots + a_{i_r}x^{i_r}$ *with* $0 < i_1 < i_2 < \ldots < i_r$ *and* $a_{i_j} \neq 0$ *real constants for* $j \in \{1, 2, \ldots, r\}$*. When* $a_{i_j}a_{i_{j+1}} < 0$ *we say that* a_{i_j} *and* $a_{i_{j+1}}$ *have a variation of sign. If the number of variations of sign is* m*, then* $p(x)$ *has at most* m *positive real roots. Moreover, it is always possible to choose the coefficients of* $p(x)$ *in such a way that* $p(x)$ *has exactly* $r-1$ *positive real roots.*

For a proof of this theorem see, [11]. With this result in mind, we prove theorem 5 in the following.

Proof of statement (a) *of Theorem* 5. We analize the existence of limit cycles that intersects the discontinuity curve R in the two points $(x, 0)$ and $(0, y)$. So we must study the solutions of the system

$$\begin{array}{l} Q_1 = H(x,0) - H(0,y) = 0, \\ Q_2 = H_4(x,0) - H_4(0,y) = 0, \end{array} \tag{2.3}$$

or equivalently,

$$\begin{aligned} Q_1 = \;& d^2x^2 - (a^2+\omega^2)y^2, \\ Q_2 = \;& -a_1^2x^2 + 4a_1^4x^4 - 4a_1^6x^6 + b_1^2y^2 - 9a_1^4b_1^2x^4y^2 + 9a_1^6b_1^2x^6y^2 - 4b_1^4y^4 + 9a_1^2b_1^4x^2y^4 \\ & +4b_1^6y^6 - -9a_1^2b_1^6x^2y^6 - x^2\alpha_1^2 + 9b_1^2x^2y^2\alpha_1^2 - 27b_1^4x^2y^4\alpha_1^2 + 27b_1^6x^2y^6\alpha_1^2 + y^2\beta_1^2 \\ & -9a_1^2x^2y^2\beta_1^2 + 27a_1^4x^4y^2\beta_1^2 - 27a_1^6x^6y^2\beta_1^2 = 0. \end{aligned}$$

Using the Gröebner basis, we obtain an equation given by a polynomial $p(y^2)$ in the variable y^2 of degree three without the variable x. Due to the large size of the Gröebner basis, this basis will not be exposed here. Therefore, system (2.3) has at most three positive values for the variable y. But studying the variation of signs in the consecutive coefficients of this polynomial $p(y^2)$ with the help of a software and the Theorem 11, we obtain that $p(y^2)$ has at most one positive real solution. So in this case the discontinuous piecewise differential systems have at most one limit cycle. ■

Proof of statement (b) of Theorem 5. The same proof of statement (b) of Theorem 4 works here. ■

Proof of statement (c) *of Theorem* 5. Now the discontinuous piecewise differential systems are the same of the ones of statement (b) with the difference that the position of the two vector fields involved is inverted. Here the system that we must solve is

$$\begin{array}{l} S_1 = H_4(x_1,0) - H_4(0,y_1) = 0, \\ S_2 = H(0,y_1) - H(0,y_2) = 0, \\ S_3 = H_4(0,y_2) - H_4(x_2,0) = 0, \\ S_4 = H(x_2,0) - H(x_1,0) = 0. \end{array}$$

Since

$$S_2 = \left(a^2+\omega^2\right)(y_1 - y_2)(y_1 + y_2) = 0,$$

we get that $y_1 = y_2$ or $y_1 = -y_2$, so the condition $0 < y_1 < y_2$ is not satisfied. This completes the proof of this statement. ■

2.5 Exhibition of Limit Cycles

2.5.1 Exhibition of Limit Cycles under the Assumptions of Statement (a) of Theorem 2

We shall exhibit a limit cycle that pass through the points $(1,0)$ and $(0,1)$ under the assumptions of statement (a) of Theorem 2. The linear differential center forming the discontinuous piecewise differential system is

$$X_c = \begin{cases} \dot{x} = x + 3y, \\ \dot{y} = -3x - y, \end{cases}$$

and the isochronous center of first type is

$$Y_1 = \begin{cases} \dot{x} = \dfrac{5y}{3} + \dfrac{4x^2y}{3} + x\left(2 + \dfrac{8y^2}{9}\right), \\ \dot{y} = -2y + \dfrac{8y^3}{9} + x\left(-3 + \dfrac{4y^2}{3}\right). \end{cases}$$

Two first integrals for these two systems are

$$H(x,y) = 8y^2 + (3x+y)^2 \quad \text{and} \quad H_1(x,y) = \frac{\left(x + \dfrac{y}{3}\right)^2 + (x+y)^2}{1 + 2\left(x + \dfrac{y}{3}\right)(x+y)},$$

respectively. So, we get a periodic orbit living on the curves

$$8y^2 + (3x+y)^2 = 9 \quad \text{and} \quad \frac{\left(x + \frac{y}{3}\right)^2 + (x+y)^2}{1 + 2\left(x + \frac{y}{3}\right)(x+y)} = \frac{2}{3}.$$

These periodic orbits are plotted in Figure 2.1.

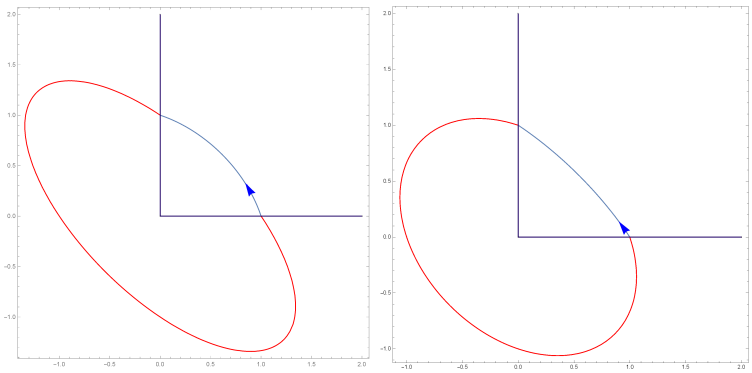

Figura 2.1: Examples of limit cycles. Figure made by the author.

Now we need to verify that this periodic orbit is a limit cycle and for this we will see that this periodic orbit is the unique periodic orbit of the discontinuous piecewise differential system formed by the systems X_c and X_1. In other words we verify that the solution of the following system

$$E_1 = 9x^2 - 9y^2 = 0, \qquad E_2 = \frac{2x^2}{1+2x^2} - \frac{10y^2}{9\left(1 + 2y^2/3\right)} = 0,$$

is unique. This system has the solutions $(-1,-1)$, $(-1,1)$, $(0,0)$ and $(1,1)$. The only solution that fits in our discontinuous piecewise differential system verifying $x>0$ and $y>0$ is $(1,1)$. So, we have an isolated periodic solution and, consequently, a unique limit cycle passing through the points $(1,0)$ and $(0,1)$.

In Figure 2.1, we have that the limit cycle on the left part of the figure has the linear center located in the first quadrant, and on the right it has the isochronous center located in the first quadrant.

2.5.2 Exhibition of Limit Cycles under the Assumptions of Statement (a) of Theorem 3

We shall exhibit a limit cycle that pass through the points $(1,0)$ and $(0,1)$ for a discontinuous piecewise differential system under the assumptions of statement (a) of Theorem 3. The linear differential center is

$$X_c=\begin{cases}\dot{x}=-x-3y,\\ \dot{y}=3x+y,\end{cases}$$

and the isochronous center of type X_2 is

$$X_2=\begin{cases}\dot{x}=0.8472692451281911x^3-2.139401725939056y-0.8364103556343343x^2y-\\ \qquad 4.278803451878112y^3+x\left(-1.1394017259390556-6.836410355634334y^2\right),\\ \dot{y}=0.13999358700066028x^3+1.1394017259390556y+3.43271792887313x^2y+\\ \qquad 2.2788034518781113y^3+x\left(1.0742425161240468+6.44545509674428y^2\right).\end{cases}$$

Two first integrals for these systems are

$$H\left(x,y\right)=8y^2+\left(3x+y\right)^2,$$

and

$$H_2=\frac{(x+y)^2+\left(\frac{1}{3}\left(-1-4\left(\frac{10}{19+3\sqrt{129}}\right)^{\frac{1}{3}}+2^{\frac{2}{3}}\left(\frac{1}{5}\left(19+3\sqrt{129}\right)\right)^{\frac{1}{3}}x+y\right)^2\right)^2}{1+4\left(x+y\right)\left(\frac{1}{3}\left(-1-4\left(\frac{10}{19+3\sqrt{129}}\right)^{\frac{1}{3}}+2^{\frac{2}{3}}\left(\frac{1}{5}\left(19+3\sqrt{129}\right)\right)^{\frac{1}{3}}\right)x+y\right)},$$

respectively and we get a periodic orbit on the level curves $H\left(x,y\right)=9$ and

$$H_2=\frac{\left(1+\frac{1}{9}\left(-1-4\left(\frac{10}{19+3\sqrt{129}}\right)^{\frac{1}{3}}+2^{\frac{2}{3}}\left(\frac{1}{5}\left(19+3\sqrt{129}\right)\right)^{\frac{1}{3}}\right)^2\right)^2}{1+\frac{4}{3}\left(-1-4\left(\frac{10}{19+3\sqrt{129}}\right)^{\frac{1}{3}}+2^{\frac{2}{3}}\left(\frac{1}{5}\left(19+3\sqrt{129}\right)\right)^{\frac{1}{3}}\right)}=\frac{4}{5}.$$

This periodic orbit is plotted in Figure 2.2. The limit cycle on the left part of the figure has the linear center located in the first quadrant, and on the right it has the isochronous center located in the first quadrant.

Now we need to verify that this periodic orbit is a limit cycle, i.e., that the system

$$I_1=9\left(x-y\right)\left(x+y\right)=0,$$

and

$$I_2=\frac{2.799\cdot10^{-6}\left(5.404\cdot10^6x^4+2.161\cdot10^{-7}x^4y^2-2.143\cdot10^7y^4-5.586\cdot10^6x^2y^4\right)}{\left(15+3.909x^2\right)\left(1+4y^2\right)}=0,$$

has only one solution that fits in our case and we find $(0,0)$, $(-1,1)$, $(-1,-1)$, $(1,-1)$ and $(1,1)$. Therefore, the unique solution with $x>0$ and $y>0$ is $(1,1)$, which confirms that the periodic orbit is a limit cycle.

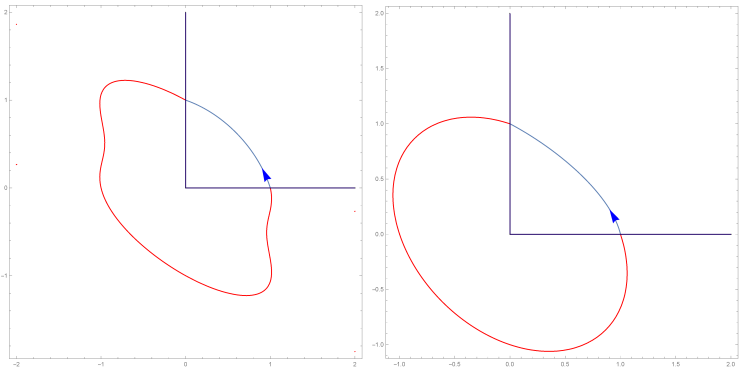

Figura 2.2: Examples of limit cycles. Figure made by the author.

2.5.3 Exhibition of Three Limit Cycles under the Assumptions of Statement (a) of Theorem 4

Under the assumptions of statement (a) of Theorem 4, we shall exhibit three limit cycles that pass through the points $(18.549009361227327, 0)$ and $(0, 25.722847831141028)$ for the first limit cycle, for the second limit cycle through the points $(25.388714134116643, 0)$ and $(0, 35.20781178025187)$ and finally for the third limit cycle passing through the other two points $(41.038816629476216, 0)$ and $(0, 56.91059909305413)$. The linear differential center is

$$X_c = \begin{cases} \dot{x} = -2x - \dfrac{13y}{5}, \\ \dot{y} = 5x + 2y, \end{cases}$$

and the isochronous center of type X_3 is

$$X_3 = \begin{cases} \dot{x} = & -0.105098x^3 - 2.11124y + 0.00392714x^2y - 0.00196024y^3 \\ & -x\left(-2.75169 - 0.00557864y^2\right), \\ \dot{y} = & 0.00724939x^3 - 2.75169y - 0.0107282x^2y + 0.0054651y^3 \\ & -x\left(-4.06008 + 0.00392714y^2\right). \end{cases}$$

Two particular first integrals for these two systems are

$$H\left(x, y\right) = 9y^2 + \left(5x + 2y\right)^2$$

and

$$H_3\left(x, y\right) = \frac{4 + 27\left(x/10 - 0.072111y\right)^2 - 9\left(0.0176073x + 0.0126968y\right)^2}{\left(1 - 3\left(0.0176073x + 0.0126968y\right)^2\right)^3}.$$

Three periodic orbits for this discontinuous piecewise differential system are plotted in Figure 2.3. For these three limit cycles, we have in the first quadrant the vector field related to the third isochronous center.

Now we verify that these three periodic orbits are limit cycles, i.e., we will verify that the system formed by the equations M_1 and M_2 below have only three solutions. More precisely, the equations M_1 and M_2 are given by

$$M_1 = 25x^2 - 13y^2 = 0$$

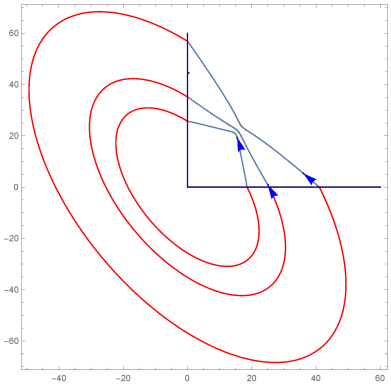

Figura 2.3: Examples of limit cyles. Figure made by the author.

and

$$M_2 = -\frac{27}{\left(0.000930054x^2-1\right)^3\left(0.000483628y^2-1\right)^3}\Big(-0.01031x^2+3.84445.10^{-7}x^4 \\ -1.19185.10^{-10}x^6+0.00536121y^2+6.77626.10^{-21}x^2y^2+1.33546.10^{-8}x^4y^2 \\ -4.14016.10^{-12}x^6y^2-1.03954.10^{-7}y^4-6.94437.10^{-9}x^2y^4+1.67583.10^{-11}y^6 \\ +1.1195.10^{-12}x^2y^6\Big)=0,$$

and these two equations have only the following three solutions (x, y), with $x > 0$ and $y > 0$:

$$(18.54900936122732, 25.72284783114102), \quad (25.38871413411664, 35.2078117802518)$$

and

$$(41.03881662947621, 56.9105990930541).$$

Therefore, this confirms that the three periodic orbits are limit cycles.

2.5.4 Exhibition of Limit Cycles Under the Assumptions of Statement (a) of Theorem 5

Under the assumptions of statement (a) of Theorem 5 we shall exhibit one limit cycle that pass through the points $(0.0124707, 0)$ and $(0, 0.0223083)$. The linear differential center is

$$X_c = \begin{cases} \dot{x} = -x - 5y/4, \\ \dot{y} = 4x + y, \end{cases}$$

and the isochronous center of type X_4 is

$$X_4 = \begin{cases} \dot{x} = -0.7698y + 13943.1x^3 - 249414x^2y - 9742.71y^3 - x\left(0.946727 + 161212y^2\right), \\ \dot{y} = -4357.22y^3 + 99765.3x^3 + 0.946727y + 515879x^2y + x\left(2.46336 + 249414y^2\right). \end{cases}$$

Two first integrals for these two systems are

$$H(x, y) = 4y^2 + (4x + y)^2,$$

and

$$H_4(x, y) = \frac{4 - 27\left(100x - 55.9017y\right)^2 + 9\left(232.379x + 129.904y\right)^2}{\left(1 + 3\left(232.379x + 129.904y\right)^2\right)^3},$$

respectively. A periodic orbit is plotted in Figure 2.4. The limit cycle on the left part of the figure has the linear center located in the first quadrant and on the right it has the isochronous center located in the first quadrant.

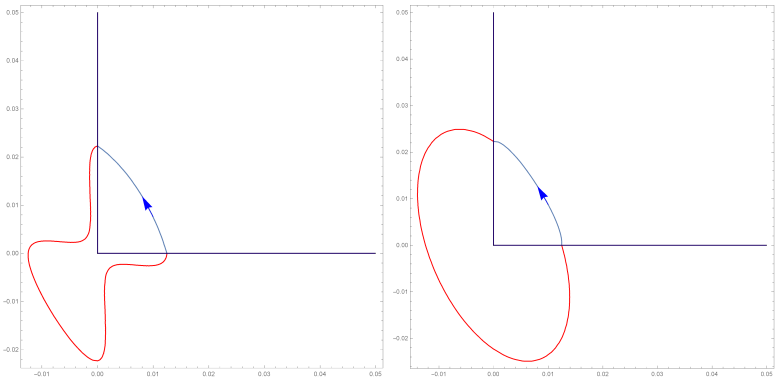

Figura 2.4: Examples of limit cyles. Figure made by the author.

Now we verify that this periodic orbit is a limit cycle, i.e., that the system

$$\begin{aligned} Q_1 = \;& 16x^2 - 5y^2 = 0, \\ Q_2 = \;& 63999.8x^2 + 1.16639.10^{10}x^4 + 6.2985.10^14x^6 - 19999.9y^2 + \\ & 1.96828.10^{14}x^4y^2 + 1.06287.10^{19}x^6y^2 - 1.13906.10^9y^4 - \\ & 6.15086.10^{13}x^2y^4 - 1.92215.10^{13}y^6 - 1.03795.10^{18}x^2y^6 = 0, \end{aligned}$$

has a unique solution (x, y) satisfying $x > 0$ and $y > 0$, that is $(0.0124707, 0.0223083)$. Therefore this periodic orbit is a limit cycle.

3 Results on New Families of Global Cubic Centers

This chapter begins with the statement of the Theorem 12, proved in [64] and of the main Theorem 13 of this chapter. Due to the large extension of the Theorem 13, we begin its proof by a general sketch valid for all cases studied. The cases that emerge fit in one of three different patterns and an respective sample of each case is proved.

Theorem 12. *If the origin of system* (1.3) *is a center if and only if one of the following sets of conditions holds:*

(*a*) $H = P = G = K = 0$;

(*b*) $H = B = E = 0$;

(*c*) $H = 0$, $(DE - BC)(G - K) - P(B^2 + 4BD + 4CE + E^2) = 0$, $B^3C + B^3E + 3B^2DE - 3BCE^2 - BE^3 - DE^3 = 0$, $DE - BC \neq 0$;

(*d*) $H = 0$, $B = -4D$, $E = -4C$, $C^4P + C^3DG - C^3DK - 6C^2D^2P - CD^3G + CD^3K + D^4P = 0$;

(*e*) $H = P = C = E = 0$;

(*f*) $H = P = 0$, $B = E$, $C = D$;

(*g*) $H = P = 0$, $B = -E$, $C = -D$;

(*h*) $H = P = B = D = 0$;

(*i*) $H = 0$, $(DE - BC)K = 2P(C^2 + D^2)$, $(DE - BC)G = P(B^2 - 6C^2 - 6D^2 + E^2)$, $BD + 2C^2 + CE + 2D^2 = 0$, $DE - BC \neq 0$;

(*j*) $H = P = 0$, $B = -2D$, $E = -2C$, $G = -K$;

(*k*) $H = P = C = D = K = 0$.

The theorem above estabilishes specific conditions for the parameters to get a local center at the origin, for the system (1.3). For example, the condition (a) estabilishes that, for $H = P = G = K = 0$, we get a local center for the equilibrium point $(0, 0)$ and so on for the remaining conditions. The main theorem brings specific parameters conditions for the system (1.3) to get a global center in the equilibrium point located at the origin $(0, 0)$ and is the following.

Theorem 13. *The origin of system* (1.3) *is a global center and the polynomials* $\dot{x}$ *and* $\dot{y}$ *have no common factors that are non-constant if and only if one of the following sets of conditions holds:*

(b.1) $H = B = E = C = D = 0$, $G = (2P^2 - K^2)/K$ *and* $K > 0$.

(b.2) $H = B = E = C = D = P = 0$, $G = -K$ *and* $K > 0$.

(d.1) $H = P = C = E = 0$, $B = -4D$, $G = K$ *and* $D^2 - 4K < 0$.

(d.2) $H = P = D = 0$, $B = -4D$, $E = -4C$, $G = K$ *and* $C^2 - 4K < 0$.

(d.3) $H = P = 0$, $B = -4D$, $E = -4C$, $D = \pm C$, $G = K$ *and* $C^2 - 2K < 0$.

(e.1) $H = P = C = E = 0$, $B = -2D$, $K = -G$, $K > 0$ *and* $D^2 + 4G < 0$.

(f.1) $H = P = K = D = C = 0$, $B = E$ *and* $E^2 - 4G < 0$.

(f.2) $H = P = 0$, $G = K$, $B = E$, $C = D$, $E = -4D$ *and* $D^2 - 2K < 0$.

(f.3) $H = P = 0$, $G = -K$, $B = E$, $C = D$, $E = -2D$, *and* $D^2 - K < 0$.

(g.1) $H = P = K = D = C = 0$, $B = -E$ *and* $E^2 - 4G < 0$.

(g.2) $H = P = 0$, $G = K$, $B = -E$, $C = -D$, $E = 4D$ *and* $D^2 - 2K < 0$.

(g.3) $H = P = 0$, $G = -K$, $B = -E$, $C = -D$, $E = 2D$, *and* $D^2 - K < 0$.

(h.1) $H = P = B = D = 0$, $E = -2C$, $G = -K$ *and* $C^2 - 4K < 0$.

(j.1) $H = P = 0$, $B = -2D$, $E = -2C$, $G = -K$, $(C + D)^2 - 4K < 0$, $(C - D)^2 - 4K < 0$ *and* $C^2 + D^2 - 4K \pm \sqrt{(D^2 + 4K - C^2)^2 - 16D^2K} < 0$.

(k.1) $H = P = C = D = K = 0$, $B^2 - 4G < 0$ *and* $E^2 - 4G < 0$.

3.0.1 Skecth of the Proof of Theorem 13

In general ideas, first we take one of the cases of Theorem 12 applying its conditions. Then we apply the Poncaré compactification to system. After this we analyze if the origin is an equilibrium point in the chart U_2, considering in this stage cases that the origin is an infinite equilibrium point and cases that the origin is not an equilibrium point. Then we analyze the presence or not of infinite equilibria in the chart U_1. After this, we calculate the Jacobian matrix in these equilibria if they exist, forcing these matrices to be null and picking up conditions in the parameters that become these matrices null. Then we do a vertical blow up process in the vector fields of the charts U_1 and U_2 in their equilibria for verifying when these equilibria present a meeting of two hyperbolic sectors. For this happen, all the equilibria must be saddles. Finally, we analyze the existence of more than one finite equilibrium point in the original system with all the parameters conditions applied.

From statement (a) of Theorem 12, we can not obtain a global center, because with the application of the condition $H = P = G = K = 0$, the vector field obtained has degree two.

From statement (b) of Theorem 12, we have six cases to analyze (based on the origin being a equilibrium point or not in the chart U_2 and parameters conditions that become viable the Jacobian matrices to be null) and we find global centers in only two of them. They are given in statements $(b.k)$ for $k = 1, 2$ of Theorem 13. In the first five cases, the origin of the local chart U_2 in the Poincaré compactification is not an equilibrium point. In statement (b.2) initially we find $H = B = E = C = D = P = 0$, $G = \pm K$ and $K > 0$ for a global center at the origin, but for $G = K$ we have that the system (1.3) becomes $\dot{x} = y\,(1 + Kx^2 + Ky^2)$, $\dot{y} = -x\,(1 + Kx^2 + Ky^2)$. Since $1 + Kx^2 + Ky^2$ is a common factor of $\dot{x}$ and $\dot{y}$, this diferential system rescaled with the time can be reduced to the system $\dot{x} = y$, $\dot{y} = -x$ and we do not consider such systems. When $G = -K$, system (1.3) becomes $\dot{x} = y\,(1 - Kx^2 + Ky^2)$, $\dot{y} = -x\,(1 + Kx^2 - Ky^2)$, and then we consider it. In six cases, the origin of U_2 is an equilibrium point and it will be a particular case from conditions of statement (f.1), and so presenting a global center.

From statement (c) of Theorem 12, when we solve the three equations $(DE - BC)(G - K) - P\,(B^2 + 4BD + 4CE + E^2) = 0$, $B^3C + B^3E + 3B^2DE - 3BCE^2 - BE^3 - DE^3 = 0$ and $H = 0$, taking into account that $DE - BC \neq 0$, we do not have solutions for analyze the existence of global centers.

From statement (d) of Theorem 12, when we solve the equation $C^4P + C^3DG - C^3DK - 6C^2D^2P - CD^3G + CD^3K + D^4P = 0$, we get six different cases to analyze. Each case is separated in two subcases, either the origin of U_2 is an equilibrium point or not. One of the subcases that has global center presents the same parameters conditions of case (b.2) and the subcases that have global center are given in statements $(d.r)$ for $r = 1, 2, 3$ of Theorem 13.

Under the conditions of statement (e) of Theorem 12, we get four cases to study. Each case is separated in two subcases, either the origin of U_2 is an equilibrium point or not. The subcase that has global center is given in statement $(e.1)$ of Theorem 13. One of the subcases obtained will be a particular case of statement (k.1) and another subcase presents the same parameters conditions of statement (d.1).

From the conditions of statements (f) and (g), we get eight subcases to study, two of them having an equilibrium point at the origin of U_2 and for the other six, this origin is not an equilibrium point. The subcases with global center are $(f.k)$ and $(g.k)$ for $k = 1, 2, 3$. We remark that the conditions for having a global center are the same under conditions (f) and (g).

From the conditions of statement (h), we obtain four cases to analyze and only in one case the origin of U_2 is an equilibrium point. The subcase with global center is given in statement $(h.1)$. We get a subcase that will be a particular case of (k.1) with $B = 0$ and other case is a particular case of (d.2) with the parameter condition $B = 0$.

From the conditions of statement (i) and solving the equations

$$(DE - BC)K = 2P(C^2 + D^2), \quad (DE - BC)G = P(B^2 - 6C^2 - 6D^2 + E^2),$$

$$BD + 2C^2 + CE + 2D^2 = 0, \quad H = 0,$$

and taking into account that $DE - BC \neq 0$, we get five cases to analize, but for these cases, in order to have a global center, we must have $DE - BC = 0$, which is a contradiction. So we cannot have global center for statement (i).

From the conditions of statement (j), we get four cases to study and in one case the origin of U_2 is an equilibrium point. Only one of these cases allows the existence of a global center, that is given in statement $(j.1)$.

Finally, from statement (g), we have only one subcase to analize and it is a global center, given in statement $(g.1)$.

Many cases not mentioned in Theorem 13 do not have a global center at the origin of system (1.3), due to one of the following five reasons:

(i) System (1.3) becomes quadratic for some values of the parameters. For instance, this is the case under the conditions of statement (a) of Theorem 12.

(ii) It is not possible to become zero the Jacobian matrices at the infinite equilibria of the charts U_1 or U_2 in the Poincaré compactification.

(iii) When studying the local phase portrait of some infinite equilibrium point, doing blow up's, appears some parabolic sector inside a saddle-node or a node, because they produce in the local phase portrait of the infinite equilibrium point orbits that go to infinity or come from infinity.

(iv) System (1.3) presents more than one finite equilibria, i.e., some equilibrium point distinct of the center localized at the origin of coordinates.

(v) By the existence of some indetermination, for example, in one of the cases analyzed, the origin of the local chart U_2 is an equilibrium point and the parameter $G = (-C^4P+6C^2D^2P-D^4P)/(C^3D-CD^3)$ must be zero, but in order that the Jacobian matrix of this case be zero at the infinite equilibria, we must have $C = P = 0$, but then G becomes indetermined.

The distinct cases described in the statements of Theorem 13 fit in one of following three different patterns:

(I) There are no infinite equilibria, i.e., the infinity is a periodic orbit. Then, to prove that system (1.3) has a global center, it is reduced to prove that the unique finite equilibrium is the origin of coordinates. This sometimes is a difficult computational problem. For instance, this situation occurs in inside the case of statement (c) of Theorem 12 when $D = (-B^3C - B^3E + 3BCE^2 + BE^3)/(E\,(3B^2 - E^2))$ and $K = (-B^3EG+BE^3G+B^4P-6B^2E^2P+E^4P)/(BE\,(-B^2+E^2))$ is a solution of $(DE - BC)\,(G - K) - P(B^2 + 4BD\, +4CE + E^2) = 0$. Also it occurs in the case of statement (d) of Theorem 12 when $K = (C^3DG - CD^3G + C^4P - GC^2D^2P + D^4P)/(C^3D - CD^3)$ is a solution of $C^4P + C^3DG - C^3DK - 6C^2D^2P - CD^3G + CD^3K + D^4P = 0$.

(II) All the infinite equilibria are in the local charts $U_1 \cup V_1$. Since the linear part at these equilibria will be the zero matrix, we need to do blow up's trying to see that the local phase portraits of such equilibria are formed by two hyperbolic sectors.

(III) The origin of the chart U_2 is an equilibrium point. As in the case (II), we must do blow up's.

In what follows, we shall illustrate **some cases showing** these patterns.

3.0.2 The Proofs According to the Previous Sketch

Cases (b.1) and (b.2). Based on the conditions of statement (b) of Theorem 12, we have $H = B = E = 0$, then system (1.3) becomes

$$\begin{aligned} \dot{x} &= y - Cx^2 + 2Dxy + Cy^2 + Px^3 + Gx^2y - 3Pxy^2 + Ky^3, \\ \dot{y} &= -x + Dx^2 + 2Cxy - Dy^2 - Kx^3 - 3Px^2y - Gxy^2 + Py^3. \end{aligned} \tag{3.1}$$

This system in the chart U_2 writes

$$\begin{aligned} \dot{u} = \;& 2Gu^2 + 4Pu\left(u^2-1\right) + K\left(1+u^4\right) + Cv + 3Duv - 3Cu^2v \\ & -Du^3v + v^2 + u^2v^2, \\ \dot{v} = \;& v\left(Gu + Ku^3 + P\left(3u^2-1\right) + Dv - 2Cuv - Du^2v + uv^2\right). \end{aligned} \tag{3.2}$$

First we consider that the origin of system (3.2) is not an equilibrium, i.e, $K \neq 0$. In the chart U_1 of the Poincaré compactification, system (3.1) becomes

$$\begin{aligned} \dot{u} = \;& -2Gu^2 + 4Pu\left(u^2-1\right) - K\left(1+u^4\right) + Dv + 3Cuv - 3Du^2v \\ & -Cu^3v - v^2 - u^2v^2, \\ \dot{v} = \;& -v\left(P + Gu - 3Pu^2 + Ku^3 - Cv + 2Duv + Cu^2v + uv^2\right). \end{aligned} \tag{3.3}$$

We get four infinite equilibria of system (3.3), namely $p_1 = (u_{-+}, 0)$, $p_2 = (u_{--}, 0)$, $p_3 = (u_{++}, 0)$ and $p_4 = (u_{+-}, 0)$, where

$$\begin{aligned} u_{\pm\pm} = \;& \frac{1}{2K}\Big(2P \pm \sqrt{2}\Big(\sqrt{-K\left(G+K\right)+2P^2} \\ & \pm\sqrt{-GK + K^2 + 4P^2 - 2P\sqrt{-2K\left(G+K\right)+4P^2}}\Big)\Big). \end{aligned}$$

Let J_i be the Jacobian matrix of system (3.3) evaluated at p_i, for $i = 1, 2, 3, 4$. By Proposition 9, these four matrices must be the zero matrix. This provides three conditions, the ones of the following three cases.

Case (b.1). $C = 0$, $D = 0$ and $G = (2P^2 - K^2)/K$. Now we have to do blow up's for studying the local phase portraits at the four infinite equilibria of the chart U_1. We translate the equilibrium p_1 at the origin of coordinates doing the change of variables $(u, v) = (u_1 + u_{-+}, v_1)$, and we get the system

$$\begin{aligned} \dot{u_1} = \;& \frac{1}{K^2}\left(-K^3u_1^2\left(4 - 4\sqrt{1+\frac{P^2}{K^2}}u_1 + u_1^2\right) - 2P^2v_1^2\right. \\ & +K^2\left(-2 + 2\sqrt{1+\frac{P^2}{K^2}}u_1 - u_1^2\right)v_1^2 \\ & \left.-2KP\left(2Pu_1^2 + \left(-\sqrt{1+\frac{P^2}{K^2}} + u_1\right)v_1^2\right)\right), \\ \dot{v_1} = \;& -\frac{1}{K}v_1\left(K^2u_1\left(2 - 3\sqrt{1+\frac{P^2}{K^2}}u_1 + u_1^2\right) + K\left(-\sqrt{1+\frac{P^2}{K^2}} + u_1\right)v_1^2\right. \\ & \left.+P\left(2Pu_1 + v_1^2\right)\right). \end{aligned} \tag{3.4}$$

Since $u_1 = 0$ is not a characteristic direction, we do the vertical blow up $(u_1, v_1) =$

(u_2, u_2v_2) and we obtain the system

$$\begin{aligned}
\dot{u_2} = & -\frac{1}{K^2}u_2^2\left(4K^3+4KP^2-4K^2\sqrt{(K^2+P^2)}u_2+K^3u_2^2+2Kv_2^2+2P^2v_2^2\right.\\
& \left.-2P\sqrt{K^2+P^2}v_2^2+2KPu_2v_2^2-2K\sqrt{K^2+P^2}u_2v_2^2+K^2u_2^2v_2^2\right),\\
\dot{v_2} = & -\frac{1}{K^2}u_2v_2\left(-2K^3-2KP^2+K^2\sqrt{K^2+P^2}u_2-2K^2v_2^2-2P^2v_2^2\right.\\
& \left.+2P\sqrt{K^2+P^2}v_2^2-KPu_2v_2^2+K\sqrt{K^2+P^2}u_2v_2^2\right).
\end{aligned} \tag{3.5}$$

Now we eliminate the common factor u_2 in the two components of system (3.5) doing a rescaling of the time and we get the system

$$\begin{aligned}
\dot{u_2} = & -\frac{1}{K^2}u_2\left(4K^3+4KP^2-4K^2\sqrt{(K^2+P^2)}u_2+K^3u_2^2+2Kv_2^2+2P^2v_2^2\right.\\
& \left.-2P\sqrt{K^2+P^2}v_2^2+2KPu_2v_2^2-2K\sqrt{K^2+P^2}u_2v_2^2+K^2u_2^2v_2^2\right),\\
\dot{v_2} = & -\frac{1}{K^2}v_2\left(-2K^3-2KP^2+K^2\sqrt{K^2+P^2}u_2-2K^2v_2^2-2P^2v_2^2\right.\\
& \left.+2P\sqrt{K^2+P^2}v_2^2-KPu_2v_2^2+K\sqrt{K^2+P^2}u_2v_2^2\right).
\end{aligned} \tag{3.6}$$

Since the equilibria of system (3.6) on the straight line $u_2 = 0$ are $p = (0,0)$, $p_\pm = \left(0, \pm\sqrt{K^3+KP^2}/\sqrt{-K^2-P^2+P\sqrt{K^2+P^2}}\right)$ and they are hyperbolic, the process of the blow up has ended. Note that $\sqrt{-K^2-P^2+P\sqrt{K^2+P^2}} < 0$ because $K \neq 0$, so the equilibria $p\pm$ are not real.

The eigenvalues of the linear part of the system at the equilibrium p are $2K + 2P^2/K$ and $-2\left(2K + 2P^2/K\right)$, so p is a saddle. If $K > 0$, going back through these changes of variables, we obtain that p is formed by two hyperbolic sectors, as the ones of Figure , where we have the desingularization using blow up's of the origin of coordinates of the chart U_1 in the following way: (a) the local phase portrait in a neigborhood of the straight line$u_1 = 0$ of system (3.12). (b) The local phase portrait in a neighborhood of the straight line $u_1 = 0$ of system (3.11). (c) The local phase portrait at the origin of the chart U_1.. If $K < 0$, we have that the component of the vector field before the blow up process $\dot{u_1} > 0$ for $u_1 = 0$ in the chart U_1. So the vector field flow in the region $u_2 < 0$ of the plane $u_2 \times v_2$ changes of direction, as showed in the middle of Figure 3.1, because we multiply the system in the chart U_2 by u_2. So, come back to the original system before the blow up, with the changes of variables $u_2 = u_1$ and $v_2 = \dfrac{v_1}{u_1}$ (desingularization process), we can not obtain the joining of two hyperbolic sectors, as showed in the right of Figure 3.1, where we have desingularization using blow up's of the origin of coordinates of the chart U_1 in the following way: (a) the local phase portrait in a neigborhood of the straight line $u_2 = 0$ of system (3.6). (b) The local phase portrait in a neighborhood of the straight line $u_2 = 0$ of system (3.5). (c) The local phase portrait at the origin of the chart U_1.

We do a similar analysis for the equilibrium points p_2, p_3 and p_4, obtaining the same conclusion, i.e., when $K > 0$ these four equilibria are formed by two hyperbolic sectors. So, by Proposition 10, if $K > 0$, then system (3.1) has a global center if the system has a unique finite equilibrium point.

System (3.1) after the conditions obtained reduces to

$$\begin{aligned}
\dot{x} &= y + Px^3 + \frac{2P^2-K^2}{K}x^2y - 3Pxy^2 + Ky^3,\\
\dot{y} &= -x - Kx^3 - 3Px^2y - \frac{2P^2-K^2}{K}xy^2 + Py^3.
\end{aligned}$$

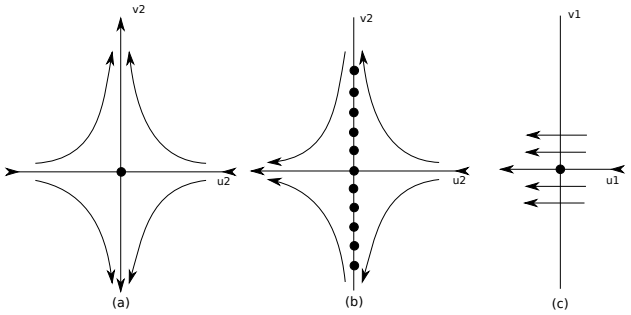

Figura 3.1: Desingularization of blow up's. Figure made by the author.

Since this system for $K > 0$ has only the origin as an equilibrium point, statement (b.1) is proved.

An analogous analysis could be applied to the statements (d.1), (e.3), (h.3) and (j.1) of Theorem 13.

Case (b.2). $C = D = P = 0$ and $G = -K$. These conditions transform the equilibrium points p_1 and p_2 into the equilibrium $\left(-\sqrt{-K^2}/K, 0\right)$ and the equilibrium points p_3 and p_4 into the equilibrium $\left(\sqrt{-K^2}/K, 0\right)$. Therefore system (3.1) has no infinite equilibrium points in the chart U_1 and, consequently, the infinity is a periodic orbit. Now we study the finite equilbria of system (3.1), which is reduced to the system

$$\dot{x} = y + Kx^2y + Ky^3, \quad \dot{y} = -x - Kx^3 - Kxy^2.$$

The three equilibria of this system are $\left(x, \pm\sqrt{-1 - Kx^2}/K\right)$ and $(0, 0)$.

If $K > 0$, we have only the origin as a finite equilibrium and then, by Proposition 10, we have a global center at the origin. If $K < 0$, for the values of x such that $K\left(-1 - Kx^2\right) > 0$, we have a continuum of equilibrium points and the system cannot present a global center. This proves the statement (b.2) of Theorem 13.

This kind of proof can be applied to the cases (d.1), (d.2), (d.3), (d.4), (e.2), (f.2), (g.2) and (h.2) of Theorem 13.

Case (b.3) Now we assume that $K = 0$, so the origin of the chart U_2 is an infinite equilibrium point. From system (3.2), the Jacobian matrix at the origin of U_2 is

$$\begin{pmatrix} -4P & C \\ 0 & -P \end{pmatrix}.$$

From Proposition 9, this matrix must be the zero matrix if we want to have a global center, so $P = C = 0$.

From system (3.3), now we get that in the local chart U_1 the system (3.1) writes

$$\dot{u} = -2Gu^2 - v\left(-D + 3Du^2 + v + u^2v\right), \quad \dot{v} = -uv\left(G + v\left(2D + v\right)\right). \tag{3.7}$$

The unique infinite equilibria of this system is $p = (0, 0)$. The Jacobian matrix of the system at p is

$$\begin{pmatrix} 0 & D \\ 0 & 0 \end{pmatrix}.$$

Due to Proposition 9, if we want to obtain a global center for system (3.1), this matrix must be the zero matrix, hence $D = 0$. Therefore, system (3.1) under the conditions $K = P = C = D = 0$ reduces to the system

$$\dot{x} = y + Gx^2y, \quad \dot{y} = -x - Gxy^2. \tag{3.8}$$

The five finite equilibria of these system are $\left(\pm 1/\sqrt{-G}, \pm 1/\sqrt{-G}\right)$ and $(0,0)$. So if $G > 0$ the origin is the unique finite equilibria.

Now we study the local phase portrait at the origin of the chart U_1 and we need to do blow up's, because this equilibrium point is linearly zero. Since $u = 0$ is not a characteristic direction, we do the change of variables $(u, v) = (u_1, u_1 v_1)$ and the system (3.7) becomes

$$\dot{u_1} = -u_1^2 \left(2G + \left(1 + u_1^2\right) v_1^2\right), \quad \dot{v_1} = u_1 v_1 \left(G + v_1^2\right). \tag{3.9}$$

Doing a rescaling of the time, we eliminate the common factor u_1 from system (3.9) and we obtain the system

$$\dot{u_1} = -u_1 \left(2G + \left(1 + u_1^2\right) v_1^2\right), \; \dot{v_1} = v_1 \left(G + v_1^2\right). \tag{3.10}$$

The equilibrium points of this system on $u_1 = 0$ are $(0,0)$ and $\left(0, \pm\sqrt{-G}\right)$, but with the restriction $G > 0$ we only have the equilibria $(0,0)$. The Jacobian matrix at the origin of the system has eigenvalues $-2G$ and G, so the $(0,0)$ is a hyperbolic saddle. Going back through the change of variables, we get that the origin of U_1 is formed by two hyperbolic sectors, as showed in Figure 3.1.

The origin of the chart U_2 from system (3.2) with $K = P = C = D = 0$ is a linearly zero equilibrium point. Then, for studying its local phase portrait we must do blow up's. Since $u = 0$ is not a characteristic direction, we do the change of variables $(u, v) = (u_1, u_1 v_1)$, getting the system

$$\dot{u_1} = u_1^2 \left(2G + \left(1 + u_1^2\right) v_1^2\right), \quad \dot{v_1} = -u_1 v_1 \left(G + v_1^2\right). \tag{3.11}$$

Rescaling the time, we eliminate the common factor u_1, and we obtain the system

$$\dot{u_1} = u_1 \left(2G + \left(1 + u_1^2\right) v_1^2\right), \quad \dot{v_1} = -v_1 \left(G + v_1^2\right). \tag{3.12}$$

The equilibrium points of this system on $u_1 = 0$ are $(0,0)$ and $\left(0, \pm\sqrt{-G}\right)$. Again, with the restriction $G > 0$, the unique equilibrium is the $(0,0)$. The Jacobian matrix at the origin has the eigenvalues $2G$ and $-G$. So the origin is a saddle. Again, going back through the change of variables, we get that the origin of U_2 is formed by two hyperbolic sectors as shown in Figure 3.1, where we have desingularization using blow up's of the origin of coordinates of the chart U_1 in the following way: (a) The local phase portrait in a neigborhood of the straigh line$u_1 = 0$ of system (3.12). (b) The local phase portrait in a neighborhood of the straight line $u_1 = 0$ of system (3.11). (c) The local phase portrait at the origin of the chart U_1. By Proposition (10). under all these conditions, system (3.1) has a global center at the origin and statement (b.3) is proved.

The cases (e.1), (f.1), (g.1), (h.1) and (k.1) are proved in an analogous way.

Case (f.3) This case happens when we analyze the case (f) or (g) of Theorem 12, assuming that the origin of the chart U_2 is not an equilibrium. Since $H = P = 0$, $B = E$ and $C = D$, system (1.3) becomes

$$\begin{aligned} \dot{x} &= y - Dx^2 + (2D + E)\, xy + Gx^2 y + Dy^2 + Ky^3, \\ \dot{y} &= -x + Dx^2\, (2D + E)\, xy - Dy^2 - Kx^3 - Gxy^2. \end{aligned} \tag{3.13}$$

This system in the chart U_2 is

$$\begin{aligned} \dot{u} &= 2Gu^2 + K\left(1 + u^4\right) + v\left(D(1 + 3u - u^3) + Eu - (3D + E)u^2 + v + u^2 v\right), \\ \dot{v} &= v\left(Gu + Ku^3 + v\left(D - 2Du - Eu - Du^2 + uv\right)\right). \end{aligned} \tag{3.14}$$

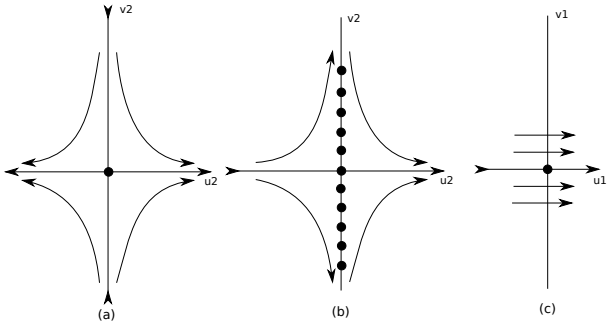

Figura 3.2: Desingularization of blow up's. Figure made by the author.

We have that the origin is not an equilibria when $K \neq 0$.
In the chart U_1, system (3.13) becomes

$$\begin{aligned} \dot{u} &= -2Gu^2 - K\left(1+u^4\right) - (u-1)\,uv - D\left(1+3u-3u^2-u^3\right) + \left(1+u^2\right)v, \\ \dot{v} &= -v\left(Gu + Ku^3 + v\left(D\left(-1+2u+u^2\right) + u\left(E+v\right)\right)\right). \end{aligned} \tag{3.15}$$

The infinite equilibrium points of this system are the four equilibria

$$p_{\pm} = \left(\pm\sqrt{-(G+\sqrt{G^2-K^2})/K}, 0\right) \text{ and } q_{\pm} = \left(\pm\sqrt{-(G-\sqrt{G^2-K^2})/K}, 0\right).$$

From Proposition 9, we do zero the four Jacobian matrices of system (3.15) at these four equilibria and we obtain the solution $E = -2D$ and $G = -K$, which origins $p_{\pm} = q_{\pm} = (\pm 1, 0)$.

Moving the equilibria $(-1, 0)$ to the origin of coordinates, system (3.15) becomes

$$\begin{aligned} \dot{u_1} &= -K\left(-2+u_1\right)^2 u_1^2 - v_1\left(D\left(-2+u_1\right)u_1^2 + \left(2-2u_1+u_1^2\right)v_1\right), \\ \dot{v_1} &= -v_1\left(Ku_1(2-3u_1+u_1^2) + v_1\left(D_1\left(-2+u_1\right)u_1 + \left(-1+u_1\right)v_1\right)\right). \end{aligned} \tag{3.16}$$

Then we apply the blow up $u_1 = u_2$, $v_1 = u_2 v_2$ and system (3.16) is given by

$$\begin{aligned} \dot{u_2} &= -u_2^2\left(4K - 4Ku_2 + Ku_2^2 - 2Du_2v_2 + Du_2^2v_2 + 2v_2^2 - 2u_2v_2^2 + u_2^2v_2^2\right), \\ \dot{v_2} &= \left(2-u_2\right)u_2v_2\left(K+v_2^2\right). \end{aligned} \tag{3.17}$$

Doing a rescaling of the time, we eliminate the common factor u_2 from system (3.17) and we obtain

$$\begin{aligned} \dot{u_2} &= -u_2\left(4K - 4Ku_2 + Ku_2^2 - 2Du_2v_2 + Du_2^2v_2 + 2v_2^2 - 2u_2v_2^2 + u_2^2v_2^2\right), \\ \dot{v_2} &= \left(2-u_2\right)v_2\left(K+v_2^2\right). \end{aligned} \tag{3.18}$$

The equilibrium points of system (3.18) at $u_2 = 0$ are $(0,0)$, $\left(0, -i\sqrt{K}\right)$, $\left(0, i\sqrt{K}\right)$. The Jacobian matrix calculated at origin has eigenvalues $-4K$ and $2K$, so the origin is a hyperbolic saddle. If $K > 0$, only the origin is the equilibria of system (3.18) on $u_2 = 0$. Going back through the change of variables, we obtain that the origin of the system (3.17) is formed by two hyperbolic sectors when $K > 0$, as shown in Figure 3.1. If $K < 0$, we have the three equilibrium points of system (3.18), but the eigenvalues of $\left(0, \pm i\sqrt{K}\right)$ are $-2K$ and $-4K$, so these equilibrium points are nodles and the system can not have a global center.

Doing the same analysis made for the equilibrium $(-1, 0)$ for the other equilibrium $(1, 0)$ of system (3.15), i.e., first we translate the equilibrium $(1, 0)$ to the origin of coordinates, after we do the blow up process and the rescaling of the time by the common factor

u_2 and we obtain the following three equilibrium points $(0,0)$, $\left(0,-D\pm\sqrt{D^2-K}\right)$ on $u_2=0$. The origin is a saddle and if the other two equilibria are not real, going back through the change of variables we get, again, that the origin of system (3.17) is formed by two hyperbolic sectors.

Before studying when the equilibrium points $\left(0,-D\pm\sqrt{D^2-K}\right)$ exist or not, we study the finite equilibrium points. The system (3.13) with the conditions $E=-2D$ and $G=-K$ becomes

$$\dot{x}=y-Dx^2+Dy^2-Kx^2y+Ky^3,\quad \dot{y}=-x+Dx^2-Dy^2-Kx^3+Kxy^2. \tag{3.19}$$

Then the unique finite equilibrium point of system (3.19) is the origin when $D^2-K<0$. So the equilibrium points $\left(0,-D\pm\sqrt{D^2-K}\right)$ do not exist and, consequently, the system has a global center under the conditions $H=P=0$, $B=E$, $C=D$, $K>0$, $E=-2D$, $G=-K$ and either $-\sqrt{K}<D<0$, or $0<D<\sqrt{K}$.

4 Canard Limit Cycles in Piecewise Linear Differential Systems Through Regularization and Blow Up

We shall begin by studying ordinary differential equations in which some variables have derivatives of much larger magnitude than those of other variables. This scenario yields a system with different time scales. The easiest case is a separation, which splits the variables into two groups.

Definition 6. *A fast-slow vector field is a system of ordinary differential equations taking the form:*

$$\begin{cases} \epsilon\frac{dx}{d\tau} = \epsilon\dot{x} = f(x,y,\epsilon), \\ \frac{dy}{d\tau} = \dot{y} = g(x,y,\epsilon), \end{cases}$$

where $f : \mathbb{R}^m \times \mathbb{R}^n \times \mathbb{R} \to \mathbb{R}^m$, $g : \mathbb{R}^m \times \mathbb{R}^n \times \mathbb{R} \to \mathbb{R}^n$ *and* $0 < \epsilon << 1$. *Furthermore, the* x *variables are called fast variables and the* y *variables are called slow variables. Setting* $t = \frac{\tau}{\epsilon}$ *gives the equivalent form*

$$\begin{cases} \frac{dx}{dt} = x' = f(x,y,\epsilon), \\ \frac{dy}{dt} = y' = \epsilon g(x,y,\epsilon). \end{cases}$$

We refer to τ *as the fast time scale and* t *as the slow time scale. From now on, the variable notation* $\dot{x}$ *refers to the fast time and* x' *refers to slow time (analogously for* y*).*

The study of limit cycles is one of the most important objectives in the qualitative theory of the planar ordinary differential equations, because has many applications in control theory [50] and other science areas.

Here we consider a discontinuous piecewise differential system on $\mathbb{R}^2$ composed by a pair of C^r (with $r \geq 1$) differential systems in $\mathbb{R}^2$ separated by a smooth curve Λ. The line of discontinuity Λ of the discontinuous piecewise differential system is given by $\Lambda = h^{-1}(0)$, where $h : \mathbb{R}^2 \longrightarrow \mathbb{R}$ is a C^1 function having 0 as a regular value. Observe that Λ is the boundary between the regions $\Lambda^+ = \{(x,y) \in \mathbb{R}^2; h(x,y) > 0\}$ and $\Lambda^- = \{(x,y) \in \mathbb{R}^2; h(x,y) < 0\}$. Hence

$$Z(x,y) = \begin{cases} X(x,y), & if \ \ h(x,y) \geq 0, \\ Y(x,y), & if \ \ h(x,y) \leq 0, \end{cases} \tag{4.1}$$

is the vector field corresponding to a piecewise differential system with a discontinuity line Σ.

Definition 7 (Sotomayor-Teixeira regularization)**.** *A C^∞ function $\phi : \mathbb{R} \to \mathbb{R}$ is a transition function if $\phi(x) = -1$ for $x \leq -1$, $\phi(x) = 1$ for $x \geq 1$ and $\phi'(x) > 0$ if $x \in (-1, 1)$. The ϕ-regularization of $Z = (X, Y)$ is the one parameter family $Z_\epsilon \in C^r$ given by*

$$Z_\epsilon(q) = \left(\frac{1}{2} + \frac{\phi_\epsilon(h(q))}{2}\right) X(q) + \left(\frac{1}{2} - \frac{\phi_\epsilon(h(q))}{2}\right) Y(q),$$

with $\phi_\epsilon(x) = \phi\left(\frac{x}{\epsilon}\right)$, for $\epsilon > 0$, h is a smooth function $h : K \subset \mathbb{R}^2 \to \mathbb{R}$ having $0 \in \mathbb{R}$ as a regular value, K a compact set and $\Sigma \subset K$ with $\Sigma = h^{-1}(0)$.

In article [17], the relations between slow fast systems and piecewise linear continuous vector fields are estabilished through theorems below.

Theorem 14. *Consider $X \in \Omega^r$ (space of the C^r piecewise smooth vector fields), X_ϵ its ϕ-regularization and $p \in \Sigma$. Suppose that ϕ is a polynomial of degree k in a small interval $I \subset (-1, 1)$ with $0 \in I$. Then the trajectories of X_ϵ in $V_\epsilon = \left\{q \in K; \frac{h(q)}{\epsilon} \in I\right\}$ are in correspondence with the solutions of an ordinary differential equation $z' = p(z, \epsilon)$, satisfying that p is smooth in both variables and $p(z, 0) = 0$ for any $z \in \Sigma$. Moreover, if $(X_1 - X_2) h^k(p) \neq 0$, then we can take a C^{r-1}-local coordinate system $\left\{\left(\frac{\delta}{\delta x}\right)(p), \left(\frac{\delta}{\delta y}\right)(p)\right\}$ such that this smooth ordinary differential equation is a slow fast system problem.*

Let $\Omega_d \subset \Omega^r$ be the set of piecewise smooth vector fields X=(X_1, X_2) in Ω^r such that there exists a continuous function h that is a solution of

$$\nabla h (X_1 - X_2) = \Pi_i (X_1 - X_2),$$

where Π_i denote the canonical projections, for $i = 1$ or $i = 2$.

Theorem 15. *Consider $X \in \Omega^r$ and X_ϵ its ϕ-regularization. Suppose that ϕ is a polynomial of degree k in a small interval $I \subset \mathbb{R}$ with $0 \in I$. Then the trajectories of X_ϵ on $V_\epsilon = \left\{q \in K; \frac{h(q)}{\epsilon} \in I\right\}$ are solutions of a slow fast system problem.*

In the same article [17], the parameter of regularization and the parameter of slow fast system are the same, but in our case, after the regularization, the existence of the parameter in the denominator at the components of the vector field has become a problem when the blow up is done. So, we separated in two parameters for analysis: η is the regularization parameter and ϵ is the slow fast parameter.

This work is based on the article [58], where is treated the problem of piecewise smooth linear Liénard differential system of the form:

$$\frac{dx}{dt} = y - f(x), \quad \frac{dy}{dt} = \epsilon(a - x),$$

where $\epsilon > 0$ is sufficiently small and f is a linear function. Yet in [58], the singularities worked are hyperbolic or elementary (points that presents at least one eigenvalue with real part $\neq 0$). So, the necessity of application of the blow up method does not exist and the treatment is more direct to obtain the canard cycles.

In this thesis we work with planar piecewise linear slow-fast Liénard differential systems with three zones separated by two vertical lines. The existence and uniqueness of canard limit cycles for systems with a unique singular point located in the middle zone. In our case, we find canard limit cycles using regularization of vector fields and the blow up

method, which consists in a desingularization of singular points in the critical manifold, with the aim of a regularization of singular points non hyberbolic, becoming them hyperbolic points, which enable us the application of the Fenichel theory. The main objective of this thesis is to prove the theorem below:

Theorem 16. *Consider the discontinuous piecewise vector system in* $\mathbb{R}^2$*:*

$$X : \begin{cases} x' = y - f(x), \\ y' = a - x, \end{cases}$$

where $f(x) = -x$*, if* $x < 0$ *and* $f(x) = x^2$*, if* $x > 0$*. When we apply the Sotomayor-Teixeira regularization to regularize this system, canard limit cycles appears in the two new singularities that emerge on the range of regularization, whose length is* 2η*.*

The theorem is proved in the following sections.

First we regularize the vector field of Theorem 16, then the existence of limit cycles is showed beyond the Hopf bifurcation theory. After this, a detailed computation of vector fields on the charts are showed together with the blow up method for one of the two non hyperbolic singularities of the vector field in question. Finally, in section 5 we show the existence of canard limit cycles by use of Melnikov integral.

4.1 Regularization

How it was commented in the beginning of this chapter, we analyze the system:

$$X : \begin{cases} \dot{x} = y - f(x), \\ \dot{y} = a - x, \end{cases} \tag{4.2}$$

where $f(x) = -x$, if $x < 0$ and $f(x) = x^2$, if $x > 0$. The Figure 4.1 below shows the graph of the function $y = f(x)$ from the system above.

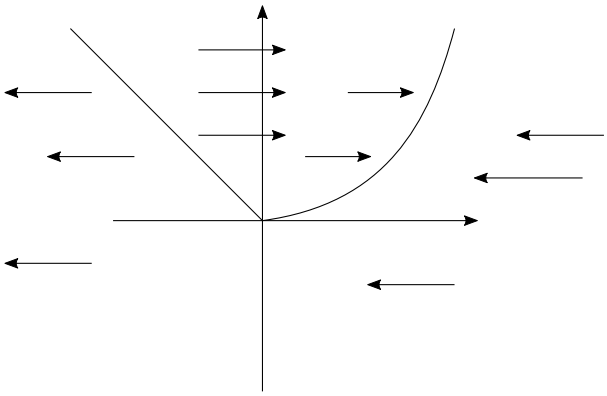

Figura 4.1: Critical manifold. Figure made by the author.

The aim of this work is to find canard limit cycles using regularization of the vector fields of the system (4.2).

Using the Sotomayor-Teixeira regularization on the vector field (4.2), we stay with:

$$X_{reg} = (1 - \phi_\eta(x)) X_l + \phi_\eta(x) X_r,$$

where X_l is the vector field for $x < 0$ (left) and X_r (right) is the vector field for $x > 0$, with $\phi_\eta(x) = \frac{x}{\eta}$. Continuing with the vector field X_{reg}, we have

$$X_{reg} = \left(\left(1 - \frac{x}{\eta}\right)(y + x) + \frac{x}{\eta}\left(y - x^2\right), a - x\right),$$

$$X_{reg} : \begin{cases} \dot{x} = \left(1 - \frac{x}{\eta}\right)(y + x) + \frac{x}{\eta}\left(y - x^2\right), \\ \dot{y} = a - x, \end{cases}$$

Doing the transformation of variables $(x = \epsilon\overline{x})$ and $(y = \overline{y})$ for perturbing the system above and, after the transformation of variables, we keep $\overline{x} = x$, we stay with

$$X_{reg} : \begin{cases} \epsilon\dot{x} = \left(1 - \frac{x}{\eta}\right)(y + x) + \frac{x}{\eta}\left(y - x^2\right), \\ \dot{y} = a - x. \end{cases}$$

Transforming the variables of the slow-fast system, i.e., $\tau = \epsilon t$, we stay with (we keep the same notation for the derivative in fast and slow systems):

$$X_{reg} = \begin{cases} \dot{x} = \left(1 - \frac{x}{\eta}\right)(y + x) + \frac{x}{\eta}\left(y - x^2\right), \\ \dot{y} = \epsilon\left(a - x\right). \end{cases} \tag{4.3}$$

Altering the form of the initial problem through a vertical translation of the slow manifold of X_l by one unit up, we stay with:

$$X^- : \begin{cases} \dot{x} = y + x - 1, \\ \dot{y} = \epsilon\left(a - x\right), \end{cases} \qquad X^+ = \begin{cases} \dot{x} = y - x^2, \\ \dot{y} = \epsilon\left(a - x\right), \end{cases}$$

where $f_1(x) = -x + 1$ and $f_2(x) = x^2$. Therefore, we have that $\left(X^- h\right)\left(X^+ h\right)|_{\Sigma=\{x=0\}} = (y - 1)\, y = y^2 - y < 0 \Leftrightarrow 0 < y < 1$ is the sliding region of this vector field. This system is shown in the Figure 4.2.

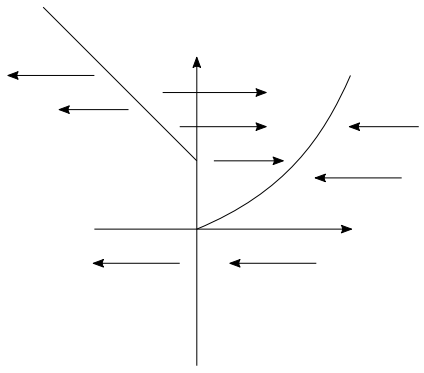

Figura 4.2: Sliding region between the interval $(0, 1)$ on the y axis. Figure made by the author.

The sliding vector field is given by

$$X^\Sigma = \frac{\left(X^+ h\right) X^- - \left(X^- h\right) X^+}{\left(X^+ h - X^- h\right)} =$$

$$= \frac{y\left(y - 1, \epsilon a\right) - (y - 1)\left(y, \epsilon a\right)}{(y - y + 1)} = (0, \epsilon a).$$

Another case of modification is when we translate by one unit up the slow manifold of the system X_r.

$$X^- : \begin{cases} \dot{x} = y + x \\ \dot{y} = \epsilon (a - x) \end{cases} \qquad X^+ : \begin{cases} \dot{x} = y - x^2 - 1 \\ \dot{y} = \epsilon (a - x) \end{cases},$$

with $f_1(x) = -x$ e $f_2(x) = x^2 - 1$. The Figure 4.3 shows this situation.

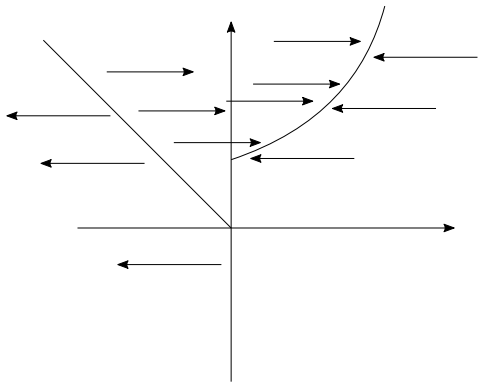

Figura 4.3: Sliding region between the interval $(0, 1)$ on the y axis. Figure made by the author.

So, we have that $(X^- h)(X^+ h)|_{\Sigma=\{x=0\}} = y(y-1) = y^2 - y < 0 \Leftrightarrow 0 < y < 1$.

$$X^\Sigma = \frac{(y-1)(y, \epsilon a) - y(y-1, \epsilon a)}{y - 1 - y} = (0, \epsilon a).$$

Therefore, we have sliding regions in the y axis, when modifying the slow manifolds by vertical translation on the left side and on the right side of the vertical axis.

4.2 Hopf Bifurcation

The analysis of this section is based on the theorem below.

Theorem 17. *Any bidimensional system*

$$\frac{dx}{dt} = f(x, \alpha), \quad x \in \mathbb{R}^2, \alpha \in \mathbb{R}$$

with $f \in C^n(\Omega), \Omega \subset \mathbb{R}^2 \times \mathbb{R}$, *having a singularity at* $x = 0$, $\forall |\alpha| << 1$, *with eigenvalues* $\lambda_{1,2}(\alpha) = \gamma(\alpha) \pm i\omega(\alpha)$, *where* $\gamma(0) = 0$, $\omega(0) = \omega_0 > 0$, *satisfying the conditions below*

$$1) l_1(0) \neq 0 \ \textit{non degeneriscity condition},$$

$$2) \gamma'(0) \neq 0 \ \textit{transversality condition},$$

is locally topologically equivalent around the origin, to the one of the normal forms showed below

$$\begin{cases} \dot{y_1} = \alpha y_1 - y_2 \pm (y_1^2 + y_2^2) y_1, \\ \dot{y_2} = y_1 + \alpha y_2 \pm (y_1^2 + y_2^2) y_2. \end{cases}$$

The conditions (1) and (2) will be elucidated posteriorly in the text. The normal forms above are related to the existence of limit cycles at the system considered. For more information about limit cycles and normal forms, study the reference [51]. The proposition that is proved in this section is the next.

Proposition 18. *When we regularize the system* (4.2)*, limit cycles appear in the singularities* $(a_1, f(a_1))$ *and* $(a_2, f(a_2))$ *inside the range of regularization. Without regularization, we do not have any limit cycles at the singularity point* $(0, 0)$*.*

The aim of this section is calculate Lyapunov coefficient and transversality of the regularized vector field. After the Sotomayor-Teixeira regularization, the regularized system becomes:

$$X_{reg} = \begin{cases} \dot{x} = \left(1 - \frac{x}{\eta}\right)(y + x) + \frac{x}{\eta}(y - x^2), \\ \dot{y} = a - x. \end{cases}$$

Now we need to perturb the system with the parameter ϵ, which origins:

$$X_{per} : \begin{cases} \dot{x} = \left(1 - \frac{x}{\eta}\right)(y + x) + \frac{x}{\eta}(y - x^2), \\ \dot{y} = \epsilon(a - x). \end{cases}$$

After some computations, the regularized system stays in the form

$$X_{per} : \begin{cases} \dot{x} = y - \frac{x^3}{\eta} - \frac{x^2}{\eta} + x, \\ \dot{y} = \epsilon(a - x). \end{cases} \tag{4.4}$$

For $\epsilon = 0$, the system X_{pert} from (4.4) is given by

$$X_{per} = \begin{cases} \dot{x} = y - \frac{x^3}{\eta} - \frac{x^2}{\eta} + x, \\ \dot{y} = 0. \end{cases}$$

The slow manifold is given by

$$L = \left\{(x, y) \in \mathbb{R}^2; y = \frac{x^3}{\eta} + \frac{x^2}{\eta} - x\right\},$$

and doing this curve analysis, we get that the points

$$s = \left(\frac{1}{3}\left(-1 + \sqrt{1 + 3\eta}\right), \frac{(-1 + \sqrt{1 + 3\eta})(-1 + \sqrt{1 + 3\eta} - 12\eta)}{27\eta}\right),$$

and

$$n = \left(\frac{1}{3}\left(-1 - \sqrt{1 + 3\eta}\right), \frac{(1 + \sqrt{1 + 3\eta})(1 + \sqrt{1 + 3\eta} + 12\eta)}{27\eta}\right),$$

are local minimum and maximum respectively. All points of L, except s and n, are elementary singular points, i.e., the Jacobian matrix in these points present an eigenvalue non-null. The phase portrait for X_{pert} in $\epsilon = 0$ is represented in Figure 4.4 below.

The lines L_1 and L_3 are attractor hyperbolic singularities lines and L_2 is a repulsor hyperbolic singularity line. For $\epsilon > 0$, the vector field X_{pert} has only one singular point $p_a = (a, F(a))$, with $F(a) = \frac{a^3}{\eta} + \frac{a^2}{\eta} - a$. The Jacobian matrix of the system X_{pert} stays as

$$DX_{pert} = \begin{pmatrix} 1 - \frac{2x}{\eta} - \frac{3x^2}{\eta} & 1 \\ -\epsilon & 0 \end{pmatrix}.$$

We denote by Z the Jacobian matrix computed at the singularity p_a. Therefore,

$$Z = DX_{pert} = \begin{pmatrix} 1 - \frac{2a}{\eta} - \frac{3a^2}{\eta} & 1 \\ -\epsilon & 0 \end{pmatrix}.$$

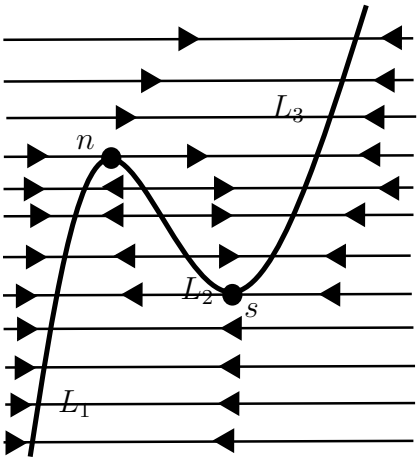

Figura 4.4: Phase portrait for the vector field X_{pert} in $\epsilon = 0$. Figure made by the author.

Using the fact that the eigenvalues of Z are given by $\lambda_{\epsilon,a} = \dfrac{trZ \pm \sqrt{\Delta}}{2}$, where $\Delta = (trZ)^2 - 4\det Z$, we have

$$\lambda_{\epsilon,a} = \frac{-2a - 3a^2 + \eta \pm \sqrt{(2a + 3a^2 - \eta)^2 - 4\epsilon\eta^2}}{2\eta}.$$

We analyse three cases here: $\Delta = 0$, $\Delta < 0$ and $\Delta > 0$. The case $\Delta < 0$ gives origin to the Hopf bifurcation through the variation of the parameter a with $\epsilon > 0$ fixed. We study the behavior of the limit cycle that emerges from this bifurcation when $\epsilon \to 0$.

Considering the parameters space (a, ϵ), we see that Δ becomes null on the quadratic surface $\epsilon = \dfrac{(2a + 3a^2 - \eta)^2}{4\eta^2}$, $\Delta < 0$ above this surface and $\Delta > 0$ below this surface, see Figure 4.5. Observe that $trZ = 0 \Leftrightarrow a = \dfrac{1}{3}(-1 \pm \sqrt{1 + 3\eta})$. We denote $\lambda^1_{\epsilon,a}$ the

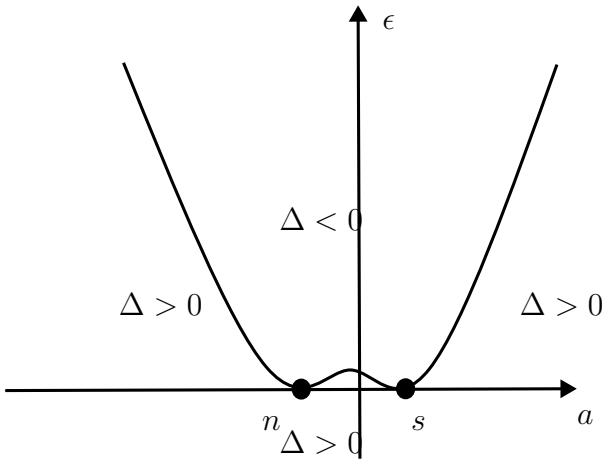

Figura 4.5: Graph of the quadratic surface. Figure made by the author.

eigenvalue of the matrix Z that corresponds to the signal "+"and by $\lambda^2_{\epsilon,a}$ the eigenvalue that corresponds to the signal "−".

When $\Delta > 0$, on the parameters space (a, ϵ), we are considering the region $(2a + 3a^2 - \eta)^2 - 4\epsilon\eta^2 > 0$. In this region, $a \neq \dfrac{1}{3}(-1 \pm \sqrt{1 + 3\eta})$. The eigenvalues are real and distinct. If

$a < \frac{1}{3}(-1 - \sqrt{1+3\eta})$, both eigenvalues are negative and $\lambda^2_{\epsilon,a} < \lambda^1_{\epsilon,a}$. Given a determined pair (a, ϵ) in this region, the phase portrait for the singularity is an attractor node, as showed in the Figure 4.6 below.

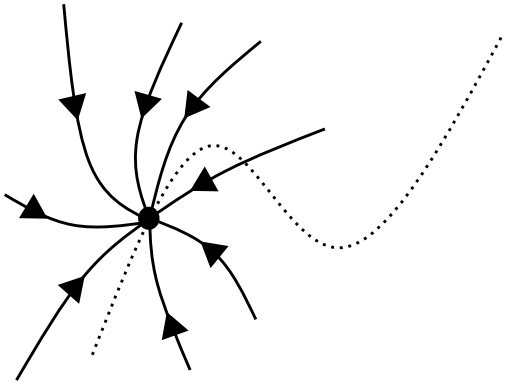

Figura 4.6: Atractor node. Figure made by the author.

If $\frac{1}{3}(-1 - \sqrt{1+3\eta}) < a < \frac{1}{3}(-1 + \sqrt{1+3\eta})$, the eigenvalues $\lambda^1_{\epsilon,a}$ and $\lambda^2_{\epsilon,a}$ are positive and $\lambda^2_{\epsilon,a} < \lambda^1_{\epsilon,a}$. The equiibrium point is a repulsor node for the singularity, as showed in Figure 4.7.

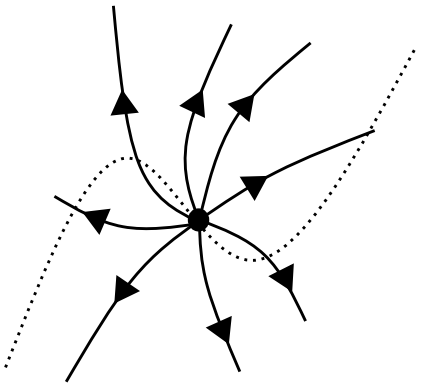

Figura 4.7: Repulsor node. Figure made by the author.

If $a > \frac{1}{3}(-1 + \sqrt{1+3\eta})$, the eigenvalues $\lambda^1_{\epsilon,a}$ and $\lambda^2_{\epsilon,a}$ are negative and $\lambda^2_{\epsilon,a} < \lambda^1_{\epsilon,a}$. In this region the phase portrait is an atractor node for this singularity, represented in the Figure 4.8 below.

When $\Delta = 0$, the eigenvalues are real and equal, i.e., $\lambda^1_{\epsilon,a} = \lambda^2_{\epsilon,a} = \dfrac{-2a - 3a^2 + \eta}{2\eta} = \lambda_a$. If $a < \frac{1}{3}(-1 - \sqrt{1+3\eta})$, the phase portrait for this configuration is an improper attractor node for this singularity, because $\lambda_a < 0$ for small enough values from η, as showed in Figure 4.9 below.

If $\frac{1}{3}(-1 - \sqrt{1+3\eta}) < a < \frac{1}{3}(-1 + \sqrt{1+3\eta})$, we have an improper repulsor node for the singularity, because $\lambda_a > 0$ in this region as showed in Figure 4.10 below.

If $a > \frac{1}{3}(-1 + \sqrt{1+3\eta})$, we have $\lambda_a < 0$ and an improper attractor node for this singularity, represented in Figure 4.11 below.

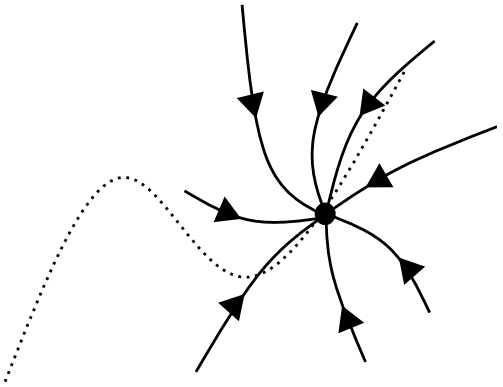

Figura 4.8: Attractor node. Figure made by the author.

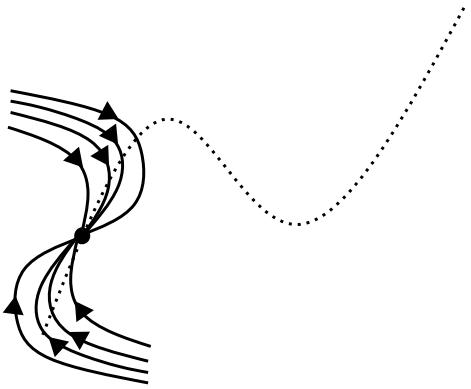

Figura 4.9: Improper attractor node. Figure made by the author.

When $\Delta < 0$, the eigenvalues are conjugated complex. They are given by

$$\lambda_{\epsilon,a} = \frac{-2a - 3a^2 + \eta \pm i\sqrt{4\epsilon\eta^2 - (2a + 3a^2 - \eta)^2}}{2\eta}.$$

The Figure 4.12 shows a bifurcation diagram for the family X_{pert}. The singularity s is an attractor node for $a > \frac{1}{3}\left(-1 + \sqrt{1+3\eta}\right)$ and a repulsor node for $\frac{1}{3}\left(-1 - \sqrt{1+3\eta}\right) < a < \frac{1}{3}\left(-1 + \sqrt{1+3\eta}\right)$. In some neighborhood of $a = \frac{1}{3}\left(-1 + \sqrt{1+3\eta}\right)$, we have a change of stability and the same occurs for $a = \frac{1}{3}\left(-1 - \sqrt{1+3\eta}\right)$, as showed in the same Figure 4.12 below.

In Figure 4.12 we see a symmetry around the point $a = -\frac{1}{3}$. The lines

$$H = \left\{a = \frac{1}{3}\left(-1 + \sqrt{1+3\eta}\right), \epsilon > 0\right\}$$

and

$$H' = \left\{a = \frac{1}{3}\left(-1 - \sqrt{1+3\eta}\right), \epsilon > 0\right\}$$

are denominated bifurcation lines and X_{pert} has only one attractor limit cycle $\Gamma_{\epsilon,a}$ for $a \in \left(\frac{1}{3}\left(-1 - \sqrt{1+3\eta}\right), \frac{1}{3}\left(-1 + \sqrt{1+3\eta}\right)\right)$, as proved ahead in this paper. For the symmetry of the problem and because the singularity n stays out of the regularization range for η

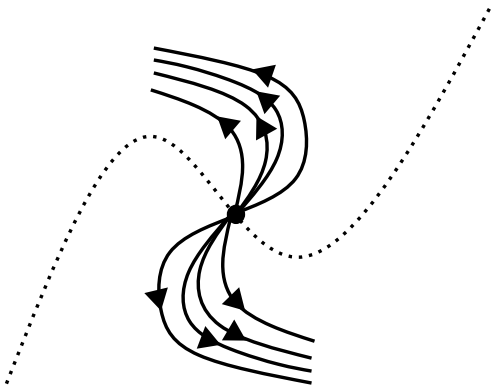

Figura 4.10: Improper repulsor node. Figure made by the author.

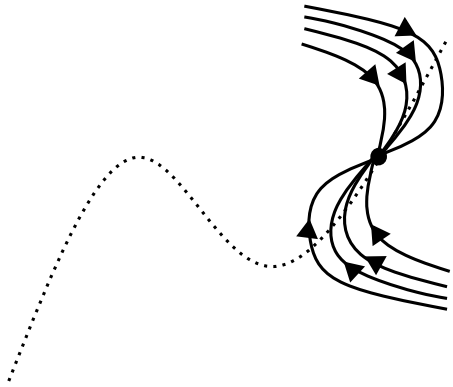

Figura 4.11: Improper attractor node. Figure made by the author.

small enough, we analyse only the singularity s from now on (this singularity s always stays inside the regularization range for any value of η). Outside the interval

$$\left(\frac{1}{3}\left(-1-\sqrt{1+3\eta}\right),\frac{1}{3}\left(-1+\sqrt{1+3\eta}\right)\right)$$

the system does not present limit cycle.

The limit cycle through the continuous curves

$$\epsilon \mapsto a = c(\epsilon), c(\epsilon) \in \left[\frac{1}{3}\left(-1-\sqrt{1+3\eta}\right),\frac{1}{3}\left(-1+\sqrt{1+3\eta}\right)\right]$$

collapses in one of the curves showed in Figure 4.13 below, when $\epsilon \to 0$. These kind of curves are denominated by limit periodic sets (lps).

More precisely, limit periodic sets are compact invariant subsets through the flow of X_{pert} with $\epsilon = 0$, which are approximated in the Hausdorff metric by one parameter families of limit cycles $\Gamma_{\epsilon,c(\epsilon)}$, associated with the one parameter subfamilies of X_{pert} with ϵ and $a = c(\epsilon)$. The Hausdorff metric is based in the following notion of distance between two non empty sets $V, W \subset \mathbb{R}^{m+n}$, which is defined by

$$d_H(V,W) = max\left\{\sup_{v\in V}\inf_{w\in W}||v-w||, \sup_{w\in W}\inf_{v\in V}||v-w||\right\}.$$

As long as we are considering $a \geq -\frac{1}{3}$, it is enough to do the analysis of the limit periodic sets (1) to (5) in the Figure 4.13 taking curves $c(\epsilon)$ such that

$$c(0) \in \left[-\frac{1}{3},\frac{1}{3}\left(-1+\sqrt{1+3\eta}\right)\right].$$

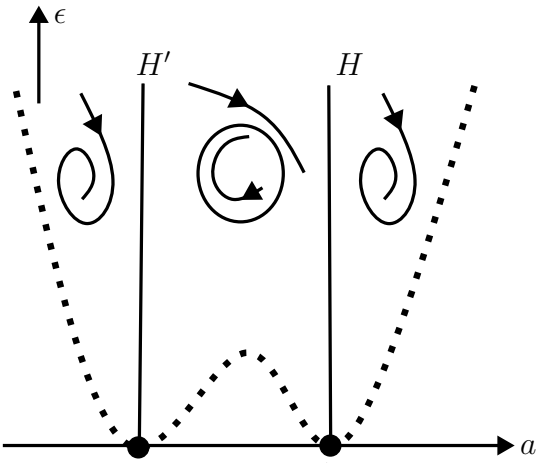

Figura 4.12: Bifurcation diagram for X_{pert}. Figure made by the author.

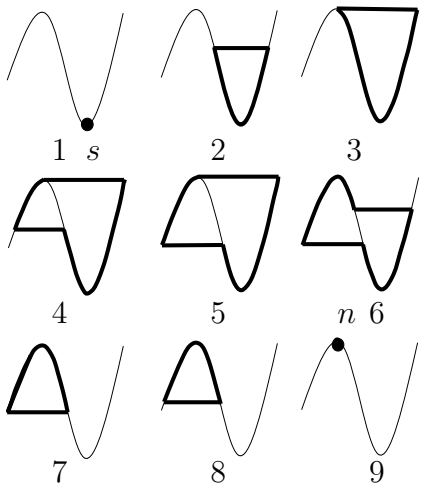

Figura 4.13: Limit periodic sets. Figure made by the author.

The others are symmetrically equivalent.

The limit periodic set (lps) (1) is called "small"and denoted by Γ_0, while the lps (5) is called "big"and denoted by Γ_B. The cases (2), (3) and (4) are known as "canards"and we use the following terminology respectively: lps of type I, denoted by Γ^I, lps of type II, denoted by Γ^{II} and lps of type III, denoted by Γ^{III}. Moreover, we introduce the terminology $\Gamma^I_{y-y_0}$ and $\Gamma^{III}_{y-y_0}$, where $y_0 = \dfrac{(-1+\sqrt{1+3\eta})\,(-1-6\eta+\sqrt{1+3\eta})}{27\eta}$, to represent the situations of the Figure 4.14.

In Figure 4.14, we have $y_1 = \dfrac{(1+\sqrt{1+3\eta})\,(1+6\eta+\sqrt{1+3\eta})}{27\eta}$. Observe that $\Gamma^I_{y_0-y_0} = \Gamma^I_0 = \Gamma_0$, $\Gamma^{III}_{y_0-y_0} = \Gamma^{III}_0 = \Gamma_B$ and $\Gamma^I_{y_1-y_0} = \Gamma^{III}_{y_1-y_0} = \Gamma^{II}$. For $\Gamma^I_{y-y_0}$ and $\Gamma^{III}_{y-y_0}$ we only refer to limit periodic sets of the type canard when $y - y_0 > 0$. The orientation of the limit periodic set is the induced in the neighborhood of the limit cycle and is compatible with the flow of X_{pert}. The next theorem is proved in [32].

Theorem 19. *There exists a curve $C_0 = \{a = c_0(\epsilon)\}$ with $c_0(\epsilon) = \sqrt{\epsilon}\overline{a}(\sqrt{\epsilon})$, $\overline{a} \in C^\infty$, with $\overline{a}(0) = 0$ and $\overline{a}'(0) = -1$, such that for some continuous curve $C = \{a = c(\epsilon)\}$ with $c(\epsilon) \leq 0$ and $c(0) \in \left[-\dfrac{1}{3}, 0\right]$, we have by taking $y \in]y_0, y_1[$:*

- *(I) $\lim_{\epsilon\to 0}\Gamma_{\epsilon,c(\epsilon)} = \Gamma_0 \Leftrightarrow \forall \epsilon > 0; c(\epsilon) \geq c_0(\epsilon)$ and $lim_{\epsilon\to 0}\log(c(\epsilon) - c_0(\epsilon)) \leq 0$;*

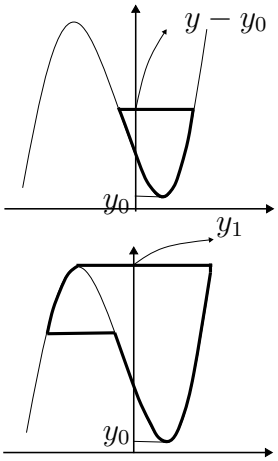

Figura 4.14: lps of type I and III. Figure made by the author.

- *(II)* $\lim_{\epsilon\to 0}\Gamma_{\epsilon,c(\epsilon)} = \Gamma^I_{y-y_0} \Leftrightarrow \forall\epsilon > 0; c(\epsilon) \geq c_0(\epsilon)$ *and* $\lim_{\epsilon\to 0}(-\epsilon\log(c(\epsilon) - c_0(\epsilon))) = k(y - y_0)$*;*
- *(III)* $\lim_{\epsilon\to 0}\Gamma_{\epsilon c(\epsilon)} = \Gamma^{II} \Leftrightarrow \lim_{\epsilon\to 0}(-\epsilon\log|c(\epsilon) - c_0(\epsilon)|) \geq k\left(\frac{1}{6}\right)$*;*
- *(IV)* $\lim_{\epsilon\to 0}\Gamma_{\epsilon,c(\epsilon)} = \Gamma^{III}_y \Leftrightarrow \forall\epsilon > 0; c(\epsilon) \leq c_0(\epsilon)$ *and* $\lim_{\epsilon\to 0}(-\epsilon\log(c_0(\epsilon) - c(\epsilon))) = k(y - y_0)$*;*
- *(V)* $\lim_{\epsilon\to 0}\Gamma_{\epsilon,c(\epsilon)} = \Gamma^B \Leftrightarrow \forall\epsilon > 0; c(\epsilon) < c_0(\epsilon)$ *and* $\lim_{\epsilon\to 0}(-\epsilon\log(c_0(\epsilon) - c(\epsilon))) \leq 0$*;*

where $k(y - y_0)$ *is given by*

$$k(y) = \int_0^{x(y-y_0)} x(1+x)^2\,dx,$$

being $y \in [y_0, y_1]$.

Here k is C^1, $k'(y - y_0) = 1 + x(y - y_0)$, k is analytic in $]y_0, y_1[$, $k(y_0)$ near from 0 and $k(y_1 - y_0)$ near from 1/12.

This theorem describes precisely the canard form in function of the asymptotic behavior from $c(\epsilon)$, when $\epsilon \to 0$.

The curve c_0 plays an important role. We can expand the function $\overline{a}$ in a Taylor series of order two around 0:

$$\overline{a}(x + h) = \overline{a}(x) + \overline{a}'(x)h + R(h),$$

with $\lim_{h\to 0}\dfrac{R(h)}{h} = 0$. Therefore, $\overline{a}(h)$ is approximately $-h$ and $c(\epsilon)$ is approximately $-\epsilon$. Those curves $c(\epsilon)$ described on the itens (II), (III) and (IV) have a flat contact with $c_0(\epsilon)$, as showed in the Figure 4.15. For $\epsilon > 0$ fixed, the transition between the big canard and the small canard occurs in an interval $I_\epsilon = [c(\epsilon) - a_\epsilon, c(\epsilon) + b_\epsilon]$ with $a \in I_\epsilon$, whose length is $b_\epsilon + a_\epsilon$ goes exponentially fast to zero when $\epsilon \to 0$. The limit cycle collapses in one of the cases from (I) to (V), depending on which curve $c(\epsilon)$ we are considering.

The proof of the next theorem can be found too in [32].

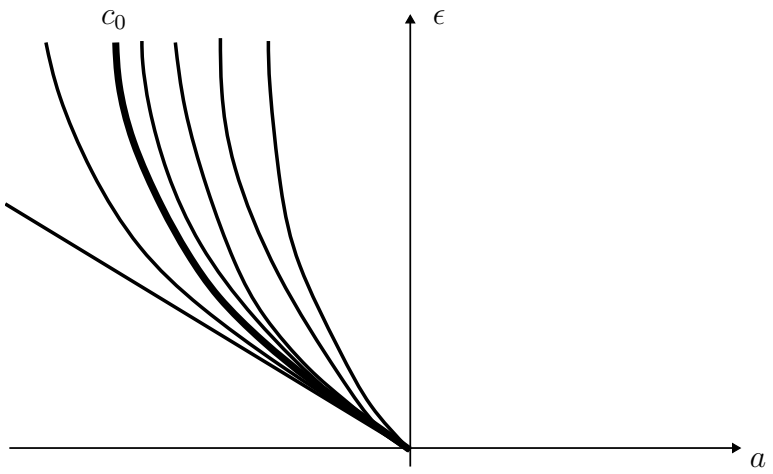

Figura 4.15: The curve c_0. Figure made by the author.

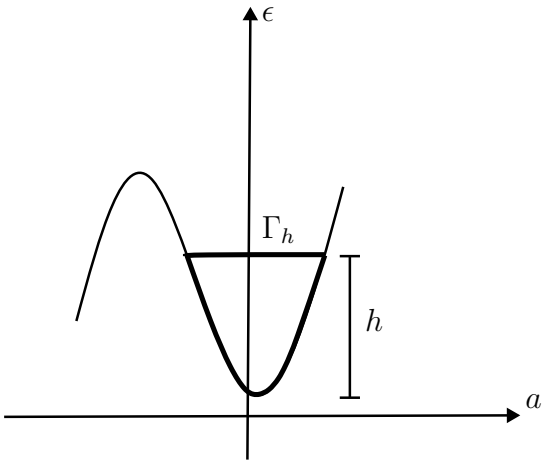

Figura 4.16: The canard cycle Γ_h. Figure made by the author.

Theorem 20. *For all $h \in (y_0, y_1)$, there exists a curve $a = c_h(\epsilon) = \epsilon^{\frac{1}{2}} c\left(\epsilon^{\frac{1}{2}}\right)$ with $c \in C^\infty$, $c(0) = 0$, such that $\Gamma_{\epsilon, c_h(\epsilon)} \longrightarrow \Gamma_h$ when $\epsilon \to 0$, where Γ_h is represented in Figure 4.16.*

Consider a generic system $\dot{x} = f(x, a)$, with $(x, a) \in \mathbb{R}^2 \times \mathbb{R}$ and $f \in C^n(\mathbb{R}^2 \times \mathbb{R})$. We denote $x = (x_1, x_2)^T$ and consider the one parameter family

$$Y = \begin{cases} \dot{x} = ax_1 - x_2 \pm (x_1^2 + x_2^2)\, x_1, \\ \dot{y} = x_1 + ax_2 \pm (x_1^2 + x_2^2)\, x_2, \end{cases} \tag{4.5}$$

where $a \in \mathbb{R}$ and $(x_1, x_2)^T = (0, 0)^T$ is a singularity. The system (4.5) presents the eigenvalues $\lambda_{1,2} = a \pm i$.

If we consider the complex variable $z = x_1 + ix_2$, from (4.5) we obtain $\dot{z} = z(a + i) \pm z|z|^2$ with $|z|$ being the norm of a complex number. In polar coordinates with $z = \rho e^{i\theta}$, system (4.5) takes the following form

$$Y_p = \begin{cases} \dot{\rho} = \rho(a \pm \rho^2), \\ \dot{\theta} = 1. \end{cases} \tag{4.6}$$

Considering the above system with the minus sign, we have

- (i) for $a < 0$, ρ is decreasing because $\dot{\rho} < 0$;

- (ii) for $a = 0$, ρ is decreasing too because $\dot{\rho} < 0$;
- (iii) for $a > 0$, ρ is decreasing if it is greater than $\sqrt{a}$ and is increasing if it is less than $\sqrt{a}$. There is no variation when $\rho = \sqrt{a}$ or $\rho = 0$ and so a limit cycle appears.

An analogous analysis could be apllied with the plus sign substituting the minus sign in (4.6). This is what is called the Hopf bifurcation and the system (4.5) is denominated the normal form of Hopf bifurcation.

Consider the family $\dot{x} = f(x, a)$ such that for $a = 0$, we have $f(0, 0) = 0$ and the Jacobian matrix $Jf(0, 0)$ has the eigenvalues $\lambda_{1,2} = \pm i\omega_0$, with $\omega_0 > 0$. This system can be written as $\dot{x} = A(a)x + F(x, a)$, where $A(a) = Jf(0, a)$ and $F(x, a) = (F_1(x, a), F_2(x, a))$ is of class C^n, $F_i : \mathbb{R}^2 \times \mathbb{R} \to \mathbb{R}$, for $i = 1, 2$ and F presents its Taylor expansion beginning with terms of order $O(|x|^2)$. The matrix $A(a)$ has the eigenvalues $\lambda_1(a) = \lambda(a)$ and $\lambda_2 = \overline{\lambda(a)}$, where $\lambda(a) = \gamma(a) + i\omega(a)$. We calculate $\lambda(0) = \gamma(0) + i\omega(0) = 0 + i\omega_0$, with $\omega_0 > 0$.

Let $q(a) \in \mathbb{C}^2$ a complex eigenvector of $A(a)$ associated to $\lambda(a)$, i.e., $A(a)q(a) = \lambda(a)q(a)$. Let $p(a) \in \mathbb{C}^2$ be such that

$$A(a)^T p(a) = \overline{\lambda(a)p(a)}. \tag{4.7}$$

It is always possible to choose $p(a) \in \mathbb{C}^2$ such that $\langle p(a), q(a)\rangle = 1$, where the inner product used here is given by $\langle p, q\rangle = \overline{p_1}q_1 + \overline{p_2}q_2$ with $p = (p_1, p_2)$ and $q = (q_1, q_2)$. Any vector $x \in \mathbb{R}^2$ can be written as $x = zq(a) + \overline{z}\overline{q(a)}$ for some $z \in \mathbb{C}$.

The system $\dot{x} = A(a)x + F(x, a)$ can be written, for a small enough, in the form $\dot{z} = \lambda(a)z + g(z, \overline{z}, a)$, where $g = O(|z|^2)$ is a function C^n given by

$$g(z, \overline{z}, a) = \langle p(a), F\left(zq(a) + \overline{z}\overline{q(a)}, a\right)\rangle.$$

Suppose that for $a = 0$, $F(x, a)$ can be represented by

$$F(x, 0) = \frac{1}{2}B(x, x) + \frac{1}{6}C(x, x, x) + O\left(|x|^4\right),$$

where $B(x, y)$ and $C(x, y, u)$ are multilinear simetric forms, with $x, y, u \in \mathbb{R}^2$. From this, we get

$$B_i(x, y) = \sum_{j,k=1}^{2} \frac{\partial^2 F_i(\alpha, 0)}{\partial\alpha_j\alpha_k}|_{\alpha=0} x_j x_k, \text{ for } i = 1, 2,$$

and

$$C_i(x, y, u) = \sum_{j,k,l=1}^{2} \frac{\partial^3 F_i(\alpha, 0)}{\partial\alpha_j\partial\alpha_k\partial\alpha_l}|_{\alpha=0} x_j x_k x_l, \text{ for } i = 1, 2.$$

The quadratic terms and the cubic term of $g(z, \overline{z}, 0)$ that is interesting for us are the following ones

$$\begin{aligned} g_{11} &= \langle p, B(q, \overline{q})\rangle, \\ g_{20} &= \langle p, B(q, q)\rangle, \\ g_{02} &= \langle p, B(\overline{q}, \overline{q})\rangle, \\ g_{21} &= \langle p, C(q, q, \overline{q})\rangle. \end{aligned}$$

The Lyapunov function l_1 calculated at 0 is known as the first Lyapunov coefficient and it is given by

$$l_1(0) = \frac{1}{2\omega_0^2} Re\left(ig_{20}g_{11} + \omega_0 g_{21}\right).$$

Joining the previous explanations about Hopf bifurcation, we obtain the following theorem.

Theorem 21. *Any bidimensional system* $\frac{dx}{dt} = f(x,a)$, $x \in \mathbb{R}^2$, $a \in \mathbb{R}$ *with* $f \in C^n(\Omega)$, $\Omega \subset \mathbb{R}^2 \times \mathbb{R}$, *having the singularity* $x = 0$, $\forall |a| << 1$, *with eigenvalues* $\lambda_{1,2}(a) = \gamma(a) + i\omega(a)$, *where* $\gamma(0) = 0$, $\omega(0) = \omega_0 > 0$, *satisfying the following conditions*

- *(i)* $l_1(0) \neq 0$,
- *(ii)* $\gamma'(0) \neq 0$,

is locally topologically equivalent around the origin to one of the normal forms showed in system (4.5).

The regularized system

$$X_{pert} = \begin{cases} \dot{x} = y - \dfrac{x^3}{\eta} - \dfrac{x^2}{\eta} + x \\ \dot{y} = \epsilon(a - x) \end{cases},$$

has only one singularity $p_a = \left(a, \dfrac{a^3}{\eta} + \dfrac{a^2}{\eta} - a\right)$, whose eigenvalues are

$$\lambda_{1,2}(a) = \frac{-2a - 3a^2 + \eta \pm \sqrt{(2a + 3a^2 - \eta)^2 - 4\epsilon\eta^2}}{2\eta}.$$

The real part of $\lambda_{1,2}(a)$ are

$$\gamma(a) = \frac{-2a - 3a^2 + \eta}{2\eta}$$

and

$$\omega(a) = \frac{\sqrt{4\epsilon\eta^2 - (2a + 3a^2 - \eta)^2}}{2\eta},$$

because here we are considering $\Delta < 0$. Therefore, $\gamma(a) = 0 \Leftrightarrow a = \dfrac{1}{3}(-1 \pm \sqrt{1 + 3\eta})$ and we consider only the value $a_1 = \dfrac{1}{3}(-1 + \sqrt{1 + 3\eta})$, because the other value (with -"sign) stays out of the regularization range forη small enough, while a with the "+"sign always stays in the range of the regularization when $\eta \to 0$.

In these conditions, the eigenvalues are given by $\lambda_a = \lambda\left(\dfrac{1}{3}(-1 + \sqrt{1 + 3\eta})\right) = \pm 2\eta\sqrt{\epsilon}$ and p_a is an attractor focus when $a > a_1 = \dfrac{1}{3}(-1 + \sqrt{1 + 3\eta})$, near a_1 and p_a is a repulsor focus when $a < a_1$, near a_1. The condition (ii) of Theorem 21 is verified below:

$$\gamma'(a) = -\frac{1 + 3a}{\eta},$$

and therefore

$$\gamma'(a_1) = -\frac{1 + 3\eta}{\eta} \neq 0,$$

for $\eta > 0$. To verify the condition (i) from Theorem 21, we must compute the first Lyapunov coefficient in a_1. So, fixing $a = a_1$, we have

$$p_a = p_{a_1} = \left(\frac{1}{3}\left(-1 + \sqrt{1 + 3\eta}\right), \frac{(-1 - 6\eta + \sqrt{1 + 3\eta})}{9(1 + \sqrt{1 + 3\eta})}\right).$$

Therefore, we must do the translation of p_{a_1} to the origin, obtaining the following system:

$$X = \begin{cases} \dot{x} = y - \dfrac{x^2\left(x + \sqrt{1+3\eta}\right)}{\eta} \\ \dot{y} = -x\epsilon \end{cases} . \tag{4.8}$$

The Jacobian matrix now is given by

$$A_0 = \begin{pmatrix} 0 & 1 \\ -\epsilon & 0 \end{pmatrix}.$$

So, the system (4.8) for $a = a_1$, writes as

$$\dot{\mathbf{x}} = A_0\mathbf{x} + \mathbf{F}\left(\mathbf{x}, \mathbf{0}\right),$$

where $\mathbf{x} = (\mathbf{x}, \mathbf{y}) \in \mathbb{R}^{\mathbf{2}}$. From now on, we denote the ordering pair (x, y) by (x_1, x_2). In this way

$$F\left(\mathbf{x}, \mathbf{0}\right) = \left(-\frac{x^3}{\eta} - \frac{x^2}{\eta}\sqrt{1+3\eta} + x, 0\right) = \left(F_1\left(\mathbf{x}, \mathbf{0}\right), F_2\left(\mathbf{x}, \mathbf{0}\right)\right),$$

where, expanding $F\left(\mathbf{x}, \mathbf{0}\right)$, we have

$$F\left(\mathbf{x}, \mathbf{0}\right) = \frac{1}{2}B\left(\mathbf{x}, \mathbf{x}\right) + \frac{1}{6}C\left(\mathbf{x}, \mathbf{x}, \mathbf{x}\right),$$

with $B\left(\mathbf{x}, \mathbf{x}\right) = \left(B_1\left(\mathbf{x}, \mathbf{x}\right), B_2\left(\mathbf{x}, \mathbf{x}\right)\right)$ and $C\left(\mathbf{x}, \mathbf{x}, \mathbf{x}\right) = \left(C_1\left(\mathbf{x}, \mathbf{x}, \mathbf{x}\right), C_2\left(\mathbf{x}, \mathbf{x}, \mathbf{x}\right)\right)$.

We see that

$$B_i\left(\mathbf{x}, \mathbf{y}\right) = B_i\left(x_1, x_2, y_1, y_2\right) = \sum_{j,k=1}^{2} \frac{\partial^2 F_i\left(\mathbf{z}, \mathbf{0}\right)}{\partial z_j, \partial z_k}|_{\mathbf{z}=(\mathbf{0},\mathbf{0})} x_j y_k,$$

with $\mathbf{z} = (\mathbf{z_1}, \mathbf{z_2})$ and $\mathbf{x}$, $\mathbf{y} \in \mathbb{R}^2$. Therefore $B_1\left(\mathbf{x}, \mathbf{y}\right) = -\dfrac{2\sqrt{1+3\eta}}{\eta} x_1 y_1$ and $B_2\left(\mathbf{x}, \mathbf{y}\right) = 0$, due to the fact that $F_2\left(\mathbf{x}\right) = 0$. Now

$$C_i\left(\mathbf{x}, \mathbf{y}, \mathbf{v}\right) = \sum_{j,k,l=1}^{2} \frac{\partial^3 F_i\left(\mathbf{z}, \mathbf{0}\right)}{\partial z_j \partial z_k \partial z_l}|_{\mathbf{z}=(\mathbf{0},\mathbf{0})} x_j y_k v_l,$$

with $\mathbf{z} = (\mathbf{z_1}, \mathbf{z_2})$ and $\mathbf{x}$, $\mathbf{y}$, $\mathbf{v} \in \mathbb{R}^2$ and $\mathbf{v} = (v_1, v_2)$. So we get

$$C_1\left(\mathbf{x}, \mathbf{y}, \mathbf{v}\right) = -\frac{6}{\eta} x_1 y_1 v_1$$

and $C_2\left(\mathbf{x}, \mathbf{y}, \mathbf{v}\right) = 0$. Therefore, we get

$$B\left(\mathbf{x}, \mathbf{y}\right) = \left(-\frac{2\sqrt{1+3\eta}}{\eta} x_1 y_1, 0\right) \text{ and } C\left(\mathbf{x}, \mathbf{y}, \mathbf{v}\right) = \left(-\frac{6}{\eta} x_1 y_1 v_1, 0\right).$$

Let $q\left(1, i\sqrt{\epsilon}\right)$ and $\overline{q} = \left(1, -i\sqrt{\epsilon}\right)$ the eigenvectors associated to the eigenvalors from the matrix A_0. We compute the vector $\overline{p\left(\alpha\right)}$, whose expression is found in (4.7), obtaining $\overline{p} = \left(i\sqrt{\epsilon}, 1\right)$. Multiplying $\overline{p}$ by $\dfrac{1}{2i\sqrt{\epsilon}}$, we obtain the vector $p = \dfrac{1}{2i\sqrt{\epsilon}}\overline{p}$. So,

$$\langle p, q\rangle = \langle\left(\frac{1}{2}, \frac{1}{2i\sqrt{\epsilon}}\right), \left(1, i\sqrt{\epsilon}\right)\rangle = \frac{1}{2} + \frac{1}{2} = 1.$$

Finally, we have to calculate the terms g_{20}, g_{11} and g_{21}, as follows below

$$g_{20} = \langle p, B\left(q,q\right)\rangle = \langle\left(\frac{1}{2}, \frac{1}{2i\sqrt{\epsilon}}\right), \left(-\frac{2\sqrt{1+3\eta}}{\eta}, 0\right)\rangle = -\frac{\sqrt{1+3\eta}}{\eta},$$

$$g_{11} = \langle p, B\left(q,\overline{q}\right)\rangle = \langle\left(\frac{1}{2}, \frac{1}{2i\sqrt{\epsilon}}\right), \left(-\frac{2\sqrt{1+3\eta}}{\eta}, 0\right)\rangle = -\frac{\sqrt{1+3\eta}}{\eta},$$

$$g_{21} = \langle\left(\frac{1}{2}, \frac{1}{2i\sqrt{\epsilon}}\right), \left(-\frac{6}{\eta}, 0\right)\rangle = -\frac{3}{\eta},$$

and finally

$$l_1\left(0\right) = \frac{1}{2\omega\left(a_1\right)^2} Re\left(ig_{20}g_{11} + \omega_0 g_{21}\right) =$$

$$\frac{1}{2\epsilon} Re\left(i\left(-\frac{\sqrt{1+3\eta}}{\eta}\right)\left(-\frac{\sqrt{1+3\eta}}{\eta}\right) + \sqrt{\epsilon}\left(-\frac{3}{\eta}\right)\right) = -\frac{3\sqrt{\epsilon}}{2\epsilon\eta} < 0,$$

ensuring that the system analyzed presents a Hopf bifurcation for $a_1 = \frac{1}{3}\left(-1+\sqrt{1+3\eta}\right)$.

4.3 Analysis for the Perturbed Regularized Fields in the Charts

The concepts of blow-up methods used in this section are taken from the reference [49], chapter 7. From the regularized field obtained before

$$X_{pert} = \begin{cases} \dot{x} = y - \frac{x^3}{\eta} - \frac{x^2}{\eta} + x, \\ \dot{y} = \epsilon\left(a - x\right), \end{cases}$$

we made a translation of the point

$$p_1 = \left(a_1, f\left(a_1\right)\right) = \left(\frac{-1+\sqrt{1+3\eta}}{3}, \frac{-1-6\eta+\sqrt{1+3\eta}}{9\left(1+\sqrt{1+3\eta}\right)}\right)$$

to the origin of the coordinate system, where

$$f\left(a_1\right) = \frac{a_1^3}{\eta} + \frac{a_1^2}{\eta} - a_1.$$

The singularity p_2 is not considered because, as long as $\eta \to 0$,

$$p_2 = \left(\frac{-1-\sqrt{1+3\eta}}{3}, \frac{1+6\eta+\sqrt{1+3\eta}}{9\left(1+\sqrt{1+3\eta}\right)}\right)$$

does not go to zero, staying, at a determined moment, out of the regularization range. The corresponding change of variables applied is

$$\overline{x} = x - \frac{\left(-1+\sqrt{1+3\eta}\right)}{3},$$

and

$$\overline{y} = y - \frac{-1-6\eta+\sqrt{1+3\eta}}{9\left(1+\sqrt{1+3\eta}\right)},$$

furthermore $\overline{\epsilon} = \epsilon$, $\overline{a} = a$.

After the computations to obtain the new vector field X_{pert} through the change of variables, we get

$$\overline{X}_{pert} = \begin{cases} \dot{\overline{x}} = \overline{y} - \frac{\overline{x}^3}{\eta} - \frac{\overline{x}^2\left(1+3\eta+\sqrt{1+3\eta}\right)}{\eta\left(1+\sqrt{1+3\eta}\right)}, \\ \dot{\overline{y}} = -\frac{1}{3}\overline{\epsilon}\left(-1-3a+3x+\sqrt{1+3\eta}\right). \end{cases} \tag{4.9}$$

The blow up process now begins at the singularity point p_1.

The blow up process applied at the singularity p_1 begins with the establishment of weights for the variables $\overline{x}$, $\overline{y}$, $\overline{\epsilon}$ and $\overline{a}$. After choose the weights of the variables, we can divide the system by some $u^\tau, \tau \in \mathbb{N}$, which gives origin to the system desingularization, eliminating the non elementary singularities.

$$\phi_2 : \mathbb{S}^3 \times [0, U'[\longrightarrow M - \{p_2\}$$

$$(\overline{x}, \overline{y}, \overline{\epsilon}, \overline{a}, u) \to \left(u\overline{x}, u^2\overline{y}, u^3\overline{\epsilon}, u\overline{a}\right).$$

The radius of the blow up above should be small than the distance between the two singularities p_1 and p_2. Let M be the dominium of the perturbed vector field $\overline{X}_{pert}$.

Let $q \in M - \{p_2\}$ and $p \in \mathbb{S}^3 \times [0, U'[$. The blow up vector field stays as

$$\widehat{X}_2(p) = \left(D\phi_2^{-1}(q)\right)\left(\overline{X}_2(q)\right) = \left(D\phi_2(p)\right)^{-1}\left(\overline{X}_2(\phi_2(p))\right),$$

where

$$D\phi_2 = \begin{pmatrix} u & 0 & 0 & \overline{x} \\ 0 & u^2 & 0 & 2u\overline{y} \\ 0 & 0 & 0 & 3u^2 \\ 0 & 0 & u & \overline{a} \end{pmatrix},$$

for the chart $\{\overline{\epsilon} = 1\}$. The inverse matrix of $D\phi_2$ is represented as:

$$\left(D\phi_2\right)^{-1} = \begin{pmatrix} u^{-1} & 0 & -\frac{-u^{-3}\overline{x}}{3} & 0 \\ 0 & u^{-2} & -\frac{2u^{-3}\overline{y}}{3} & 0 \\ 0 & 0 & -\frac{u^{-3}\overline{a}}{3} & u^{-1} \\ 0 & 0 & \frac{u^{-2}}{3} & 0 \end{pmatrix}.$$

Therefore, $\left(D\phi_2\right)^{-1}\left(\overline{X}_2\right) =$

$$= \begin{pmatrix} u^{-1} & 0 & -\frac{-u^{-3}\overline{x}}{3} & 0 \\ 0 & u^{-2} & -\frac{2u^{-3}\overline{y}}{3} & 0 \\ 0 & 0 & -\frac{u^{-3}\overline{a}}{3} & u^{-1} \\ 0 & 0 & \frac{u^{-2}}{3} & 0 \end{pmatrix} \cdot \begin{pmatrix} u^2\overline{y} - \frac{u^3\overline{x}^3}{\eta} - \frac{u^2\overline{x}^2\left(1+3\eta+\sqrt{1+3\eta}\right)}{\eta\left(1+\sqrt{1+3\eta}\right)} \\ -\frac{1}{3}u^3\left(-1-3au+3u\overline{x}+\sqrt{1+3\eta}\right) \\ 0 \\ 0 \end{pmatrix} =$$

$$= \begin{pmatrix} u\left(\overline{y} - \frac{u\overline{x}^3}{\eta} - \frac{\overline{x}^2\left(1+3\eta+\sqrt{1+3\eta}\right)}{\eta\left(1+\sqrt{1+3\eta}\right)}\right) \\ -\frac{1}{3}u\left(-1-3au+3ux+\sqrt{1+3\eta}\right) \\ 0 \\ 0 \end{pmatrix}.$$

We get, therefore,

$$\widehat{X_2} = \left(u\left(\overline{y} - \frac{u\overline{x}^3}{\eta} - \frac{\overline{x}^2\left(1+3\eta+\sqrt{1+3\eta}\right)}{\eta\left(1+\sqrt{1+3\eta}\right)} \right), u\left(\frac{1}{3} + au - ux - \frac{\sqrt{1+3\eta}}{3} \right), 0, 0 \right).$$

$$X_2^* = \frac{1}{u}\widehat{X_2} = \left(\overline{y} - \frac{u\overline{x}^3}{\eta} - \frac{\overline{x}^2\left(1+3\eta+\sqrt{1+3\eta}\right)}{\eta\left(1+\sqrt{1+3\eta}\right)}, \left(\frac{1}{3} + au - ux - \frac{\sqrt{1+3\eta}}{3} \right), 0, 0 \right).$$

For $u \to 0$, we get the following vector field

$$X_2^* = \left(\overline{y} - \frac{\overline{x}^2\left(1+3\eta+\sqrt{1+3\eta}\right)}{\eta\left(1+\sqrt{1+3\eta}\right)}, \frac{1}{3} - \frac{\sqrt{1+3\eta}}{3}, 0, 0 \right). \tag{4.10}$$

The phase portrait for the vector field (4.10) above becomes as showed in Figure 4.17.

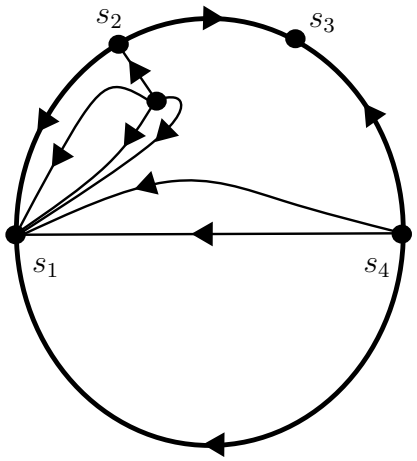

Figura 4.17: Phase portrait for the chart $\{\overline{\epsilon} = 1\}$. Figure made by the author.

For the chart $\{\overline{a} = 1\}$, we get:

$$D\phi_2 = \begin{pmatrix} u & 0 & 0 & \overline{x} \\ 0 & u^2 & 0 & 2u\overline{y} \\ 0 & 0 & u^3 & 3u^2\overline{\epsilon} \\ 0 & 0 & 0 & 1 \end{pmatrix},$$

and the inverse matrix of $D\phi_2$ is

$$(D\phi_2)^{-1} = \begin{pmatrix} u^{-1} & 0 & 0 & -u^{-1}\overline{x} \\ 0 & u^{-2} & 0 & -2u^{-1}\overline{y} \\ 0 & 0 & u^{-3} & -3\overline{\epsilon}u^{-1} \\ 0 & 0 & 0 & 1 \end{pmatrix}.$$

Therefore,

$$(D\phi_2)^{-1}\left(\overline{X_2}\right) = \begin{pmatrix} u^{-1} & 0 & 0 & -u^{-1}\overline{x} \\ 0 & u^{-2} & 0 & -2u^{-1}\overline{y} \\ 0 & 0 & u^{-3} & -3\overline{\epsilon}u^{-1} \\ 0 & 0 & 0 & 1 \end{pmatrix} \begin{pmatrix} u^2\overline{y} - \frac{u^3\overline{x}^3}{\eta} - \frac{u^2\overline{x}^2\left(1+3\eta+\sqrt{1+3\eta}\right)}{\eta\left(1+\sqrt{1+3\eta}\right)} \\ -\frac{1}{3}u^3\overline{\epsilon}\left(-1-3u+3u\overline{x}+\sqrt{1+3\eta}\right) \\ 0 \\ 0 \end{pmatrix} =$$

$$= \begin{pmatrix} u\left(\overline{y} - \frac{u\overline{x}^3}{\eta} - \frac{\overline{x}^2\left(1+3\eta+\sqrt{1+3\eta}\right)}{\eta\left(1+\sqrt{1+3\eta}\right)}\right) \\ -\frac{1}{3}u\overline{\epsilon}\left(-1+3u\left(-1+\overline{x}\right)+\sqrt{1+3\eta}\right) \\ 0 \\ 0 \end{pmatrix}.$$

Then, we get

$$\widehat{X_2} = \left(u\left(\overline{y} - \frac{u\overline{x}^3}{\eta} - \frac{\overline{x}^2\left(1+3\eta+\sqrt{1+3\eta}\right)}{\eta\left(1+\sqrt{1+3\eta}\right)}\right), -\frac{1}{3}u\overline{\epsilon}\left(-1+3u\left(-1+\overline{x}\right)+\sqrt{1+3\eta}\right), 0, 0\right).$$

$$X_2^* = \frac{1}{u}\widehat{X_2} = \left(\overline{y} - \frac{u\overline{x}^3}{\eta} - \frac{\overline{x}^2\left(1+3\eta+\sqrt{1+3\eta}\right)}{\eta\left(1+\sqrt{1+3\eta}\right)}, -\frac{1}{3}\overline{\epsilon}\left(-1+3u\left(-1+\overline{x}\right)+\sqrt{1+3\eta}\right), 0, 0\right).$$

Now, doing $u \to 0$, we obtain

$$X_2^* = \left(\overline{y} - \frac{\overline{x}^2\left(1+3\eta+\sqrt{1+3\eta}\right)}{\eta\left(1+\sqrt{1+3\eta}\right)}, -\frac{1}{3}\overline{\epsilon}\left(-1+\sqrt{1+3\eta}\right), 0, 0\right).$$

The phase portrait for this chart is given by Figure 4.18.

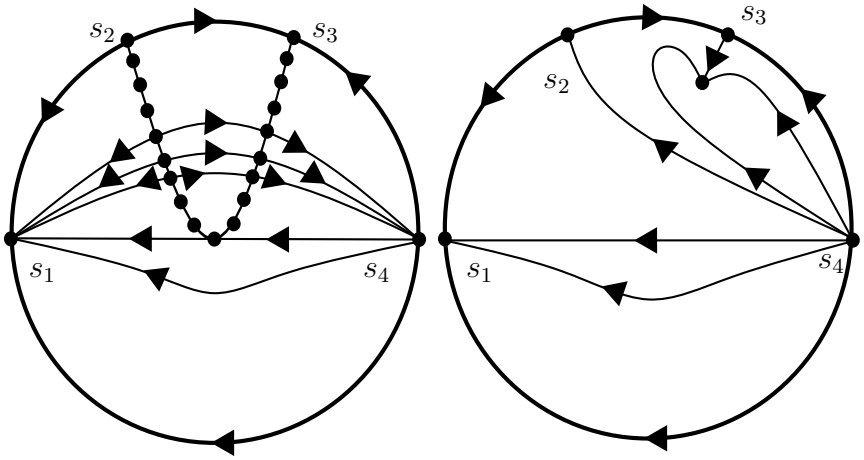

$\overline{\epsilon} = 0$ $\overline{\epsilon} > 0$

Figura 4.18: Phase portrait for the charts $\{\overline{a} = \pm 1\}$. Figure made by the author.

For the chart $\{\overline{a} = -1\}$, we obtain

$$(D\phi_2)^{-1}\left(\overline{X}_2\right) = \begin{pmatrix} u^{-1} & 0 & 0 & xu^{-1} \\ 0 & u^{-2} & 0 & 2yu^{-1} \\ 0 & 0 & u^{-3} & 3u^{-1}\overline{\epsilon} \\ 0 & 0 & 0 & -1 \end{pmatrix} \begin{pmatrix} u^2\overline{y} - \frac{u^3\overline{x}^3}{\eta} - \frac{u^2\overline{x}^2\left(1+3\eta+\sqrt{1+3\eta}\right)}{\eta\left(1+\sqrt{1+3\eta}\right)} \\ -\frac{1}{3}u^3\overline{\epsilon}\left(-1+3u+3ux+\sqrt{1+3\eta}\right) \\ 0 \\ 0 \end{pmatrix} =$$

$$\begin{pmatrix} u\left(\overline{y} - \frac{u\overline{x}^3}{\eta} - \frac{\overline{x}^2\left(1+3\eta+\sqrt{1+3\eta}\right)}{\eta\left(1+\sqrt{1+3\eta}\right)}\right) \\ -\frac{1}{3}u\overline{\epsilon}\left(-1+3u\left(1+\overline{x}\right)+\sqrt{1+3\eta}\right) \\ 0 \\ 0 \end{pmatrix}.$$

Then, we get $\widehat{X_2} = u\left(\overline{y} - \frac{u\overline{x}^3}{\eta} - \frac{\overline{x}^2\left(1+3\eta+\sqrt{1+3\eta}\right)}{\eta\left(1+\sqrt{1+3\eta}\right)}, -\frac{1}{3}\overline{\epsilon}\left(-1+3u\left(1+\overline{x}\right)+\sqrt{1+3\eta}\right), 0, 0\right)$.

$$X_2^* = \frac{1}{u}\widehat{X_2} = \left(\overline{y} - \frac{u\overline{x}^3}{\eta} - \frac{\overline{x}^2\left(1+3\eta+\sqrt{1+3\eta}\right)}{\eta\left(1+\sqrt{1+3\eta}\right)}, -\frac{1}{3}\overline{\epsilon}\left(-1+3u\left(1+\overline{x}\right)+\sqrt{1+3\eta}\right), 0, 0\right).$$

Doing $u \to 0$, we stay with the following system

$$X_2^* = \left(\overline{y} - \frac{\overline{x}^2 \left(1 + 3\eta + \sqrt{1+3\eta}\right)}{\eta \left(1 + \sqrt{1+3\eta}\right)}, -\frac{1}{3}\overline{\epsilon}\left(-1 + \sqrt{1+3\eta}\right), 0, 0 \right).$$

So, the phase portrait for the chart $\{\overline{a} = -1\}$ is the same as the phase portrait for the chart $\{\overline{a} = 1\}$, due to the fact that X_2^* is the same for both charts $\{\overline{a} = \pm 1\}$.

For the chart $\{\overline{x} = +1\}$, we have

$$D\phi_2 = \begin{pmatrix} 0 & 0 & 0 & 1 \\ u^2 & 0 & 0 & 2u\overline{y} \\ 0 & u^3 & 0 & 3u^2\overline{\epsilon} \\ 0 & 0 & u & \overline{a} \end{pmatrix},$$

$$(D\phi_2)^{-1} = \begin{pmatrix} -2\overline{y}u^{-1} & u^{-2} & 0 & 0 \\ -3\overline{\epsilon}u^{-1} & 0 & u^{-3} & 0 \\ -\overline{a}u^{-1} & 0 & 0 & u^{-1} \\ 1 & 0 & 0 & 0 \end{pmatrix}.$$

Therefore, $\overline{X}_2 =$

$$(D\phi_2)^{-1}\left(\overline{X_2}\right) = \begin{pmatrix} -2\overline{y}u^{-1} & u^{-2} & 0 & 0 \\ -3\overline{\epsilon}u^{-1} & 0 & u^{-3} & 0 \\ -\overline{a}u^{-1} & 0 & 0 & u^{-1} \\ 1 & 0 & 0 & 0 \end{pmatrix} \begin{pmatrix} u^2\overline{y} - \frac{u^3}{\eta} - \frac{u^2\left(1+3\eta+\sqrt{1+3\eta}\right)}{\eta\left(1+\sqrt{1+3\eta}\right)} \\ -\frac{1}{3}u^3\overline{\epsilon}\left(-1 + 3u - 3au + \sqrt{1+3\eta}\right) \\ 0 \\ 0 \end{pmatrix} =$$

$$= \begin{pmatrix} \frac{u\left(6u\overline{y} - 6\overline{y}^2\eta + 3(-1+\overline{a})u\overline{\epsilon}\eta + 6\overline{y}\sqrt{1+3\eta} - \overline{\epsilon}\eta\left(-1+\sqrt{1+3\eta}\right)\right)}{3\eta} \\ -\frac{3\overline{\epsilon}u\left(u - \overline{y}\eta + \sqrt{1+3\eta}\right)}{\eta} \\ -\frac{\overline{a}u\left(u - \overline{y}\eta + \sqrt{1+3\eta}\right)}{\eta} \\ -\frac{u^2\left(u - \overline{y}\eta + \sqrt{1+3\eta}\right)}{\eta} \end{pmatrix} =$$

$$= u \begin{pmatrix} \frac{6u\overline{y} - 6\overline{y}^2\eta + 3(-1+\overline{a})u\overline{\epsilon}\eta + 6\overline{y}\sqrt{1+3\eta} - \overline{\epsilon}\eta\left(-1+\sqrt{1+3\eta}\right)}{3\eta} \\ -\frac{3\overline{\epsilon}\left(u - \overline{y}\eta + \sqrt{1+3\eta}\right)}{\eta} \\ -\frac{\overline{a}\left(u - \overline{y}\eta + \sqrt{1+3\eta}\right)}{\eta} \\ -\frac{u\left(u - \overline{y}\eta + \sqrt{1+3\eta}\right)}{\eta} \end{pmatrix}.$$

Doing the transformation $\widehat{X_2} = \frac{1}{u}\overline{X}_2$, we get the following vector field:

$$\widehat{X_2} : \begin{cases} \dot{\overline{y}} = \frac{6u\overline{y} - 6\overline{y}^2\eta + 3(-1+\overline{a})u\overline{\epsilon}\eta + 6\overline{y}\sqrt{1+3\eta} - \overline{\epsilon}\eta\left(-1+\sqrt{1+3\eta}\right)}{3\eta}, \\ \dot{\overline{\epsilon}} = -\frac{3\overline{\epsilon}\left(u - \overline{y}\eta + \sqrt{1+3\eta}\right)}{\eta}, \\ \dot{\overline{a}} = -\frac{\overline{a}\left(u - \overline{y}\eta + \sqrt{1+3\eta}\right)}{\eta}, \\ \dot{u} = -\frac{u\left(u - \overline{y}\eta + \sqrt{1+3\eta}\right)}{\eta}. \end{cases}$$

Doing $\overline{\epsilon} \to 0$ and $\overline{a} \to 0$, we obtain

$$X_2^* : \begin{cases} \dot{\overline{y}} = \frac{2\overline{y}\left(u - y\eta + \sqrt{1+3\eta}\right)}{\eta}, \\ \dot{u} = -\frac{u\left(u - \overline{y}\eta + \sqrt{1+3\eta}\right)}{\eta}. \end{cases}$$

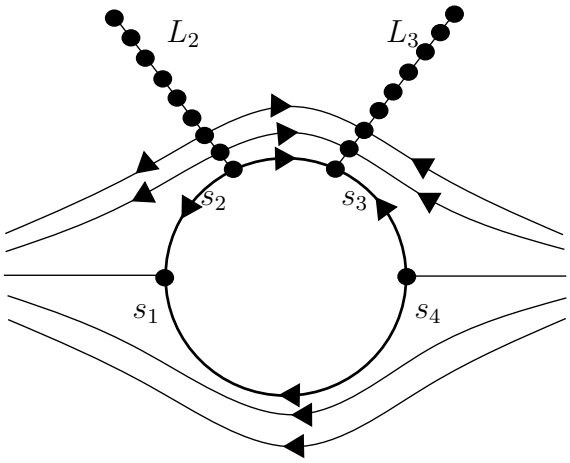

Figura 4.19: Phase portrait for the charts $\{\overline{x} = \pm 1\}$. Figure made by the author.

The phase portrait for the chart $\{\overline{x} = 1\}$ is given by Figure 4.19 below.
For the chart $\{\overline{x} = -1\}$, initially we have

$$\overline{X}_2 = (D\phi_2)^{-1}(X_2) = \begin{pmatrix} 2\overline{y}u^{-1} & u^{-2} & 0 & 0 \\ 3\overline{\epsilon}u^{-1} & 0 & u^{-3} & 0 \\ \overline{a}u^{-1} & 0 & 0 & u^{-1} \\ -1 & 0 & 0 & 0 \end{pmatrix} \begin{pmatrix} u^2\overline{y} + \frac{u^3}{\eta} - \frac{u^2\left(1+3\eta+\sqrt{1+3\eta}\right)}{\eta\left(1+\sqrt{1+3\eta}\right)} \\ -\frac{1}{3}u^3\overline{\epsilon}\left(-1-3u-3\overline{a}u+\sqrt{1+3\eta}\right) \\ 0 \\ 0 \end{pmatrix} =$$

$$= \begin{pmatrix} \frac{u\left(6u\overline{y}+\left(6\overline{y}^2+\overline{\epsilon}+3(1+\overline{a})u\overline{\epsilon}\right)\eta-6\overline{y}\sqrt{1+3\eta}-\overline{\epsilon}\eta\sqrt{1+3\eta}\right)}{3\eta} \\ \frac{3u\overline{\epsilon}\left(u+\overline{y}\eta-\sqrt{1+3\eta}\right)}{\eta} \\ \frac{\overline{a}u\left(u+\overline{y}\eta-\sqrt{1+3\eta}\right)}{\eta} \\ -\frac{u^2\left(u+\overline{y}\eta-\sqrt{1+3\eta}\right)}{\eta} \end{pmatrix} =$$

$$= u \begin{pmatrix} \frac{6u\overline{y}+\left(6\overline{y}^2+\overline{\epsilon}+3(1+\overline{a})u\overline{\epsilon}\right)\eta-6\overline{y}\sqrt{1+3\eta}-\overline{\epsilon}\eta\sqrt{1+3\eta}}{3\eta} \\ \frac{3\overline{\epsilon}\left(u+\overline{y}\eta-\sqrt{1+3\eta}\right)}{\eta} \\ \frac{\overline{a}\left(u+\overline{y}\eta-\sqrt{1+3\eta}\right)}{\eta} \\ -\frac{u\left(u+\overline{y}\eta-\sqrt{1+3\eta}\right)}{\eta} \end{pmatrix}.$$

Through the transformation $\widehat{X}_2 = \frac{1}{u}\overline{X}_2$, we arrive at the following system

$$\widehat{X}_2 : \begin{cases} \dot{\overline{y}} = \frac{6u\overline{y}+\left(6\overline{y}^2+\overline{\epsilon}+3(1+\overline{a})u\overline{\epsilon}\right)\eta-6\overline{y}\sqrt{1+3\eta}-\overline{\epsilon}\eta\sqrt{1+3\eta}}{3\eta}, \\ \dot{\overline{\epsilon}} = \frac{3\overline{\epsilon}\left(u+\overline{y}\eta-\sqrt{1+3\eta}\right)}{\eta}, \\ \dot{\overline{a}} = \frac{\overline{a}\left(u+\overline{y}\eta-\sqrt{1+3\eta}\right)}{\eta}, \\ \dot{u} = -\frac{u\left(u+\overline{y}\eta-\sqrt{1+3\eta}\right)}{\eta}. \end{cases}$$

Doing $\overline{\epsilon} \to 0$ and $\overline{a} \to 0$, we have

$$X_2^* : \begin{cases} \dot{\overline{y}} = \frac{2\overline{y}\left(u+\overline{y}\eta-\sqrt{1+3\eta}\right)}{\eta}, \\ \dot{u} = -\frac{u\left(u+\overline{y}\eta-\sqrt{1+3\eta}\right)}{\eta}. \end{cases}$$

The phase portrait for this chart is the same as for the chart $\{\overline{x}=1\}$ and it is given by Figure 4.19.

For the chart $\{\overline{y}=1\}$, we stay with

$$D\phi_2=\begin{pmatrix} u & 0 & 0 & \overline{x} \\ 0 & 0 & 0 & 2u \\ 0 & u^3 & 0 & 3u^2\overline{\epsilon} \\ 0 & 0 & u & \overline{a} \end{pmatrix},$$

$$(D\phi_2)^{-1}=\begin{pmatrix} u^{-1} & -\frac{u^{-2}\overline{x}}{2} & 0 & 0 \\ 0 & -\frac{3\overline{\epsilon}u^{-2}}{2} & u^{-3} & 0 \\ 0 & -\frac{\overline{a}u^{-2}}{2} & 0 & u^{-1} \\ 0 & \frac{u^{-1}}{2} & 0 & 0 \end{pmatrix}.$$

$$(D\phi_2)^{-1}(X_2)=\begin{pmatrix} u^{-1} & -\frac{u^{-2}\overline{x}}{2} & 0 & 0 \\ 0 & -\frac{3\overline{\epsilon}u^{-2}}{2} & u^{-3} & 0 \\ 0 & -\frac{\overline{a}u^{-2}}{2} & 0 & u^{-1} \\ 0 & \frac{u^{-1}}{2} & 0 & 0 \end{pmatrix}\begin{pmatrix} u^2-\frac{u^3\overline{x}^3}{\eta}-\frac{u^2\overline{x}^2\left(1+3\eta+\sqrt{1+3\eta}\right)}{\eta\left(1+\sqrt{1+3\eta}\right)} \\ -\frac{1}{3}u^3\overline{\epsilon}\left(-1-3\overline{a}u+3u\overline{x}+\sqrt{1+3\eta}\right) \\ 0 \\ 0 \end{pmatrix}=$$

$$=\begin{pmatrix} \frac{1}{2}u\left(2-\overline{a}u\overline{x}\overline{\epsilon}-\frac{2\overline{x}^2}{\eta}+\frac{u\overline{x}^2(-2\overline{x}+\overline{\epsilon}\eta)}{\eta}-\frac{6\overline{x}^2}{1+\sqrt{1+3\eta}}+\frac{\overline{x}\overline{\epsilon}\eta}{1+\sqrt{1+3\eta}}\right) \\ \frac{1}{2}u\overline{\epsilon}^2\left(-1-3\overline{a}u+3u\overline{x}+\sqrt{1+3\eta}\right) \\ \frac{1}{6}\overline{a}u\overline{\epsilon}\left(-1-3\overline{a}u+3u\overline{x}+\sqrt{1+3\eta}\right) \\ \frac{1}{6}u^2\overline{\epsilon}\left(1+3\overline{a}u-3u\overline{x}-\sqrt{1+3\eta}\right) \end{pmatrix}=$$

$$=u\begin{pmatrix} \frac{1}{2}\left(2-\overline{a}u\overline{x}\overline{\epsilon}-\frac{2\overline{x}^2}{\eta}+\frac{u\overline{x}^2(-2\overline{x}+\overline{\epsilon}\eta)}{\eta}-\frac{6\overline{x}^2}{1+\sqrt{1+3\eta}}+\frac{\overline{x}\overline{\epsilon}\eta}{1+\sqrt{1+3\eta}}\right) \\ \frac{1}{2}\overline{\epsilon}^2\left(-1-3\overline{a}u+3u\overline{x}+\sqrt{1+3\eta}\right) \\ \frac{1}{6}\overline{a\epsilon}\left(-1-3\overline{a}u+3u\overline{x}+\sqrt{1+3\eta}\right) \\ \frac{1}{6}u\overline{\epsilon}\left(1+3\overline{a}u-3u\overline{x}-\sqrt{1+3\eta}\right) \end{pmatrix}.$$

From the system above, we get that $\frac{1}{2}\overline{\epsilon}\left(-1-3\overline{a}u+3u\overline{x}+\sqrt{1+3\eta}\right)=\frac{\dot{\overline{\epsilon}}}{\overline{\epsilon}}$. Therefore, we get the final system on the chart $\{\overline{y}=1\}$.

$$\frac{\dot{\overline{\epsilon}}}{\overline{\epsilon}}=\frac{3\dot{\overline{a}}}{\overline{a}}=-\frac{3\dot{u}}{u}.$$

$$X_2^*:\begin{cases} \dot{\overline{x}}=\frac{1}{2}\left(2-\overline{a}u\overline{x}\overline{\epsilon}-\frac{2\overline{x}^2}{\eta}+\frac{u\overline{x}^2(-2\overline{x}+\overline{\epsilon}\eta)}{\eta}-\frac{6x^2}{1+\sqrt{1+3\eta}}+\frac{\overline{x}\overline{\epsilon}\eta}{1+\sqrt{1+3\eta}}\right) \\ \dot{u}=\frac{1}{6}u\overline{\epsilon}\left(1+3\overline{a}u-3u\overline{x}-\sqrt{1+3\eta}\right) \end{cases}.$$

Now we introduce new parameters A, E and the variable v in such a way that

$$\begin{cases} \overline{\epsilon}=v^2, \\ \overline{a}=Av, \end{cases} \tag{4.11}$$

for $A\in[-A_0,A_0]$, where A_0 is large enough or

$$\begin{cases} \overline{\epsilon}=Ev^2, \\ \overline{a}=\pm v, \end{cases}, \tag{4.12}$$

for $E\in[0,E_0[$, with E_0 small enough. In this way, we get two types of charts parameterized by A and E, where the vector field X_2^*, for $y=1$ stays as

$$X_2^*=\begin{cases} \dot{\overline{x}}=\frac{1}{6}\left(6-3Auv^3\overline{x}-\frac{6\overline{x}^2\left(u\overline{x}+\sqrt{1+3\eta}\right)}{\eta}+v^2\overline{x}\left(-1+3u\overline{x}+\sqrt{1+3\eta}\right)\right), \\ \dot{u}=\frac{1}{6}uv^2\left(1+3Auv-3u\overline{x}-\sqrt{1+3\eta}\right), \\ \dot{v}=\frac{1}{6}v^3\left(-1-3Auv+3u\overline{x}+\sqrt{1+3\eta}\right), \end{cases}$$

using the substitution (4.11). On the other hand, if we use the substitution (4.12)), we get

$$X_2^* = \begin{cases} \dot{\overline{x}} = 1 - \frac{\overline{x}^2\left(u\overline{x}+\sqrt{1+3\eta}\right)}{\eta} + \frac{1}{2}Ev^2\overline{x}\left(u\left(-v+\overline{x}\right) + \frac{\eta}{1+\sqrt{1+3\eta}}\right), \\ \dot{u} = \frac{1}{6}Euv^2\left(1+3u\left(v-\overline{x}\right) - \sqrt{1+3\eta}\right), \\ \dot{v} = \frac{1}{6}Ev^3\left(-1+3u\left(-v+\overline{x}\right) + \sqrt{1+3\eta}\right). \end{cases}$$

The coordinates of the singularities s_2 and s_3 are respectively

$$s_2 = \left(-\frac{\sqrt{\eta}}{(1+3\eta)^{\frac{1}{4}}}, 0, 0\right) \text{ and } \left(\frac{\sqrt{\eta}}{(1+3\eta)^{\frac{1}{4}}}, 0, 0\right).$$

The phase portraits of X_2^* in these charts and for $\{uv = 0\}$ are represented below in Figure 4.20.

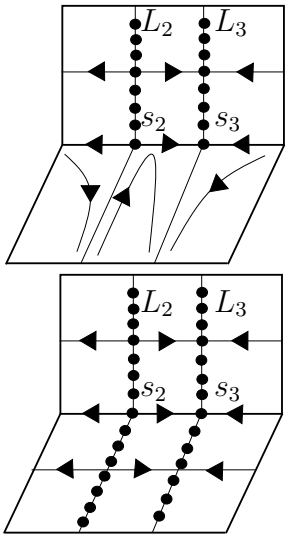

Figura 4.20: Phase portrait for the charts $\{\overline{y} = \pm 1\}$. Figure made by the author.

So, the general phase portrait for the charts worked above is showed in the Figure 4.21.

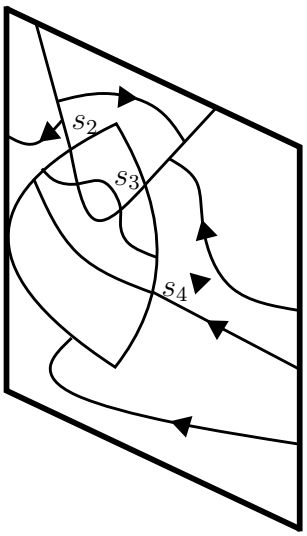

Figura 4.21: General phase portrait obtained from the charts. Figure made by the author.

For the chart $\{\overline{y}=-1\}$, we stay with

$$D\phi_2=\begin{pmatrix} u & 0 & 0 & \overline{x} \\ 0 & 0 & 0 & -2u \\ 0 & u^3 & 0 & 3u^2\overline{\epsilon} \\ 0 & 0 & u & \overline{a} \end{pmatrix},$$

$$(D\phi_2)^{-1}=\begin{pmatrix} u^{-1} & \frac{u^{-2}\overline{x}}{2} & 0 & 0 \\ 0 & \frac{3\overline{\epsilon}u^{-2}}{2} & u^{-3} & 0 \\ 0 & \frac{\overline{a}u^{-2}}{2} & 0 & u^{-1} \\ 0 & -\frac{u^{-1}}{2} & 0 & 0 \end{pmatrix}.$$

$$(D\phi_2)^{-1}(X_2)=\begin{pmatrix} u^{-1} & \frac{u^{-2}\overline{x}}{2} & 0 & 0 \\ 0 & \frac{3\overline{\epsilon}u^{-2}}{2} & u^{-3} & 0 \\ 0 & \frac{\overline{a}u^{-2}}{2} & 0 & u^{-1} \\ 0 & -\frac{u^{-1}}{2} & 0 & 0 \end{pmatrix}\begin{pmatrix} -u^2-\frac{u^3\overline{x}^3}{\eta}-\frac{u^2\overline{x}^2\left(1+3\eta+\sqrt{1+3\eta}\right)}{\eta\left(1+\sqrt{1+3\eta}\right)} \\ -\frac{1}{3}u^3\overline{\epsilon}\left(-1-3\overline{a}u+3u\overline{x}+\sqrt{1+3\eta}\right) \\ 0 \\ 0 \end{pmatrix}=$$

$$=\begin{pmatrix} -\frac{u\left(6\eta+\overline{x}\left(6u\overline{x}^2-\eta\overline{\epsilon}+3u(-a+\overline{x})\eta\overline{\epsilon}+\sqrt{1+3\eta}(6\overline{x}+\overline{\epsilon}\eta)\right)\right)}{6\eta} \\ \frac{1}{2}u\overline{\epsilon}^2\left(1+3\overline{a}u-3u\overline{x}-\sqrt{1+3\eta}\right) \\ \frac{1}{6}\overline{a}u\overline{\epsilon}\left(1+3\overline{a}u-3u\overline{x}-\sqrt{1+3\eta}\right) \\ \frac{1}{6}u^2\overline{\epsilon}\left(-1-3\overline{a}u+3u\overline{x}+\sqrt{1+3\eta}\right) \end{pmatrix}=$$

$$=u\begin{pmatrix} -\frac{\left(6\eta+\overline{x}\left(6u\overline{x}^2-\eta\overline{\epsilon}+3u(-a+\overline{x})\eta\overline{\epsilon}+\sqrt{1+3\eta}(6\overline{x}+\overline{\epsilon}\eta)\right)\right)}{6\eta} \\ \frac{1}{2}\overline{\epsilon}^2\left(1+3\overline{a}u-3u\overline{x}-\sqrt{1+3\eta}\right) \\ \frac{1}{6}\overline{a}\overline{\epsilon}\left(1+3\overline{a}u-3u\overline{x}-\sqrt{1+3\eta}\right) \\ \frac{1}{6}u\overline{\epsilon}\left(-1-3\overline{a}u+3u\overline{x}+\sqrt{1+3\eta}\right) \end{pmatrix}.$$

From the system above, we get that $\frac{1}{2}\overline{\epsilon}\left(1+3\overline{a}u-3u\overline{x}-\sqrt{1+3\eta}\right)=\frac{\dot{\overline{\epsilon}}}{\overline{\epsilon}}$. Therefore, we get the final system on the chart $\{\overline{y}=-1\}$:

$$\frac{\dot{\overline{\epsilon}}}{\overline{\epsilon}}=\frac{3\dot{\overline{a}}}{a}=-\frac{3\dot{u}}{u}.$$

$$X_2^*:\begin{cases} \dot{\overline{x}}=-\frac{\left(6\eta+\overline{x}\left(6u\overline{x}^2-\eta\overline{\epsilon}+3u(-a+\overline{x})\eta\overline{\epsilon}+\sqrt{1+3\eta}(6\overline{x}+\overline{\epsilon}\eta)\right)\right)}{6\eta}, \\ \dot{u}=\frac{1}{6}u\overline{\epsilon}\left(-1-3\overline{a}u+3u\overline{x}+\sqrt{1+3\eta}\right). \end{cases}$$

Again we use the new parameters A, E and the variable v from (4.11) and (4.12) and the vector field X_2^*, for $\overline{y}=-1$, stays as

$$X_2^*=\begin{cases} \dot{\overline{x}}=\frac{1}{6}\left(6-3Auv^3\overline{x}-\frac{6\overline{x}^2\left(u\overline{x}+\sqrt{1+3\eta}\right)}{\eta}+v^2\overline{x}\left(-1+3u\overline{x}+\sqrt{1+3\eta}\right)\right), \\ \dot{u}=\frac{1}{6}uv^2\left(1+3Auv-3u\overline{x}-\sqrt{1+3\eta}\right), \\ \dot{v}=\frac{1}{6}v^3\left(-1-3Auv+3u\overline{x}+\sqrt{1+3\eta}\right), \end{cases}$$

using the substitution (4.11). On the other hand, if we use the substitution (4.12), we get

$$X_2^*=\begin{cases} \dot{\overline{x}}=1-\frac{\overline{x}^2\left(u\overline{x}+\sqrt{1+3\eta}\right)}{\eta}+\frac{1}{2}Ev^2\overline{x}\left(u\left(-v+\overline{x}\right)+\frac{\eta}{1+\sqrt{1+3\eta}}\right), \\ \dot{u}=\frac{1}{6}Euv^2\left(1+3u\left(v-\overline{x}\right)-\sqrt{1+3\eta}\right), \\ \dot{v}=\frac{1}{6}Ev^3\left(-1+3u\left(-v+\overline{x}\right)+\sqrt{1+3\eta}\right), \end{cases},$$

equal like in the chart $\{\overline{y}=1\}$. The phase portraits are represented at the same Figures 4.20 and 4.21.

The coordinates of the singularities s_2 and s_3 are respectively

$$s_2 = \left(-\frac{\sqrt{\eta}}{(1+3\eta)^{\frac{1}{4}}}, 0, 0\right) \text{ and } \left(\frac{\sqrt{\eta}}{(1+3\eta)^{\frac{1}{4}}}, 0, 0\right).$$

So, the analysis for the chart $\{\overline{y}=-1\}$ is rigorously the same as the analysis made for the chart $\{\overline{y}=1\}$.

Blowing Up on the Lines N and S.

The lines N and S have two connected components, N_1, N_2 and S_1, S_2, respectively. Such lines are formed by singular non-elementary points, obtained when the parameter $\overline{a}$ vary with $\overline{\epsilon}=0$. Below, in the Figure 4.22, we have the representation of such lines in the space M_3, obtained after the blow up process applied at the points p_1 and p_2, which is represented by n and s respectively.

We denote by s_{11}, s_{12}, n_{21} and n_{22} the final points of the lines S_1, S_2, N_1 and N_2, respectively, inside the exceptional divisors of the blow ups already made.

The study for each one of the four connected components N_1, N_2, S_1 and S_2 is analogous. Therefore, we describe only the study for S_1 on the singularity that interest here (p_1).

Beyond the line S_1, the family is described by two equivalent vector fields: $X_{\overline{\epsilon a}}$ on the original coordinates and $\overline{X}_1$ after the blow up around the point s_{11} with $\overline{a}=-1$.

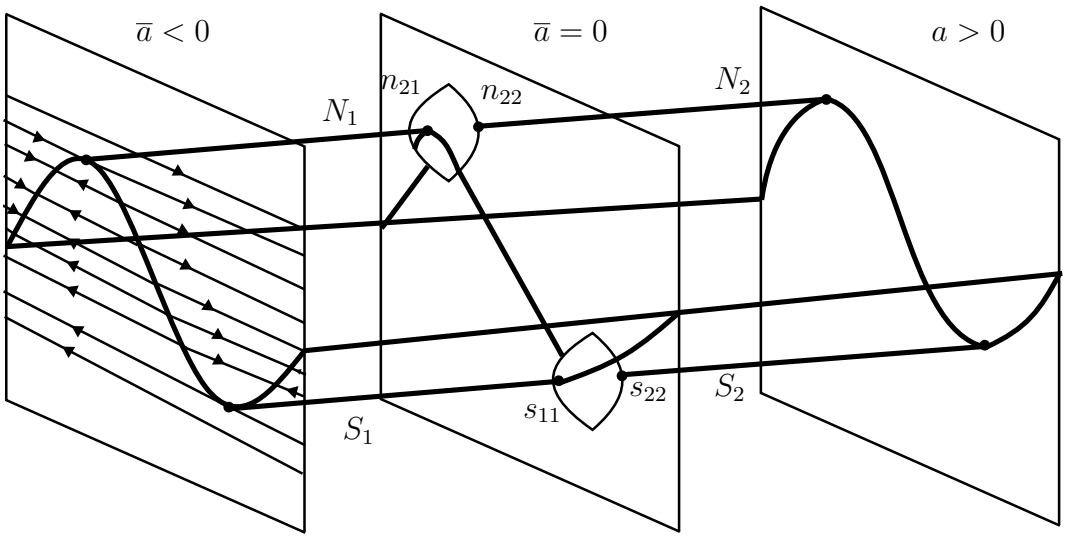

Figura 4.22: Representation of the lines N and S. Figure made by the author.

$$\overline{X}_{\overline{\epsilon},\overline{a}} = \begin{cases} \dot{\overline{x}} = \overline{y} - \frac{\overline{x}^3}{\eta} - \frac{\overline{x}^2\left(1+3\eta+\sqrt{1+3\eta}\right)}{\eta\left(1+\sqrt{1+3\eta}\right)}, \\ \dot{\overline{y}} = -\frac{1}{3}\overline{\epsilon}\left(-1-3a+3x+\sqrt{1+3\eta}\right), \end{cases}$$

$$\overline{X_1} = \begin{cases} \dot{\overline{x}} = \overline{y} - \frac{u\overline{x}^3}{\eta} - \frac{\overline{x}^2\left(1+3\eta+\sqrt{1+3\eta}\right)}{\eta\left(1+\sqrt{1+3\eta}\right)}, \\ \dot{\overline{y}} = -\frac{1}{3}\overline{\epsilon}\left(-1+3u\left(1+x\right)+\sqrt{1+3\eta}\right). \end{cases}$$

On the original coordinates (x, y, ϵ, a) we have $S_1 = \{x = y = \epsilon = 0\}$ and on the coordinates $(\overline{x}, \overline{y}, \overline{\epsilon}, u)$ we have $S_1 = \{\overline{x} = \overline{y} = \overline{\epsilon} = 0\}$.

We can write the family fields above as vector fields in $\mathbb{R}^4$,

$$\overline{X}_{\overline{\epsilon},\overline{a}} = \begin{cases} \dot{\overline{x}} = \overline{y} - \frac{\overline{x}^3}{\eta} - \frac{\overline{x}^2\left(1+3\eta+\sqrt{1+3\eta}\right)}{\eta\left(1+\sqrt{1+3\eta}\right)}, \\ \dot{\overline{y}} = -\frac{1}{3}\overline{\epsilon}\left(-1-3a+3x+\sqrt{1+3\eta}\right), \\ \dot{\overline{\epsilon}} = 0, \\ \dot{\overline{a}} = 0, \end{cases}$$

$$\overline{X_1} = \begin{cases} \dot{\overline{x}} = \overline{y} - \frac{u\overline{x}^3}{\eta} - \frac{\overline{x}^2\left(1+3\eta+\sqrt{1+3\eta}\right)}{\eta\left(1+\sqrt{1+3\eta}\right)}, \\ \dot{\overline{y}} = -\frac{1}{3}\overline{\epsilon}\left(-1+3u\left(1+x\right)+\sqrt{1+3\eta}\right), \\ \dot{\overline{\epsilon}} = 0, \\ \dot{u} = 0. \end{cases}$$

The change of coordinates is given by $x = u\overline{x}$, $y = u2\overline{y}$, $\epsilon = u^3\overline{\epsilon}$ and $a = -u$. The family fields above are equivalent for such changes. The blow ups

$$\overline{x} = \omega x'', \overline{y} = \omega^2 y'', \overline{\epsilon} = \omega^3 \epsilon'',$$

beyond $\left\{a \in \left[\frac{-1}{2}, a_0\right]\right\}$ for the field $X_{\overline{\epsilon},\overline{a}}$ and

$$\overline{x} = \omega_1 x'', \overline{y} = \omega_1^2 y'', \overline{\epsilon} = \omega_1^3 \epsilon'',$$

beyond $\{u \in [0, U[\}$ for the field $\overline{X_1}$, locally do a desingularization of the vector fields defined beyond the line S_1.

4.4 Center Manifolds and Melnikov Integral

Consider the vector field X_{pert} from the system 4.9. This vector field has non-isolated singular points, which are denominated as the set $Z_d(X)$. After the application of the desingularization process, all these points are partially hyperbolic, with one non null eigenvalue and three null eigenvalues. At the figure below, Figure 4.23, we have a tridimensional representation of M, with $Z_d(X) \subset \partial M$.

The existence of center manifolds of class C^k in each point $p \in Z_d(X)$ follows from general theorems from [32].

We are interested in the construction of center manifolds in the region

$$K = \bigcup_{\overline{\lambda_0}} \left\{ P_{\overline{\lambda_0}}; -A_0 \leq A \leq A_0, A = \frac{\overline{a_0}^2}{\overline{\epsilon_0}} \right\},$$

with A_0 small. Let $\gamma : v \mapsto (x, y, \epsilon) = (x(v), y(v), v^2)$ an arc C^∞ in the chart given by $(x, y) \in \mathbb{R}^2 \setminus \{p_1, p_2\}$, $\epsilon \in \mathbb{R}_+$ as showed in the Figure 4.24 below. Particularly, we consider the region defined here as β, which consists of connected components of the union of the final points of the lines $\overline{L_i}$ from the region F_0, that is characterized as the region from M with $\overline{a} = 0$ and $\overline{\epsilon} = 0$. The following proposition is proved in [32].

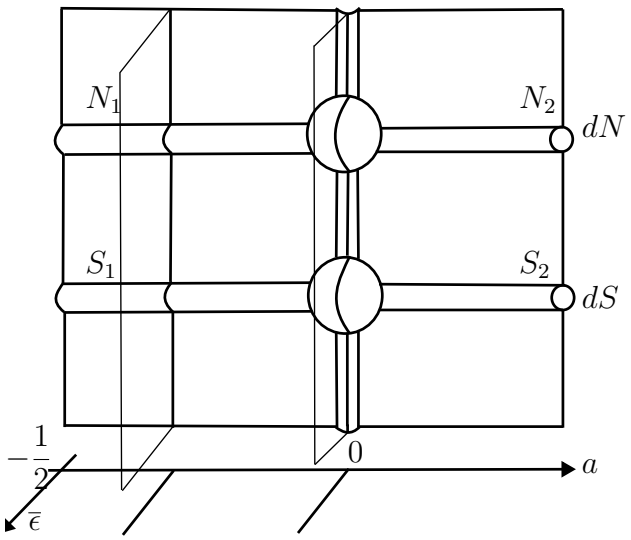

Figura 4.23: Tridimensional representation of the center manifold M. Figure made by the author.

Proposition 22. *For the region β with $\overline{\lambda} = (\overline{\epsilon}, \overline{a})$ and for all $k \in \mathbb{N}$, the germ of the vector field X_{pert} in the points s_i, $i = 2, 3$ and $A = A_0$ is C^k locally equivalent to the family $X_A = \pm\left(\overline{\epsilon}\dfrac{\partial}{\partial\overline{\epsilon}} + v^2 f(u, v, A)\left(u\dfrac{\partial}{\partial u} - v\dfrac{\partial}{\partial v}\right)\right)$ in some neighborhood of $(u, v, z, A) = (0, 0, 0, A_0)$. The function f is C^k and strictly positive. The sign is positive for s_2 and negative for s_3. Furthermore, for each A the planes $\{v = 0\}$ and $\{u = 0\}$ are respectively contained in F_0 and the disc $D_{\overline{\lambda}}$.*

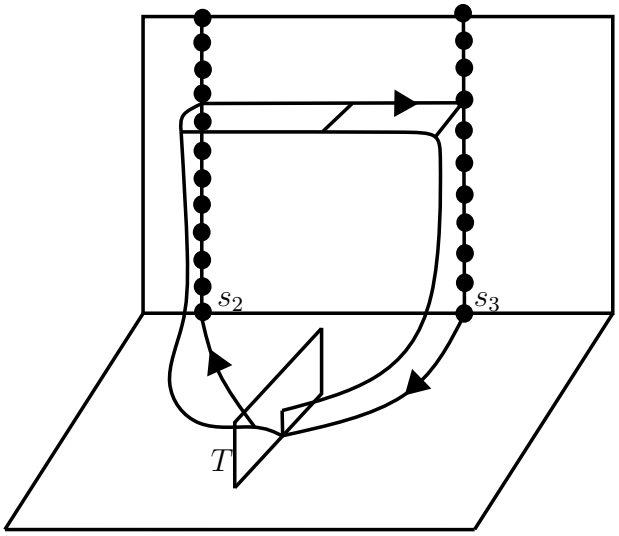

Figura 4.24: Center manifold $C_\gamma(A)$. Figure made by the author.

Let $C_\gamma(A)$ be the close of the union of orbits segments from X_A through the points of the graph of γ, taken between the first intersection of this trajectory with the transversal section T, as shown in Figure 4.24 in negative and positive time. The following theorem is proved in [32].

Theorem 23. *$C_\gamma(A)$ is well defined for $-A_0 \leq A \leq A_0$, with A_0 and v_0 small enough and it is a C^∞ manifold, with exception of two points $\alpha(\gamma) \in \overline{L_2}$ and $\beta(\gamma) \in \overline{L_3}$, which are*

limit points from vector field $X_{(0,0)}$, on the trajectory passing through $(x(0), y(0)) \in C_1$, where

$$C_1 = \left\{ \frac{x^2}{\eta} + \frac{x^3}{\eta} - x < y < \frac{(1+\sqrt{1+3\eta})(1+6\eta+\sqrt{1+3\eta})}{27\eta} \right\}.$$

4.5 Melnikov Integral

Consider the following differential equation system

$$\dot{u} = f(u, \lambda), \tag{4.13}$$

where $u = (x, y) \in \mathbb{R}^2$, $\lambda = (\epsilon, a) \in \Lambda = (\epsilon, +\infty) \times \left[-\frac{1}{3}, +\infty\right) \subset \mathbb{R}^2$ and $f(u, \lambda) = \left(y - \frac{x^3}{\eta} - \frac{x^2}{\eta} + x, \epsilon(a - x)\right)$.

Let $\xi_0 \in \mathbb{R}^2$ a regular point of the non-perturbed system

$$\dot{u} = f(u, 0), \tag{4.14}$$

and denote by $u(t, \xi, \lambda)$ the solution of (4.13) with inicial condition $u(0, \xi_0, \lambda) = \xi_0$. We define $g(u) = Rf(u, 0)$, where

$$R = \begin{pmatrix} 0 & -1 \\ 1 & 0 \end{pmatrix},$$

and let $\psi(t, \xi)$ the orthogonal system flow $\dot{u} = g(u)$. The orbit $\psi(t, \xi_0)$ is transversal to the solution $u(t, \xi_0, 0)$ of the system (4.13).

We define the transversal section

$$\Sigma = \{\psi(t, \xi_0); t \in \mathbb{R}\} \tag{4.15}$$

and we admit that there exist two solutions families $\gamma^1(t, \lambda)$, $\gamma^2(t, \lambda)$ from system (4.13), each one of them parameterized by $\lambda = (\epsilon, a)$ transversal to Σ. Furthermore, we suppose that for $\lambda = 0$ the correspondent solutions coincide with the solution of the non-perturbed system (4.14) with $\xi = \xi_0$. Our aim is obtain information about the function that measures the distance between the two families γ^1 and γ^2.

Let

$$\begin{array}{rcl} \rho^i : \Lambda \subset \mathbb{R}^2 & \longrightarrow & \mathbb{R} \\ \lambda & \mapsto & \rho^i(\lambda), \end{array}$$

where $\rho^i(0) = 0$, with $\rho^i(\lambda)$ denoting the intersection point of the family γ^i with the transversal section Σ, for $i = 1, 2$. Such point is measured by the parameterization of Σ, given by (4.15). So, we could write

$$\gamma^i(t, \lambda) = u\left(t, \psi\left(\rho^i(\lambda), \xi_0\right), \lambda\right) \quad i = 1, 2. \tag{4.16}$$

We can see these families as variations of the solution of the non-perturbed system (4.14) and $\gamma^i(t, 0) = u(t, \xi_0, 0)$, due to $\rho^i(0) = 0$ and $\psi(0, \xi_0) = \xi_0$, for $i = 1, 2$. Furthermore, as long as we have $\gamma^i(0, \lambda) = \psi(\rho^i(\lambda), \xi_0)$, so $\gamma^i(0, \lambda) \in \Sigma$.

Now we define the function

$$\begin{array}{rcl} \Delta : \Lambda \subset \mathbb{R}^2 & \longrightarrow & \mathbb{R} \\ \lambda & \mapsto & \Delta(\lambda) = \rho^1(\lambda) - \rho^2(\lambda). \end{array}$$

The function Δ measures the distance between the points where the families cross Σ and, moreover, we have that $\gamma^i(t,\lambda)\cap\Sigma=\rho^i(\lambda), i=1,2$.

For λ in a neighborhood of the origin, the function $\Delta(\lambda)$ is equivalent to the function

$$\begin{array}{rcl} sep:\Lambda\subset\mathbb{R}^2 & \longrightarrow & \mathbb{R} \\ \lambda & \mapsto & sep(\lambda)=\langle\psi(\rho^1(\lambda),\xi_0)-\psi(\rho^2(\lambda),\xi_0),g(\xi_0)\rangle. \end{array}$$

The function *sep* could be written as

$$sep(\lambda)=f(\xi_0,0)\times\left(\psi\left(\rho^1(\lambda),\xi_0\right)-\psi\left(\rho^2(\lambda),\xi_0\right),g(\xi_0)\right),$$

where $\times$ is the cross product in $\mathbb{R}^2$, defined by $u\times v=u_1v_2=v_2u_1$, with $u=(u_1,u_2)$ and $v=(v_1,v_2)$. If the solutions $\gamma^1(t,\lambda)$ and $\gamma^2(t,\lambda)$ are identical, we have that $sep(0)=0$ and $sep(\lambda)=0$.

Let's define $S=\{\lambda\in\Lambda; sep(\lambda)=0\}$. For λ small enough, the function *sep* is equivalent to the function Δ. from now on we define the separation function with some dependence of the time, as represented below.

$$\begin{array}{rcl} S:\mathbb{R}\times\Lambda & \longrightarrow & \mathbb{R} \\ (t,\lambda) & \mapsto & S(t,\lambda)=\langle\gamma^1(t,\lambda)-\gamma^2(t,\lambda),g(\phi_t(\xi_0))\rangle, \end{array}$$

or $S(t,\lambda)=f(\phi_t(\xi_0),0)\times(\gamma^1(t,\lambda)-\gamma^2(t,\lambda))$, where ϕ_t is the flow of the system (4.14).

Once we have $S(0,\lambda)=sep(\lambda)$, the technique which is used is of calculate the partial derivatives of the function $sep(\lambda)$ from the correspondent partial derivatives of the function $S(t,\lambda)$.

Defining $S^i(t,\lambda)=\langle\gamma^i(t,\lambda),g(\phi_t(\xi_0),0)\times\gamma^i(t,\lambda)$, $i=1,2$, the function S can be expressed as $S(t,\lambda)=S^1(t,\lambda)-S^2(t,\lambda)$.

We have that

$$S^i_{\lambda_j}=f(\phi_t(\xi_0),0)\times\gamma^i_{\lambda_j}(t,0). \tag{4.17}$$

As long as we have $\gamma^i(t,\lambda)$ solution from (4.13), we arrive in $\dot\gamma^i(t,\lambda)=f(\gamma^i(t,\lambda),\lambda)$. Therefore, $\dot\gamma_{\lambda_j}(t,\lambda)=f_u(\gamma^i(t,\lambda),\lambda)\gamma^i_{\lambda_j}(t,\lambda)+f_{\lambda_j}(\gamma^i(t,\lambda),\lambda)$, and so

$$\dot\gamma^i_{\lambda_j}(t,0)=f_u\left(\gamma^i(t,0),0\right)\gamma^i_{\lambda_j}(t,0)+f_{\lambda_j}\left(\gamma^i(t,0),0\right).$$

We can write $\gamma^i(t,0)=u(t,\xi_0,0)$, and therefore $\dot\gamma^i_{\lambda_j}(t,0)=f_u(u(t,\xi_0,0),0)\gamma^i_{\lambda_j}(t,0)+f_{\lambda_j}(u(t,\xi_0,0),0)$, which gives origin to

$$\dot\gamma^i_{\lambda_j}(t,0)=f_u(\phi_t(\xi_0),0)\gamma^i_{\lambda_j}(t,0)+f_{\lambda_j}(\phi_t(\xi_0),0). \tag{4.18}$$

From equation (4.17), we get $\dot S^i_{\lambda_j}(t,0)=f_u(\phi_t(\xi_0),0)\,\dot u(t,\xi_0,0)\times\gamma^i_{\lambda_j}(t,0)+f(\phi_t(\xi_0))\times\dot\gamma^i_{\lambda_j}(t,0)$ and using (4.18), we obtain

$$\begin{array}{rl} \dot S^i_{\lambda_j}(t,0)= & f_u(\phi_t(\xi_0),0)\,f(\phi_t(\xi_0),0)\times\gamma^i_{\lambda_j}(t,0)+f(\phi_t(\xi_0),0) \\ & \times\left(f_u(\phi_t(\xi_0),0)\,\gamma^i_{\lambda_j}(t,0)+f_{\lambda_j}(\phi_t(\xi_0),0)\right). \end{array}$$

Using the notation $f_u(\phi_t(\xi_0),0)=A(t)$, we arrive in

$$\begin{array}{rl} \dot S^i_{\lambda_j}(t,0)= & A(t)\,f(\phi_t(\xi_0),0)\times\gamma^i_{\lambda_j}(t,0)+f(\phi_t(\xi_0),0)\times A(t)\,\gamma^i_{\lambda_j}(t,0)+ \\ & +f(\phi_t(\xi_0),0)\times f_{\lambda_j}(\phi_t(\xi_0),0). \end{array} \tag{4.19}$$

From vector analysis, we have the result that if A is a matrix $2x2$ and $v, w \in \mathbb{R}^2$, so $Av \times w + v \times Aw = (trA)\, v \times w$. Applying this result in (4.19), we obtain

$$\dot{S}^i_{\lambda_j}(t,0) = (trA(t))\, f(\phi_t(\xi_0),0) \times \gamma^i_{\lambda_j}(t,0) + f(\phi_t(\xi_0),0) \times f_{\lambda_j}(\phi_t(\xi_0),0),$$

and as $A(t) = \begin{pmatrix} \frac{\partial f_1}{\partial u_1} & \frac{\partial f_1}{\partial u_2} \\ \frac{\partial f_2}{\partial u_1} & \frac{\partial f_2}{\partial u_2} \end{pmatrix}$, with $f(u,0) = (f_1(u,0), f_2(u,0))$, we conclude that $trA(t) = divf(\phi_t(\xi_0),0)$.

Therefore,

$$\dot{S}^i_{\lambda_j}(t,0) = divf(\phi_t(\xi_0),0)\, f(\phi_t(\xi_0),0) \times \gamma^i_{\lambda_j}(t,0) + f(\phi_t(\xi_0),0) \times f_{\lambda_j}(\phi_t(\xi_0),0),$$

and using (4.17), we obtain

$$\dot{S}^i_{\lambda_j}(t,0) = divf(\phi_t(\xi_0),0)\, S^i_{\lambda_j}(t,0) + f(\phi_t(\xi_0),0) \times f_{\lambda_j}(\phi_t(\xi_0),0). \tag{4.20}$$

Solving the ordinary differential equation (4.20) through the assumption that we know the behavior of $\gamma^1(t)$, when $t \to -\infty$ and of $\gamma^2(t,0)$, when $t \to +\infty$, we arrive in

$$S^1_{\lambda_j}(0,0) = K(t)\, S^1_{\lambda_j}(t,0) + \int_t^0 K(s)\, f(\phi_s(\xi_0)) \times f_{\lambda_j}(\phi_s(\xi_0),0)\, ds,$$

and

$$-S^2_{\lambda_2}(0,0) = -K(t)\, S^2_{\lambda_j}(t,0) + \int_0^t K(s)\, f(\phi_s(\xi_0)) \times f_{\lambda_j}(\phi_s(\xi_0),0)\, ds,$$

where $K(t) = e^{-\int_0^t divf(\phi_s(\xi_0),0)ds}$. Therefore, the partial derivative of sep in relation to λ_j stays as

$$\begin{array}{l} sep_{\lambda_j}(0) = \\ \lim_{t\to-\infty}\left[K(t)\, f(\phi_t(\xi_0)) \times \gamma^1_{\lambda_j}(t,0) + \int_t^0 K(s)\, f(\phi_s(\xi_0)) \times f_{\lambda_j}(\phi_s(\xi_0),0)\, ds\right] + \\ + \lim_{t\to+\infty}\left[-K(t)\, f(\phi_t(\xi_0)) \times \gamma^2_{\lambda_j}(t,0) + \int_0^t K(s)\, f(\phi_s(\xi_0)) \times f_{\lambda_j}(\phi_s(\xi_0),0)\, ds\right] \end{array} \tag{4.21}$$

As long as the terms between the brackets are constants, these limits from (4.21) exist.

Now we apply (4.21) for the case of perturbations of saddle connections. Let is suppose that ξ_0 denotes a regular point on the orbit of the system (4.15), which connects two hyperbolic saddles p_0 and q_0, i.e., $\lim_{t\to-\infty}\phi_t(\xi_0) = p_0$ and $\lim_{t\to+\infty}\phi_t(\xi_0) = q_0$. Let Σ as defined in (4.15). Through the application of the implicit function theorem, if λ is in the neighborhood of the origin, the system (4.13) has the perturbed hyperbolic saddle points $p_\lambda = p_0 + O(\lambda)$ and $q_\lambda = q_0 + O(\lambda)$.

We define $\gamma^1(t,\lambda)$ the solution of (4.13)) with inicial conditions in Σ that stays in the unstable manifold of p_λ and $\gamma^2(t,\lambda)$ the correspondent solution in the stable manifold of the hyperbolic saddle point q_λ. The next proposition gives an explicit equation for $sep_{\lambda_j}(0)$.

Proposition 24. *If the system* (4.13)*) with* $\lambda = 0$ *has a saddle connection and if* γ^i *given by* $\gamma^i(t,\lambda) = u(t, \psi(\rho^i(\lambda),\xi_0),\lambda), i = 1,2$ *are solutions in the stable* ($i = 1$) *and in the unstable* ($i = 2$) *manifolds of the perturbed saddle point, we have*

$$lim_{t\to-\infty} K(t)\, f(\phi_t(\xi_0)) \times \gamma^1_{\lambda_j}(t,0) = 0,$$

$$lim_{t\to+\infty} K(t) f(\phi_t(\xi_0)) \times \gamma^2_{\lambda_j}(t,0) = 0.$$

Moreover,

$$sep_{\lambda_j}(0) = \int_{-\infty}^{+\infty} e^{-\int_0^t div f(\phi_s(\xi_0),0)ds} f(\phi_t(\xi_0),0) \times f_{\lambda_j}(\phi_t(\xi_0),0)\, dt,$$

known as Melnikov integral.

Now we study the existence of a periodic orbit approaching a limit periodic set of the type I, using the integral from proposition (24).

Consider the family given by the chart $\{\overline{\epsilon} = 1\}$ from the exploded vector field X_2^* on the blow up process. For the sake of simplify the notation, consider $b = \dfrac{(1+3\eta+\sqrt{1+3\eta})}{\eta(1+\sqrt{1+3\eta})}$.

$$X_2^* = \begin{cases} \dot{\overline{x}} = \overline{y} - \dfrac{\overline{x}^2}{2} b \\ \dot{\overline{y}} = (A - b\overline{x}) \end{cases} . \tag{4.22}$$

We can multiply both equations of system (4.22) by the integral factor e^{-y} and the system stays as

$$X_2^{**} = \begin{cases} \dot{\overline{x}} = e^{-\overline{y}} \left(\overline{y} - \dfrac{\overline{x}^2}{2} b \right) \\ \dot{\overline{y}} = e^{-\overline{y}} (A - b\overline{x}) \end{cases} . \tag{4.23}$$

For $a = 0$, the system (4.23) presents as a first integral the function

$$H = -e^{-\overline{y}} \left(\overline{y} - \frac{\overline{x}}{2} + 1 \right).$$

Now we consider the transversal section T from the Figure 4.24. Let $C_\gamma(A)$ the central manifold built as explained in Theorem 23 and let ρ_1 and ρ_2 curves in T defined for the intersection of $C_\gamma(A) \cap T$. Parametrizing the section T by $(u, h = H(0,\overline{y})) \in \mathbb{R}^2 \times \mathbb{R}$, we can write ρ_1 and ρ_2 as graphs functions C^∞:

$$\rho_1 = graph\{h = F(u,A)\} \text{ and } \rho_2 = graph\{h = B(u,A)\}.$$

Let is define the function $\Delta(u,A) = F(u,A) - B(u,A)$. We see that $\Delta(0,0) = 0$. By construction, the solution equations of $\Delta(u,A) = 0$ corresponds to the intersection of periodic orbits from X_2^*, with the section T. Moreover, $\Delta \in C^\infty$ because $F, B \in C^\infty$. Below, we verify that $\dfrac{\partial \delta}{\partial A}(0,0) \neq 0$ and using the implicit function theorem, we guarantee the existence of only one $A = c(u)$ such that $c(0) = 0$ and $\Delta(u, c(u)) = 0$.

Using proposition (24), we obtain

$$\frac{\partial \Delta}{\partial A}(0,0) = \int_{-\infty}^{+\infty} e^{-\int_0^t div X_2^*(\overline{x},\overline{y},0)ds} X_2^{**}(\overline{x},\overline{y},0) \times X_{2a}^{**}(\overline{x},\overline{y},0)\, dt,$$

where $X_{2a}^{**} = D_a X_2^{**}$. We have that

$$X_2^{**}(\overline{x},\overline{y},0) = \left(e^{-\overline{y}} \left(\overline{y} - \frac{\overline{x}^2}{2} b \right), -e^{-\overline{y}} b\overline{x} \right),$$

$$X_{2a}^{**}(\overline{x},\overline{y},0) = \left(0, e^{-\overline{y}}\right),$$

$$div X_2^{**}(\overline{x},\overline{y},0) = -b\overline{x}e^{-\overline{y}} + b\overline{x}e^{-\overline{y}} = 0$$

and

$$X_2^{**}(\overline{x},\overline{y},0) \times X_{2a}^{**}(\overline{x},\overline{y},0) = e^{-2\overline{y}}\left(\overline{y} - \frac{\overline{x}^2}{2}\right) b.$$

Therefore, we obtain that

$$\frac{\partial \Delta}{\partial A} = \int_{-\infty}^{+\infty} e^{-2\overline{y}}\left(\overline{y} - \frac{\overline{x}^2}{2}b\right) dt.$$

Using the first equation of (4.22), we arrive in

$$dt = \frac{d\overline{x}}{\left(\overline{y} - \frac{\overline{x}^2}{2}b\right)e^{-\overline{y}}}$$

and so

$$\frac{\partial \Delta}{\partial A}(0,0) = \int_{-\infty}^{+\infty} e^{-\overline{y}} d\overline{x}.$$

As the integral is calculated along the equipotential manifold $\Gamma = \left\{\overline{y} = \frac{\overline{x}^2}{2} - 1\right\}$, we conclude that

$$\frac{\partial \Delta}{\partial A}(0,0) = \int_{-\infty}^{+\infty} e^{1-\frac{\overline{x}^2}{2}} d\overline{x} > 0.$$

Therefore, $\dfrac{\partial \Delta}{\partial A} \neq 0$.

Therefore, fixed $h \in (y_0, y_1)$, let is consider the curve in $\mathbb{R}^4$ given by

$$\gamma_h = \{(x, y, \epsilon, a) = (0, h, s, 0), s \in [0, s_0)\},$$

where s_0 is a fixed constant. Let is $C_{\gamma_h}(A)$ the center manifold associated. So, there exists only one curve $A = c(u)$ in the blow-up space $\{(\overline{x},\overline{y},u,A\})$ such that $\Delta(u, c(u)) = 0$. Returning to the original parameters, we can write

$$a = u\overline{a} = \epsilon^{\frac{1}{2}} c\left(\epsilon^{\frac{1}{2}}\right) = c_h(\epsilon).$$

Therefore, along the curve $a = c_h(\epsilon)$, the induced family $X_{\epsilon, a=c_h(\epsilon)}$ has a sequence of limit cycles $\Gamma_{\epsilon, c_h(\epsilon)}$ that converges to Γ_h when $\epsilon \to 0$.

5 Conclusion

In the first subject studied, we worked with a linear center at the origin and four normal different forms of isochronous centers at the origin, studying possibilities of existence of limit cycles between the linear center and one of the four different types of cubic iscochronous centers on the plane $\mathbb{R}^2$, divided by the discontinuity set Σ and two regions Σ^+ and Σ^-. We got limit cycles only in the case of one intersection of the limit cycle with Σ_1 and one intersection of the limit cycle with Σ_2, with X_c acting in Q_1 and X_i acting in the first quadrant Q_1. The cases with two intersections with Σ^+ and two intersections with Σ^- do not present limit cycles, regardless of the position of the linear center and one of the isochronous centers in Σ^+ and Σ^-.

In the second subject studied, we dealt with the existence of a global center at the origin in the system (1.3), based on ten different statements of Theorem 12. Each one of these statements present a global center for determined conditions applied in the parameters involved, with the exception of statements (a) and (c) of Theorem 12, which do not have global center at the origin of the coordinate system.

In the third subject studied, we concluded the existence of a canard limit cycle for the regularized system (4.4) through analysis of Hopf bifurcation in one of the singularities that always is inside the regularized region, followed by blow up applications in the charts of the parameters involved and, finally, finishing by an analysis using Melnikov integral.

References

[1] R. Allaoua, A. Bendjeddou, A. Berbache, R. Cheurfa, Limit cycles for piecewise differential systems formed by an arbiitrary lienar system and a cubic isochronous center, Memoirs on Differential Equations and Mathematical Physics, (2022).

[2] M.J. Alvarez, A. Ferragut and X. Jarque, *A Survey on the Blow Up Technique*, Int. J. of Bifurcation and Chaos **21**, 3103–3118, (2011).

[3] Alves M. A., Euzébio R. D., *Periodic Trajectories in Planar Discontinuous Piecewise Linear Systems with only Centers and with a Nonregular Switching Line*, Nonlinearity, (2023).

[4] A.A. Andronov, E.A. Leontovich, I.I. Gordon and A.G. Maıer, *Qualitative theory of second-order dynamic systems*, Halsted Press [John Wiley & Sons], New York-Toronto; Israel Program for Scientific Translations, Jerusalem-London, 1973.

[5] A. Andronov, A. Vitt, S. Khaikin, Theory of oscillations, Pergamon Press, Oxford, Russian edition, (1966).

[6] J.C. Artés, F. Dumortier and J. Llibre, *Qualitative Theory of Planar Differential Systems*, Springer, (2006).

[7] N.N. Bautin *On the Number of Limit Cycles which Appear with the Variation of Coefficients from an Equilibrium Position of Focus or Center Type*, Mat. Sbornik 30, 181–196 pp., (1952), Amer. Math. Soc. Transl. Vol. 100, 1–19, (1984).

[8] B.P. Belousov, A Periodic reaction and its mechanism, Collection of Short Papers on Radiation Medicine for 1958, Moscow: Med. Publ., (1959).

[9] R. Benterki, J. Llibre, Centers and limit cycles of polynomial differential systems of degree 4 via averaging theory, J. Comput. Appl. Math. **313** (2017), 273–283.

[10] R. Benterki, J. Llibre, The centers and their cyclicity for a class of polynomial differential systems of degree 7, J. Comput. Appl. Math. **368** (2020), 112456, 16 pp.

[11] I.S. Berezin, N.P. Zhikov, Computing methods, Volume II, Pergamon Press, Oxford, (1964).

[12] Braga D. C. and Mello L. F., *Limit Cycles in a Family of Discontinuous Piecewise Linear Differential System with Two Zones in the Plane*, Nonlinear Dynamics, (2013).

[13] Broucke M. E., Pugh C. and Simic S. *Structural Stability of Picewise Smooth Systems*, Comp. Appl. Math., (2001).

[14] Buzzi C. A., Carvalho T. and Euzebio R. D., *On Poincaré Bendixson Theorem and Non-Trivial Minimal Sets in Planar Non-Smooth Vector Fields*, Publ. Math., (2018).

[15] C. Buzzi, J. Llibre and P. Santana, *Phase Portraits of* $(2,0)$ *Reversible Vector Fields with Symmetrical Singularities*, J. Math. Anal. Appl. **503**, 125324, 21 pp., (2021).

[16] Buzzi C., Pessoa C. and Torregrossa J., *Piecewise Linear Perturbations of a Linear Center*, Disc. Contin. Dyn. Syst., (2013).

[17] Buzzi, C. A.; da Silva P. R.; Teixeira M. A., *A singular approach to discontinuous vector fields on the plane*, Journal of Differential Equations, Elsevier, 2006.

[18] Cardin P. and Torregrosa J. *Limit Cycles in Planar Piecewise Lienar Differential Systems with Non-regular Separation Line*, Physica D, (2016).

[19] Carmona F. and Fernández-Garcia S., Fernández-Sanches F., Garcia-Medina E. and Teruel E., *Noose Bifurcation and Crossing Tangency in Reversible Piecewise Linear Systems*, Nonlinearity, (2014).

[20] Carmona F., Fernández-Sanches F., Novaes D. D. *Uniform Upper Bound for the Number of Limit Cycles of Planar Piecewise Linear Differential Systems with Two Zones Separated by a Straight Line*, Applied Mathematics Letters, Volume 137, (2023).

[21] Chavarriga J., Giné J., García I. A., *Isochronous Centers of a Lienar Center Perturbed by Fourth Degree Homogeneous Polynomial*, Bulletin des Sciences Mathematiques, p. 77-96, 123, (1999).

[22] Chicone, C., *Ordinary differential Equations with Applications*, Springer, 2006.

[23] Chillingworth D. R. J., *Discontinuity Geometry for an Impact Oscillator*, Dyn. Syst., (2002).

[24] R. Conti *Uniformly Isochronous Centers of Polynomial Systems in* $\mathbb{R}^2$, Lect. Notes Pure Appl. Math. **152**, 21–31, (1994).

[25] R. Conti, *Centers of Planar Polynomial Systems: a Review*, Le Mathematiche. **LIII**, 207–240, (1998).

[26] Cox, A. D.; Little, J., O'Shea, D., *Ideals, Varieties, and Algorithms- An Introdiction to the Computational Algebraic Geometry and Commutative Álgebra*, Undergraduate Texts in Mathematics- Springer, Fourth Edition.

[27] da Silva, C. E. L., *Ciclos Canard e Variedades Centrais*, Dissertação IME-USP, São Paulo, 2005.

[28] B.R. de Freitas, J. Llibre, J.C. Medrado, Limit cycles of continuous and discontinuous piecewise-linear differential systems in R^3, J. Comput. Appl. Math. **338** (2018), 311–323.

[29] de Moraes, J., R.; da Silva, P. R., *Piecewise Smooth Slow Fast Systems*, Springer, 2020.

[30] M. di Bernardo, C.J. Budd, A.R. Champneys, P. Kowalczyk, Piecewise smooth dynamical systems: Theory and aplications, Appl. Math. Sci., **163**, Springer-Verlag, London, (2008).

[31] H. Dulac *Détermination et Integration d'une Certaine Classe d'Equations Différentielle ayant par Point Singulier un Centre*, Bull. Sci. Math. Sér. **32**(2), 230–252, (1908).

[32] Dumortier F., Roussarie R. Canard Cycles and Center Manifolds, American Mathematical Society, (1996).

[33] Esteban M., Llibre J. and Valls C. *The Extended 16th Hilbert Problem for Discontinuous Piecewise Linear Centers Separated by a Nonregular Line*, Int. J. Bifurcation and Chaos, (2021).

[34] Euzebio R.D., Pazim R. and Ponce E., *Jump Bifurcations in some Degenerate Planar Piecewise Linear Differential Systems with Three Zones*, Physica D, (2016).

[35] Freire E., Ponce E., Rodrigo F. and Torres F., *Bifurcation Sets of Continuous Piecewise Linear Systems with Two Zones*, Int. J. Bifurcation Chaos Appl. Sci. Eng., 2073–2097, (1998).

[36] Freire E., Ponce E. and Torres F., *Canonical Discontinuous Planar Piecewise Linear System*, SIAM J. Appl. Dyn. Syst., (2012)

[37] Filippov, A. F., *Differential Equations with Discontinuous Right Hand Sides*, Kluwer Academic: Dordrecht, The Netherlands, 1988.

[38] M. Galeotti and M. Villarini, *Some Properties of Planar Polynomial Systems of Even Degree*, Ann. Mat. Pura. Appl. **161**(1), 299–313, (1992).

[39] J. García-Saldaña, J. Llibre and C. Valls, *Linear type global centers of linear systems with cubic homogeneous nonlinearities*, **69**(3), 771-–785,(2020).

[40] Guardia M., Seara T. M. and Teixeira M. A., *Generic Bifurcations of Low Codimension of Planar Filippov Systems*, J. Diff. Eq., (2011).

[41] Han M. and Zhang W., *On Hopf Bifurcation in Non-Smooth Planar Systems*, J. Diff. Eq., (2009).

[42] H. He, D. Xiao, *On the Global Center of Planar Polynomial Differential Systems and the Related Problems*, J. Appl. Anal. Comput. **12**(3), 1141–1157, (2022).

[43] Huan S. M. and Yang X. S., *Limit Cycles in a Family of Planar Piecewise Lienar Differential Systems with a Nonregular Separation Line*, Int. J. Bifurcation and Chaos, (2019).

[44] Huan S. M. and Yang X. S., *On the Number of Limit Cycles in General Planar Piecewise Linear Systems*, Disc. Contin. Dyn. Syst., (2012).

[45] C. Huygens, *Horologium Oscillatorium Sive de Motu Pendularium*, Theory and Design of the Pendulum Clock, dedicated to Louis XIV of France, (1673).

[46] Jacquemard A., Teixeira M. A. and Tonon D. J., *Piecewise Smooth Reversible Dynamical Systems at a Two-Fold Singularity*, Int. J. Bifurcation and Chaos, (2012).

[47] W. Kapteyn, *New Investigations on the Midpoints of Integrals of Differential Equations of the First Degree*, Nederl. Akad. Wetensch. Verslag Afd. Natuurk.**19**, 1446–1457, (1911); **20**, 1354–1365, (1912) (Dutch).

[48] Kozlova V. S., *Roughness of a Discontinuous System*, Vestn. Mosk. Univ., (1984).

[49] Kuehn, C., *Multiple Time Scale Dynamics*, Springer, 2015.

[50] Kuehn, C., Kojakhmetov, H. J., *Controlling Canard Cycles*, Journal of Dynamical and Control Systems, 517-544, 28, (2022).

[51] Kusnetzov, Y. A., *Elements of Applied Bifurcation Theory*, Springer, USA, 1998.

[52] Leine R. I.; Nijmeijer, H., *Dynamics and Bifurcations of Non Smooth Mechanical Systems*, Springer, 2004.

[53] Liberzon, D., *Switching in Systems and Control: Foundations and Applications*, Birkhause, 2003.

[54] J. Llibre, Limit cycles in continuous and discontinuous piecewise linear differential systems with two pieces separated by a straight line, Bulletin of Academy of Sciences of Moldova, Matematica **2**(90), 3–12, (2019).

[55] J. Llibre, J. Itikawa, Limit cycles for continuous and discontinuous perturbations of uniform isochronous cubic centers. J. Comput. Appl. Math. **277** (2015), 171–191.

[56] Llibre J., Ordoñez M. and Ponce E., *On the Existence and Uniqueness of Limit Cycles in a Planar Piecewise Linear Systems without Simmetry*, Nonlinear Anal., (2013).

[57] Llibre J. and Ponce E. *Three Nested Limit Cycles in Discontinuous Piecewise Linear Differential Systems with Two Zones*, Dyn. Cont. Discrete Impuls. Syst., (2012).

[58] Li, Shimin; Llibre, Jaume, *Canard Limit Cycles for Piecewise Linear Liénard Systems with Three Zones*, International Journal of Bifurcation and Chaos, Vol.30, No.15 (2020) 2050232 (7 pages).

[59] J. Llibre and C. Valls, *Polynomial Differential Systems with Even Degree Have no Global Centers*, J. Math. Anal. Appl. **503**(1), 125281, 5 pp., (2021).

[60] J. Llibre and C. Valls, *Reversible Global Centres with Quintic Homogeneous Nonlinearities*, Dynamical Systems, **30**, 135–148, (2023).

[61] J. Llibre, M.A. Teixeira, Piecewise linear differential systems with only centers can create limit cycles?, Nonlin. Dyn. **91**, 249–255, (2018).

[62] W. Li, J. Llibre, J. Yang, Z. Zhang, Limit cycles bifurcating from the period annulus of quasi-homogeneous ecnters, J. Dyn. Diff. Equat. **21**, 133–152, (2009).

[63] Llibre J., Zhang X., J. Math. Anal. Appl., 467, 537–549, (2018).

[64] N.G. Lloyd, J.M. Pearson and V.A. Romanovsky, *Computing Integrability Conditions for a Cubic Differential System*, Computers Math. Applic. **32**(10), 99–107 pp., (1996).

[65] Lum R. and Chua L. O. *Global properties of Continuous Piecewise Linear Vector Fields. Part I: Simplest Case in* $\mathbb{R}^2$, Memorandum UCB/ERL M90/22, (1991).

[66] Lum R. and Chua L. O. *Global properties of Continuous Piecewise Linear Vector Fields. Part II: Simplest Simetric in* $\mathbb{R}^2$, Int. J. Circuit Theory Appl., (1992).

[67] Luo C. J., *Singularity and Dynamics on Discontinuous Vector Fields*, Monograph Series on Nonlinear Science and Complexity, Elsevier, (2006).

[68] O. Makarenkov, J.S.W. Lamb, Dynamics and bifurcations of nonsmooth systems: A survey, Physica D **241**, 1826–1844, (2012).

[69] W.I. Milham, *Time and Timekeepers*, MacMillan, New York, (1945).

[70] I.A. Pleshkan, A new method of investigating the isochronocity of a system of two differential equations, Differential Equations **5**, 796–802, (1969).

[71] H. Poincaré, *Mémoire sur les Courbes Définies par les Équations Différentielles*, J. Anal. Math. **37**, 375-422, (1881), *Oeuvres de Henri Poincaré*, vol. I, Gauthier-Villars, Paris, 3–84 pp., (1951).

[72] Ponce E. Torres F., *A General Mechanism to Generate Three Limit Cycles in Planar Filippov Systems with Two Zones*, Nonlinear Dynamics, (2014).

[73] Simpson, D. J. W., *Bifurcations in Piecewise Smooth Continuous Systems*, World Scientific Series on Nonlinear Sciences Series A; World Scientific: Singapore, 2010.

[74] Simpson D. J. W. and Kuske R., *Stochastic Perturbations of Periodic Orbits with Sliding* , J. Nonlinear Science, (2015).

[75] Teixeira M. A. *Perturbation Theory for Non-Smooth Systems*, Encyclopedia of Complexity and Systems Science, (2008).

[76] Teixeira M. A., *Stability Conditions for Discontinuous Vector Fields*, J. Diff. Eq., (1990).

[77] B. van der Pol, A theory of the amplitude of free and forced triode vibrations, Radio Review (Later Wireless World) **1** 701–710, (1920).

[78] B. van der Pol, On relaxation-oscillations, The London, Edinburgh and Dublin Phil. Mag. J. Sci. **2** 978–992, (1926).

[79] Walsh J., Widiasih E., Hahn J and Mcgehee R., *Periodic Orbits for a Discontinuous Vector Field Arising from a Conceptual Model of Glacial Cycles*, Nonlinearity, (2016).

[80] Zhao Q., Wang C. and Yu J. *Limit Cycles in Discontinuous Planar Piecewise Linear Systems Separated by a Nonregular Line of Center-Center Type*, Int. J. Bifurcation and Chaos, (2021).

[81] Zhao Q. and Yu J. *Poincaré Maps of "<-shape Planar Piecewise Linear Dynamical Systems with a Saddle*, Int. J. Bifurcation and Chaos, (2019).

[82] H. Zoladek, Quadratic Systems with Center and Their Perturbations, Journal of Differential Equations **109**, 223-273, (1994).